AD-A056 100 RAND CORP SANTA MONICA CALIF F/G 17/2.1
THE FEASIBILITY OF EMPLOYING FREQUENCIES BETWEEN 20 AND 300 GHZ--ETC(U)
MAY 78 L MUNDIE, N FELDMAN
UNCLASSIFIED RAND/R-2275/DCA NL

1 OF 2
AD
A056 100

LEVEL II

R-2275-DCA
May 1978

The Feasibility of Employing Frequencies between 20 and 300 GHz for Earth-Satellite Communications Links

L. G. Mundie, N. E. Feldman

A Report prepared for

DEFENSE COMMUNICATIONS AGENCY

Rand
SANTA MONICA, CA. 90406

The research described in this report was sponsored by the Defense Communications Agency under Contract No. DCA100-77-C-0016.

Published by The Rand Corporation

UNCLASSIFIED

SECURITY CLASSIFICATION OF THIS PAGE (When Data Entered)

REPORT DOCUMENTATION PAGE

READ INSTRUCTIONS BEFORE COMPLETING FORM

1. REPORT NUMBER: R-2275-DCA
2. GOVT ACCESSION NO.:
3. RECIPIENT'S CATALOG NUMBER:

4. TITLE (and Subtitle): The Feasibility of Employing Frequencies Between 20 and 300 GHz for Earth-Satellite Communications Links

5. TYPE OF REPORT & PERIOD COVERED: Interim rept.

6. PERFORMING ORG. REPORT NUMBER:

7. AUTHOR(s): L. Mundie, N. Feldman

8. CONTRACT OR GRANT NUMBER(s):

9. PERFORMING ORGANIZATION NAME AND ADDRESS:
The Rand Corporation
1700 Main Street
Santa Monica, Ca. 90406

10. PROGRAM ELEMENT, PROJECT, TASK AREA & WORK UNIT NUMBERS:

11. CONTROLLING OFFICE NAME AND ADDRESS:

12. REPORT DATE: May 1978

13. NUMBER OF PAGES: 121 (12) 137 P.

14. MONITORING AGENCY NAME & ADDRESS (if different from Controlling Office):

15. SECURITY CLASS. (of this report): UNCLASSIFIED

15a. DECLASSIFICATION/DOWNGRADING SCHEDULE:

16. DISTRIBUTION STATEMENT (of this Report)

Approved for Public Release; Distribution Unlimited

17. DISTRIBUTION STATEMENT (of the abstract entered in Block 20, if different from Report)

No restrictions

18. SUPPLEMENTARY NOTES

19. KEY WORDS (Continue on reverse side if necessary and identify by block number)

Millimeter Waves
Radio
Atmospheric Models
Communication Satellites
Telecommunications
Weather
Antennas

20. ABSTRACT (Continue on reverse side if necessary and identify by block number)

see reverse side

78 07 06 065

DD FORM 1 JAN 73 1473 EDITION OF 1 NOV 65 IS OBSOLETE

296 600

UNCLASSIFIED

SECURITY CLASSIFICATION OF THIS PAGE (When Data Entered)

Developes a model for estimating in a new way the statistical distributions of signal attenuation, sky noise temperature, and total atmospheric-induced degradation in millimeter-wave link performance resulting from the presence of humidity, clouds, and rain in the atmosphere. The statistical distribution of system outages is then found for certain hypothetical communications links using six frequencies and four elevation angles. To illustrate the compatibility of the communications equipment with small, mobile-user platforms, pointing and tracking, weight and power, radome considerations, and antenna options are treated. It is concluded that generally acceptable performance in the millimeter-wave frequency region can be obtained both for small, mobile users and for wide-band data relay users. See also R-1936-RC. (Author)

LEVEL II

12

R-2275-DCA

May 1978

The Feasibility of Employing Frequencies between 20 and 300 GHz for Earth-Satellite Communications Links

L. G. Mundie, N. E. Feldman

A Report prepared for

DEFENSE COMMUNICATIONS AGENCY

Rand
SANTA MONICA, CA. 90406

PREFACE

This report was prepared for the Military Satellite Communications Systems Office (MSO) of the Defense Communications Agency as the final report on a study entitled "Feasibility of Military Satellite Communications at Frequencies Above 8 GHz for Mobile and Wide-Band Data Relay Users." It follows an earlier Rand project for the same agency entitled "Advantages of Frequencies Above 8 GHz: An Overview."

These two projects for the Defense Communications Agency grew out of a Rand-supported study entitled "A New Approach to Millimeter-Wave Communications," described in Rand report R-1936-RC.

The current report presents estimates of the degradation of performance of millimeter-wave links due to atmospheric effects in a new way and draws consequent implications for the design of future systems. This information should be useful to designers of future communications satellite systems in the 20 to 300 GHz frequency region for a wide diversity of users.

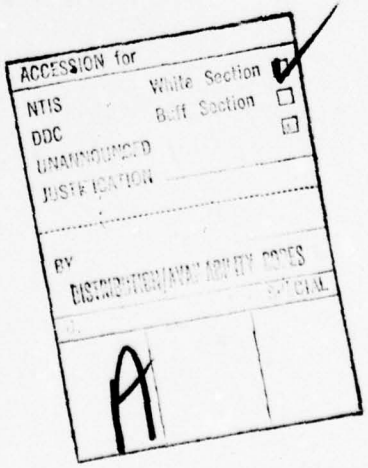

SUMMARY

This report examines the feasibility of using frequencies above 8 GHz for military satellite communications. Because communications degradation resulting from atmospheric effects (due to humidity, clouds, and rain) is the main limitation to the use of the higher frequencies, much of the report is devoted to the development of a model for the statistical distributions of signal attenuation, of sky noise temperature, and of total atmospheric-induced degradation in link performance, as a function of frequency and elevation angle. The model is then applied to a few hypothetical communications links to estimate the statistical distribution of outages due to weather as a function of data rate and other system parameters. The model was developed for Washington, D.C. (a region with relatively high rainfall), but could be extended to any location where weather data are available. The performance estimates were made for the downlink (even when the specific frequency has been allocated for uplink use) because it is usually limiting.

No attempt was made in this study to evolve an optimal communications system; rather, the basic effort was to examine the effects of varying a number of key parameters through a wide range.

Six frequencies are considered in this analysis--one in each of six bands allocated for satellite communications use. The frequencies (21.2, 31, 48, 101, 152, and 265 GHz) were selected at the positions in their respective bands at which atmospheric degradation is most severe. The performance was estimated for elevation angles (at the user) of 10, 30, 45, and 90 deg. A satellite altitude of 30,000 n mi was assumed in all cases, for reasons discussed later in this summary.

Two types of users were considered--small mobile users and wide-band data relay users. To accommodate a large number of mobile users located on small platforms (e.g., small ships, small aircraft, and land vehicles), very small (10-cm diameter) terminal antennas were postulated. The wide-band data relay users were assumed to employ 10-m diameter antennas. This range, from 10 cm to 10 m, is expected to bracket the terminal antenna diameters that will be of interest in future military communications satellite systems.

To estimate the practicality of using higher frequencies, the atmospheric degradation model was applied to four specific cases--two for each type of user. In each case, the link availability as limited by atmospheric degradation was estimated as a function of elevation angle, data rate, and frequency for the selected values of the satellite and terminal antenna diameters. Illustrative results for each of the four cases appear in the following table.

In making these performance estimates, we assumed a transmitter power of 10 W, an antenna efficiency of 0.56, and a system margin of 8 dB. When either user employed an uncooled receiver, a value of 10 was assumed for E_b/N_0, the ratio of the energy per bit to the noise power density. Because the wide-band data relay user has a much more elaborate installation than the mobile user, the option of using a cooled receiver and a more complex modem was also considered. In this case, coherent modulation permits adequate performance with an E_b/N_0 of 5 dB.

The illustrative results in the table show that practical data rates for small mobile users with uncooled receivers can be realized with only a 10-cm diameter terminal antenna. When the satellite antenna diameter is held constant at 4.4 m (Case I-A), a data rate of 10^6 bps (sufficient, for example, to provide a 16 kbps digital voice channel to each of 60 users when Time Division Multiple Access is employed) is realized, with availabilities ranging from 98.7 percent at 21.2 GHz to 89 percent at 265 GHz.

Footprint width is important as a measure of the area served by a single beam (which serves a cluster of users), as a measure of the degree of frequency reuse per satellite, and as a measure of the mutual interference problem. These issues depend on a particular system concept and antenna design, and are beyond the scope of this study. The footprint width of the beam on the earth decreases with increasing frequency, as indicated in Case I-A. When the footprint width is held constant, as in Case I-B, the associated satellite antenna diameter decreases with increasing frequency, leading to a more rapid decrease in data rate per beam with increasing frequency. This disadvantage is, however, counteracted by the advantage that a larger number of (the smaller) satellite antennas can be mounted in the same total aperture

ESTIMATED DOWNLINK PERFORMANCE AT 30 DEG ELEVATION ANGLE

Case I: Small Mobile User

(0.1 m antenna, uncooled receiver)

	A. 4.4 m (Constant) Satellite Antenna Diameter, 10^6 bps Data Rate		B. 123 n mi (Constant) Footprint Width		
Frequency (GHz)	Availability (percent)	Footprint Width (n mi)	Data Rate (bps)	Availability (percent)	Satellite Antenna Diameter (m)
21.2	98.7	123	10^6	98.7	4.4
31	98.9	83.8	10^6	97.5	3
48	96	54	10^5	98	1.94
101	94	25.7	10^4	97	0.92
152	94	17.1	10^4	96	0.61
265	89	9.8	10^3	94	0.35

Case II: Wide-Band Data Relay User

(10 m antenna, 1 m constant satellite antenna diameter)

	A. Uncooled Receiver		B. Cooled Receiver	
	10^8 bps Data Rate		Availability (percent)	
Frequency (GHz)	Availability (percent)	Footprint Width (n mi)	10^8 bps Data Rate	10^9 bps Data Rate
21.2	99.7	541	99.9	99.5
31	99.7	369	99.8	99.4
48	98.7	238	99.3	98
101	97	113	98	97
152	97	75.2	98	96
265	93	39.2	97	94

when higher frequencies are employed. Thus, at 265 GHz, 158 antennas could be mounted in the aperture completely occupied by a single 21.2 GHz antenna, giving the same footprint width.

With a 10 m antenna, the wide-band data relay user is able to achieve reasonable availabilities while communicating at 10^8 bps with an uncooled receiver (Case II-A), and at 10^9 bps with a cooled receiver (Case II-B).

The model indicates that the performance degrades rapidly as the elevation angle at the user falls below 30 deg, especially at higher frequencies. Thus, for example, in Case I-A it was found that, with an availability of 98 percent, the estimated data rate at 30 deg elevation exceeds that at 10 deg elevation by a factor ranging from 4 at 21.2 GHz to 3000 at 265 GHz. It is clear that, for communications systems which must operate during rain, the higher the frequency the more important it is to avoid elevation angles below 30 deg. This can be accomplished by putting satellites in inclined orbits rather than in geostationary orbits. Operation at elevation angles above 30 deg has the additional advantage of negligible atmospheric scintillation, decreased vulnerability to detection, interference, and jamming, and decreased blockage by surrounding objects such as terrain features and ship masts. Inclined orbits also have the advantage that they can provide full earth coverage. A number of satellite constellations were examined to determine their ability to provide continuous worldwide coverage with elevation angles above 30 deg. It was found that, for example, a constellation of nine satellites in circular orbits at 30,000 n mi altitude (60 deg inclination) provided elevation angles above 30 deg an average of 99.7 percent of the time to observers anywhere on earth. The desirable features of this constellation led to the 30,000 n mi altitude in the illustrative example.

The length, width, and area of the beam footprint on the earth's surface were calculated as a function of elevation angle, satellite altitude, and beamwidth. The illuminated area is nearly elliptical until the edge of the earth is approached, and approximately doubles as the elevation angle decreases from 90 deg (overhead) to 30 deg.

The tradeoff between complexity on the satellite and at the user terminal (while maintaining constant link performance) is examined,

particularly as it relates to the antenna sizes at the two ends of the link. The acquisition problem becomes major when communications must be maintained with large numbers of widely dispersed users having only small antennas, and when mutual interference rejection, covertness, and a high degree of security from jamming are required. This problem is briefly examined, but no attempt is made to optimize the system for its solution.

The pointing and tracking problems at high frequencies are examined in some detail. For small mobile users, the decrease in terminal antenna diameter (to 10 cm) from the values presently planned at lower frequencies (7 to 8 GHz) in the DSCS system (1 to 3 m) more than compensates for the increase in frequency, so that terminal pointing and tracking are considerably relaxed. The increased pointing and tracking accuracy required by the wide-band data relay user at higher frequencies can be provided by current techniques. Similarly, whereas the required satellite attitude reference system is more complex at higher frequencies (to attain the higher accuracy), the relative incremental cost is small--the cost of reliable, long-lifetime, space-qualified attitude reference systems capable of achieving only relatively low accuracy is already very high ($800,000). These systems require gas-bearing gyros and horizon sensors to achieve an accuracy of a few tenths of a degree. The addition of a digital sun sensor improves the performance by an order of magnitude, but adds relatively little (less than 10 percent) to the cost. The Space Sextant-Attitude Reference System now under development holds the prospect for a substantial improvement in accuracy (nearly 10^{-4} deg) with no increase in cost.

The compatibility of high-frequency communications equipment with small mobile user platforms is analyzed. The postulated small terminal antennas permit relatively flexible placement. In the case of aircraft, they might be mounted inside the fuselage or the wings beneath a conformal radome with a 10-cm diameter antenna; coverage down to 30 deg elevation could be achieved with a relatively flat, i.e., conformal, radome which is only 40 cm in diameter.

The weight and power requirements of equipment operating at the higher frequencies are strongly dependent on the efficiency of high-power output tubes. The power output capability and efficiency of a

number of tube types were examined as a function of frequency. These include the klystron, traveling wave tube (TWT), extended-interaction amplifier, ubitron tube, coupled-cavity TWT, and gyrotron. Power levels as high as 10 kW (CW) at 300 GHz may be feasible, although laboratory units have only demonstrated 12 kW at 100 GHz thus far. While the efficiency within any tube type decreases slowly with increasing frequency, measures can be taken to offset the decrease, and a change of tube type can restore high efficiency at higher frequencies.

Radomes suitable for operation in the millimeter-wave region were examined and it was found that radomes consisting of membranes supported by a random, triangular metal frame exhibit an acceptable low transmission loss (only 10 percent over a pass-band, which is selected by choosing a membrane thickness).

Multi-beam antennas such as phased arrays, reflectors, and lenses are discussed. Phased arrays are too heavy and too costly in the millimeter-wave band to be considered at all. The other approaches tend to result in high sidelobe levels. While suitable for acquisition, these antennas permit only limited data rates in the presence of interference. For communicating at high data rates, interfering sources can be rejected by adaptive pattern (null-forming) antennas and by signal-cancelling schemes. Alternatively, an antenna "farm" of conical, horn-fed, shielded parabolic single-beam antennas may be employed. These can produce far-out sidelobes which are 80 dB below the peak of the main beam (for main beam gains in excess of 40 dB).

ACKNOWLEDGMENTS

Sincere appreciation is extended to our Rand colleagues L. N. Rowell, who is the author of Section V, in which a number of satellite constellations are analyzed; W. Sollfrey, who is the author of the Appendix, which examines the size and shape of the beam footprint; E. Bedrosian and J. R. Clark, for their helpful suggestions and constructive review of this report; S. Katz, for contributions in Section IX regarding microwave tubes, radomes, and antennas; and R. R. Rapp, T. B. Garber, S. J. Dudzinsky, Jr., and P. A. CoNine for many valuable inputs.

The technical representative for the project within the Military Satellite Communications Systems Office of the Defense Communications Agency was Dr. Pravin C. Jain. The authors are indebted to him for numerous suggestions which improved the presentation of the results.

CONTENTS

SYMBOLS

A	atmospheric attenuation of communication signal, in dB
A_F	area of beam footprint on the surface of the earth
A_T	total system performance degradation caused by the atmosphere, in dB
B	depth of pivot point of communication beam beneath skin of aircraft
D, D_T, D_R	diameter of generalized antenna, of transmitting antenna, and of receiving antenna, respectively
D_{SL}, D'_{SL}	sidelobe acceptances, integrated over sidelobes which are pointed toward the earth and toward the sky, respectively
E_b	energy per information bit
f	carrier frequency used for communication
f_H, f_L	frequency at high and low ends, respectively, of the region of operation of an amplifier tube
G_F	gain of the first-stage amplifier
k	Boltzmann's constant, and a reference constant
L	signal loss factor due to atmospheric attenuation
L_c, L_L	loss factor in coupler and line, respectively
L_F	length of beam footprint on the earth
L_T	total system performance loss factor due to atmospheric attenuation and sky noise combined
M	system margin
N_0	noise power density
n	slope of line on logarithmic plot of tube efficiency as a function of frequency
R, R_w, $R_{w/o}$	data rate, data rate with atmosphere present, and data rate without atmosphere, respectively
S	slant range from terminal to satellite
T	atmospheric transmittance (from satellite to terminal)
T_a, T_c, T_L, T_g, T_F, T'_F	effective noise temperature of the absorbing medium in the atmsophere, the coupler, the line, the ground, and the first and second amplifier stages, respectively
T_{op}	the effective system operating temperature

T_{sky}, T'_{sky}	effective noise temperature of the portions of the sky which fall in the main beam and in the side-lobes, respectively
T_s	search time
t_d	stepping time of the beam from one search position to the next, including the dwell, transit, and settling times
W	width of opening in aircraft fuselage to accommodate communications beam
W_F	width of beam footprint on the earth
Δx_T, Δx_R	location errors of the transmitter and receiver, respectively
δ	angular width of communication beam, to 3-dB points
$\eta_{T'R}$	efficiencies of transmitting and receiving antennas, respectively
$\eta_{H,L}$	efficiency of a power tube at the high and low end, respectively, of its operating range
θ	angle of elevation of the satellite as observed from the terminal
θ_{min}	minimum value of θ
$\Delta\theta_x$, $\Delta\theta_y$	angular dimensions of the field of view which must be searched in the acquisition process, measured in the x- and y-directions, respectively
$\Delta\theta_{xp}$	x-component of the angular pointing error, introduced by errors in attitude reference, mechanical linkage, etc.
λ	wavelength of carrier signal
$\Delta\Omega$	solid-angular size of field of view which must be searched in the acquisition process
Ω_b	solid angle subtended by the main beam, to the 3-dB points

I. INTRODUCTION

The many attractive features that justify the consideration of frequencies above 8 GHz for military earth-satellite communications (MILSATCOM) systems have been examined in detail in two Rand study projects for the Defense Communications Agency. These higher frequencies offer relief from many of the problems faced by current MILSATCOM systems, which operate at UHF (225 to 400 MHz) and SHF (7 to 8 GHz), as discussed below.

ADVANTAGES OF HIGHER FREQUENCY OPERATION

The bandwidth available for MILSATCOM use in the lower frequency bands is inadequate, which has led to severe frequency management problems. Furthermore, these problems are apt to become much worse, because the demands for spectrum allocation are growing. At the higher frequencies considered in this study (20 to 265 GHz), the available bandwidth is larger than in the 7 to 8 GHz region by a factor ranging from 2 (in the 20 to 30 GHz band) to 30 (in the 250 to 265 GHz band). These wide regions are, moreover, presently unassigned. Wide-band data relay users typically require data rates of 10^7 to 10^8 bits per second (bps). Equipment operating at 10^9 bps and having an antijam capability has been demonstrated in the laboratory; if these users could be moved to the higher frequency bands, they would enjoy a greater available bandwidth, while leaving behind more room for mobile users.

Systems operating at UHF and SHF are probably susceptible to jamming by a determined enemy operating from a sanctuary. The narrower beams obtainable (with the same antenna size) at the higher frequencies greatly increase jam resistance and covertness and alleviate problems of interference.

Although obtained at the cost of weather-induced outages, the magnitudes of improvement at the higher frequencies are impressive. It is therefore important to carefully examine their feasibility in satellite communications systems, the purpose of the present study. A technology level is assumed that could be feasible during the next 10 to 30 years. Both fixed (wide-band data relay) and ground (ground transportable, ground vehicle, ship, and aircraft) users are considered.

Although weather-induced outages fall off rapidly with increasing aircraft altitude, the present study treats the worst case--the aircraft are assumed to be "on the deck."

ATMOSPHERIC EFFECTS

Because the primary factor in determining the feasibility of employing higher frequencies in satellite communications systems is the performance degradation associated with atmospheric effects (weather), much of our study has been devoted to this subject. Calculations were limited to the downlink, since this link usually limits system performance. The specific frequency bands considered are listed in Table 1.

Table 1

FREQUENCY BANDS USED TO DERIVE OUTAGE STATISTICS[a]

Type of User	Frequency (GHz)	
	Downlink	Uplink
Fixed (wide-band data relay)	20.2 - *21.2*	30 - 31
	102 - 105	92 - 95
	150 - *152*	140 - 142
	220 - 230	220 - 230
Mobile[b]	20.2 - *21.2*	
	30 - *31*	
	43 - *48*	
	95 - *101*	
	142 - 150	
	250 - *265*	

[a]The specific frequencies used in the computations are in italics.

[b]These mobile bands are not yet assigned to either uplink or downlink.

These bands are a subset of those allocated for satellite operation in Ref. 1 and are illustrative of those in the higher frequency region. The six italicized frequencies experience the most severe atmospheric degradation in their bands. For comparison, the performance at 8 GHz is also given.

ORGANIZATION OF THE REPORT

Section II describes a model that estimates the statistical distribution, at various frequencies and elevation angles, of the two weather-related factors limiting system performance: system operating temperature, which depends on the apparent sky temperature, and signal attenuation. The model is developed for one particular geographic location (Washington, D.C.), but could be extended to any location where appropriate weather statistics are available. The ability to predict performance degradation as a function of elevation angle is one of the strong points of the model; we know of no other model with this capability.

Section III applies the results of Section II to hypothetical communications systems suitable for serving small mobile users and estimates their performance statistics. In Section IV, similar consideration is given to systems tailored to the needs of wide-band data relay users. These statistics provide a basis for estimating the practical utility of the higher frequencies. Although the results apply only to the specific hypothetical systems selected, scaling to other parameter values, i.e., other systems, is a simple process. A discussion of tradeoffs between parameters is included in Section III.

Performance is a sensitive function of the angle of elevation to the satellite, especially at the higher frequencies, where performance degrades rapidly at low elevation angles because of increased atmospheric attenuation and sky noise. The avoidance of low elevation angles offers a number of other advantages. For example, refractive index anomalies, troublesome at low elevation angles, essentially disappear above 20 deg elevation. For all users, both the interference to and from other systems are greatly reduced. For military users, sidelobe detection and jamming by an enemy on or near the earth's surface are more difficult at other than low elevation angles. The avoidance of low elevation angles also alleviates a number of installation problems encountered by mobile users; thus, for example, obstruction of the beam by the superstructure of a ship is less troublesome at higher elevation angles. The antenna can be more deeply recessed into the user platform when low elevation angles are not required, reducing both the aerodynamic drag produced by radomes on aircraft and the size

of the silhouette presented by military vehicles. For users employing land-based stations, the line-of-sight obstruction produced at the horizon by buildings and terrain features is also reduced.

To avoid low elevation angles, geostationary orbits must be abandoned. The employment of inclined orbits has certain other advantages for military users: full earth coverage is achieved, interference between adjacent satellites (a hazard with closely spaced satellites in geostationary orbits) is reduced, and the difficulty of jamming the satellite from large jammers in sanctuaries is increased (because the jammer's antenna must now track the satellite).

These considerations led to the examination, reported in the first portion of Section V, of the elevation angle statistics of a wide range of satellite constellations with a view to determining, with each, the probability of there always being at least one satellite in view above a specified elevation. Then the number of satellites required to assure operation above any specified elevation angle can be calculated. Circular orbits at altitudes ranging from 10,000 n mi to 130,000 n mi (the limit of the stable cislunar region) as well as 24-hr and 96-hr elliptical orbits were examined.

The dimensions and area of the beam footprint on the earth are discussed and illustrated in Section VI; the mathematical details may be found in the Appendix.

Considerable attention is given throughout the report to the tradeoff among various system parameters. In Section VII, for example, the tradeoff between satellite complexity and user terminal complexity is examined. No attempt is made, however, to design an optimal system. Rather, we study the effect on system performance of varying certain parameters over regions of interest to test their limits. In selecting parameter values for small mobile users, we biased the choice in favor of simplifying the task of the user at the cost of increased satellite complexity. This bias is justified by the excellent performance record of many intricate satellites, which indicates that, when properly designed, high reliability can be achieved even by very complex satellites.[2] The acquisition problem is also briefly discussed in Section VII.

In estimating the feasibility of using higher frequencies for satellite communications, additional factors must be considered, some of which are addressed in Sections VIII through XII. Section VIII treats pointing and tracking problems. Section IX discusses the weight, size, and location constraints imposed by the characteristics of the user platform and its environment, and the restrictions imposed on the satellite equipment by the need for compatibility with the space shuttle. Special attention is paid to the prospects for producing high-efficiency, high-power amplifiers operating at the higher frequencies, since these components could dominate the weight and power requirements of the link. The availability of suitable radomes and antennas is also discussed. Section X treats the complexity, reliability, and lifetime of systems operating at higher frequencies, and Section XI reviews gaps in technology at the higher frequencies. The conclusions of the study are enumerated in Section XII.

II. ATMOSPHERIC EFFECTS

Atmospheric components, such as humidity, clouds, and rain, can degrade the performance of earth-to-satellite communications systems. This degradation is particularly troublesome at the higher microwave frequencies and has been one of the primary barriers to their employment. Accordingly, it is carefully examined in this feasibility study.

Atmospheric effects degrade performance in two ways: the communications signal is attenuated, and the operating or effective system noise temperature measured at the receiver input is increased because the apparent sky temperature is higher. In this section, a model is developed for generating the probability distribution of both the atmospheric attenuation and the total system degradation, including the effects of sky noise. Although the model is for Washington, D.C. weather, it could be extended to any geographic region for which suitable weather data are available.

WEATHER MODEL

The weather model for Washington, D.C. described in Ref. 3 is adapted as an input to our weather degradation model. The essential features of the modified weather model are presented in Table 2; all atmospheric conditions occurring in Washington, D.C. are grouped into nine categories having well-defined physical characteristics, and a specific condition is selected to represent each category. The cloud types in this table have been converted from those that would be reported by an observer to the corresponding Deirmendjian "C-1" and "C-5" models (see Refs. 4 and 5). The cloud thicknesses are nominal values, as are the thicknesses of the rain layers. The rainfall rates are approximately upper and lower quartile daily rates. The last column of Table 2 estimates the annual probability of occurrence, by hour, of the various atmospheric conditions. It is based on 11 years of data gathered at the Washington, D.C. National Airport. The probability of clear-to-scattered clouds was estimated at 40 percent, based on hourly reports of less than four-tenths of the sky being obscured by clouds. This 40 percent was assumed equally divided between "clear" and "C-1

plus humid atmosphere," with the clear portion being equally divided between "low," "medium," and "high" humidity.

Table 2

WEATHER MODEL FOR WASHINGTON, D.C.

Atmospheric Condition	Probability of Occurrence
Clear	
Dry	0.066
Medium humidity	0.067
Humid	0.067
Cloudy-plus-humid	
C-1 (0.1 km thick) plus humid atmosphere	0.20
C-5 (1.5 km thick) plus humid atmosphere	0.48
Rain	
R-1, 1 mm/hr (2 km thick) plus C-5 (3 km) plus humid atmosphere	0.04
R-2.5, 2.5 mm/hr (3 km thick) plus C-5 (4 km) plus humid atmosphere	0.04
R-10, 10 mm/hr (3 km thick) plus C-5 (4 km) plus humid atmosphere	0.035
R-50, 50 mm/hr (3 km thick) plus C-5 (4 km) plus humid atmosphere	0.005

Precipitation (rain, drizzle, and snow combined) occurred approximately 12 percent of the time. Snow was ignored on the basis of its low frequency of occurrence in Washington. Hourly rain rate data were divided into four classes (R-1, R-2.5, R-10, and R-50). The remaining 48 percent was assigned to the broken clouds and overcast category, described as "C-5 plus humid atmosphere."

This type of breakdown can only roughly approximate the probability of occurrence (cumulative duration) of weather states hindering propagation.

Zenith Attenuation Produced by Selected Atmospheric Conditions

The attenuation produced by the cloud types and rain rates specified in Table 2 has been calculated as a function of frequency by Deirmendjian.[4,6] Measured data on the attenuation produced by the three

humidity conditions of Table 2, at various frequencies and elevation angles, were gathered by Meyer,[7] who summarized all available data concerning clear air attenuation through the entire atmosphere.

Using the Deirmendjian and Meyer data, the attenuation resulting from each of the atmospheric conditions in Table 2 was calculated. The results, shown in Table 3, are zenith attenuations at the frequencies of interest. The last column in Table 3, obtained with the aid of the last column in Table 2, indicates the probability that the various attenuation values are exceeded.

Table 3

CALCULATED ZENITH ATTENUATION (in dB) THROUGH THE ENTIRE ATMOSPHERE RESULTING FROM SELECTED WEATHER CONDITIONS

Atmospheric Condition[a]	Frequency (GHz)							Probability Attenuation Is Exceeded
	15	21.2	31	48	101	152	265	
Clear								
Dry	0.1	0.5	0.22	1.05	0.92	0.64	0.85	0.93
Medium humidity	0.1	0.5	0.22	1.05	1.2	1.12	2.55	0.87
Humid	0.1	0.5	0.22	1.05	1.8	1.4	4.2	0.80
Cloudy-plus-humid								
C-1	0.1	0.5	0.23	1.06	1.83	1.46	5.2	0.60
C-5	0.26	0.77	0.80	2.08	4.1	5	12	0.12
Rain								
R-1	0.44	1.1	1.6	3.85	8	10.4	21.2	0.08
R-2.5	0.59	1.4	2.7	6.55	13.8	17.4	31.2	0.04
R-10	1.6	3.3	7.3	15.5	35.8	40.4	53.2	0.005
R-50	8.0	16	37	64	87	87	93	0[b]

[a] These conditions are described in greater detail in Table 2.

[b] In a treatment of lower communication frequencies, it would be necessary to break the "R-50" category into a number of subdivisions, extending to much higher rain rates, since these are the main cases of interest at lower frequencies. With the higher frequencies considered here, however, outages may be induced by light rain or even by heavy clouds; accordingly, it is adequate for our present purposes to represent all heavy rain by the single category, R-50. (Note that there is no higher category here.)

Sky Noise Temperature

At frequencies above 2 GHz, cosmic noise can be neglected;[8] the effective sky noise arises from thermal emission from atmospheric

constituents. It has been suggested that the sky noise temperature, T_{sky}, be expressed as[8-10]

$$T_{sky} = T_a(1 - T) = T_a(1 - 1/L) = T_a\left[1 - 10^{-A/10}\right], \quad (1)$$

where T is the atmospheric transmittance, L is the atmospheric loss factor, A is the atmospheric attenuation in dB, and T_a is the apparent absorber temperature. References 8-10 indicate that T_a is about 280°K at 16 GHz and falls to 270° to 275°K at 30 GHz. In general, the value of T_a decreases slowly with increasing frequency.

ATTENUATION STATISTICS

The calculated attenuation distribution in Table 3 and the available experimental attenuation distribution data for roughly the same climatic area and frequency were combined to evolve the attenuation model used in Sections III and IV. To accomplish this, both the calculated distributions and the measured distributions were combined on one graph.

Figure 1 shows the results obtained in the 30 to 35 GHz region. The solid circles in each case indicate the estimated cumulative zenith attenuation probability at Washington, D.C. These points were obtained from Table 3; each point, at increased attenuation, reflects an increasingly inclement atmospheric condition. The other data points represent the best available experimental measurements made in the same general geographic region at these frequencies. The crosses represent the cumulative attenuation probability observed by Wilson[11] and Ruscio* at Crawford Hill, New Jersey, during the period from December 8, 1967, to February 28, 1969, using a sun tracker at 30 GHz. Data were averaged over all elevation angles greater than 5 deg. The squares in Fig. 1 represent the results of Henry,[12] acquired during the period from August 1972 to August 1973; the sun tracker at Crawford Hill was again employed and, again, data were averaged over all elevations above 5 deg.

The data points indicated by open circles in Fig. 1 show attenuation calculated from the radiometer measurements of Wulfsberg,[13]

*Ruscio, J. T., *Attenuation Statistics on Earth-Space Path at 16 and 30 GHz Using the Crawford Hill Sun Tracker*, The Bell Telephone Company Laboratories, May 21, 1969 (unpublished).

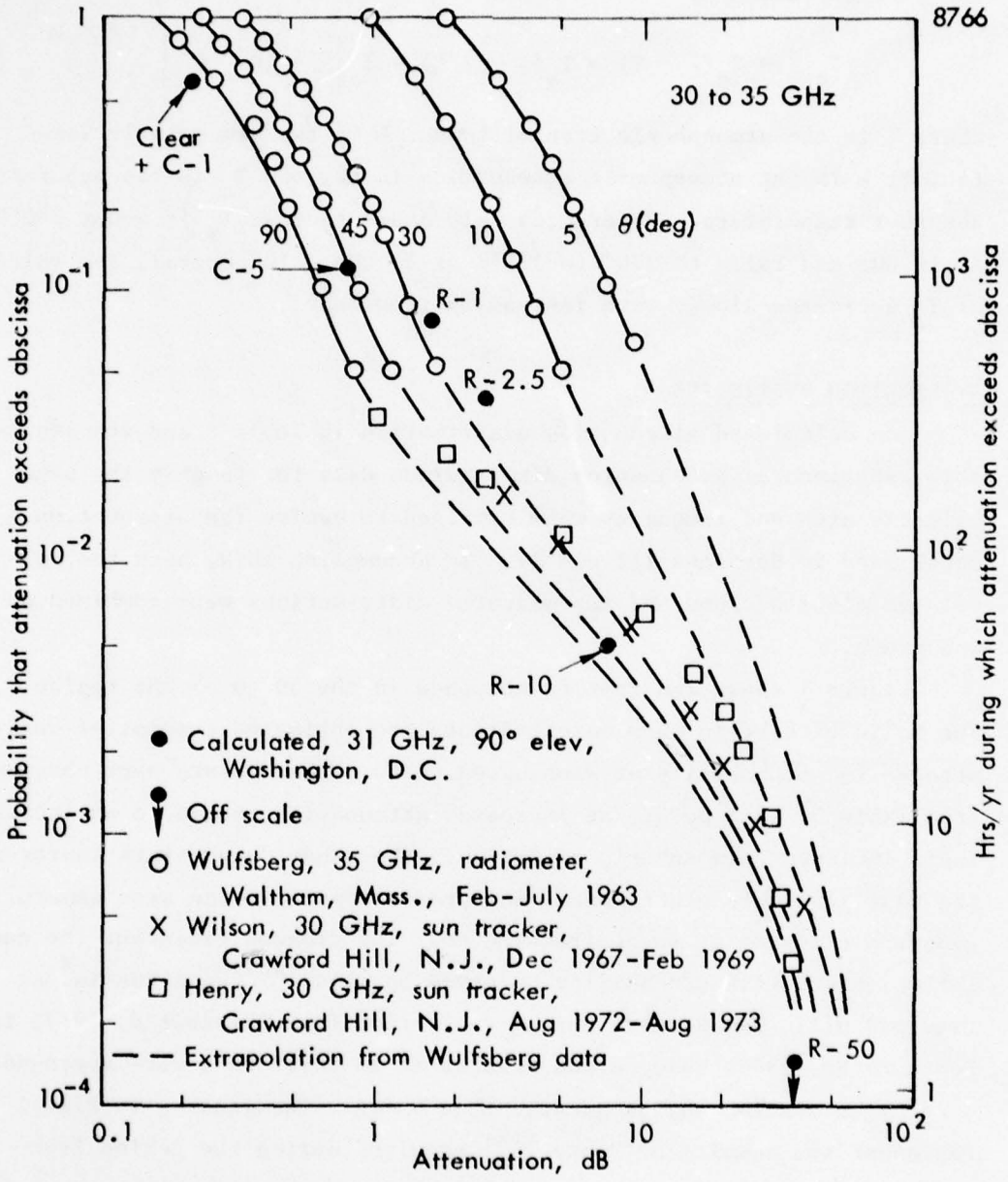

Fig. 1—Comparison of calculated and measured cumulative probability distribution of attenuation through the entire atmosphere at 30 to 35 GHz

made at Waltham, Massachusetts, during the period extending from February to July 1963. We used Eq. (1) to convert Wulfsberg's reported sky temperature data to attenuation; in this calculation, we arbitrarily assumed a value of 275 deg for the apparent absorber temperature T_a. The assumption of any other reasonable value for T_a would have had little effect on the results. Wulfsberg's measurements were made at 35 GHz and reported as a function of elevation angle. The attenuation was found to be very nearly proportional to the cosecant of the elevation angle, indicating horizontal stratification of the attenuating components (atmospheric molecules, overcast, and light rain) at the relatively low attenuation values amenable to passive radiometric determination.

Figure 2 presents similar data for the 15 to 16 GHz region. Again, the observations of Wulfsberg indicate that the cosecant law is closely followed at relatively low values of attenuation. The triangles in this figure refer to attenuation measurements by Ippolito,[14] using a beacon onboard the ATS-5 satellite as a radiation source. These measurements were made at an elevation angle of 42 deg--the satellite elevation from Rosman, North Carolina--and averaged over the entire calendar year 1970.

It is seen from Figs. 1 and 2 that the calculated attenuation statistics obtained from Table 3, represented by the solid circles in the figures, agree reasonably well with the measured values. The agreement is, in fact, suspiciously good, considering the differences in frequency, measurement technique, geographic location, and time period.

As mentioned above, the cosecant law is followed by the Wulfsberg data, which were acquired at relatively low values of attenuation. This dependence on the cosecant of the elevation angle is to be expected because the attenuation is caused by humidity, clouds, and light rain, which all can be reasonably expected to be horizontally stratified. At very high rain rates, however, a considerable vertical cloud buildup (e.g., thunderhead) is usually observed, so that high attenuation will occur at high elevation angles. Thus, the attenuation due to high rain rates is expected to be less sensitive to elevation angles, causing the curves representing different elevation angles to draw together at high values of attenuation. This was borne in mind when

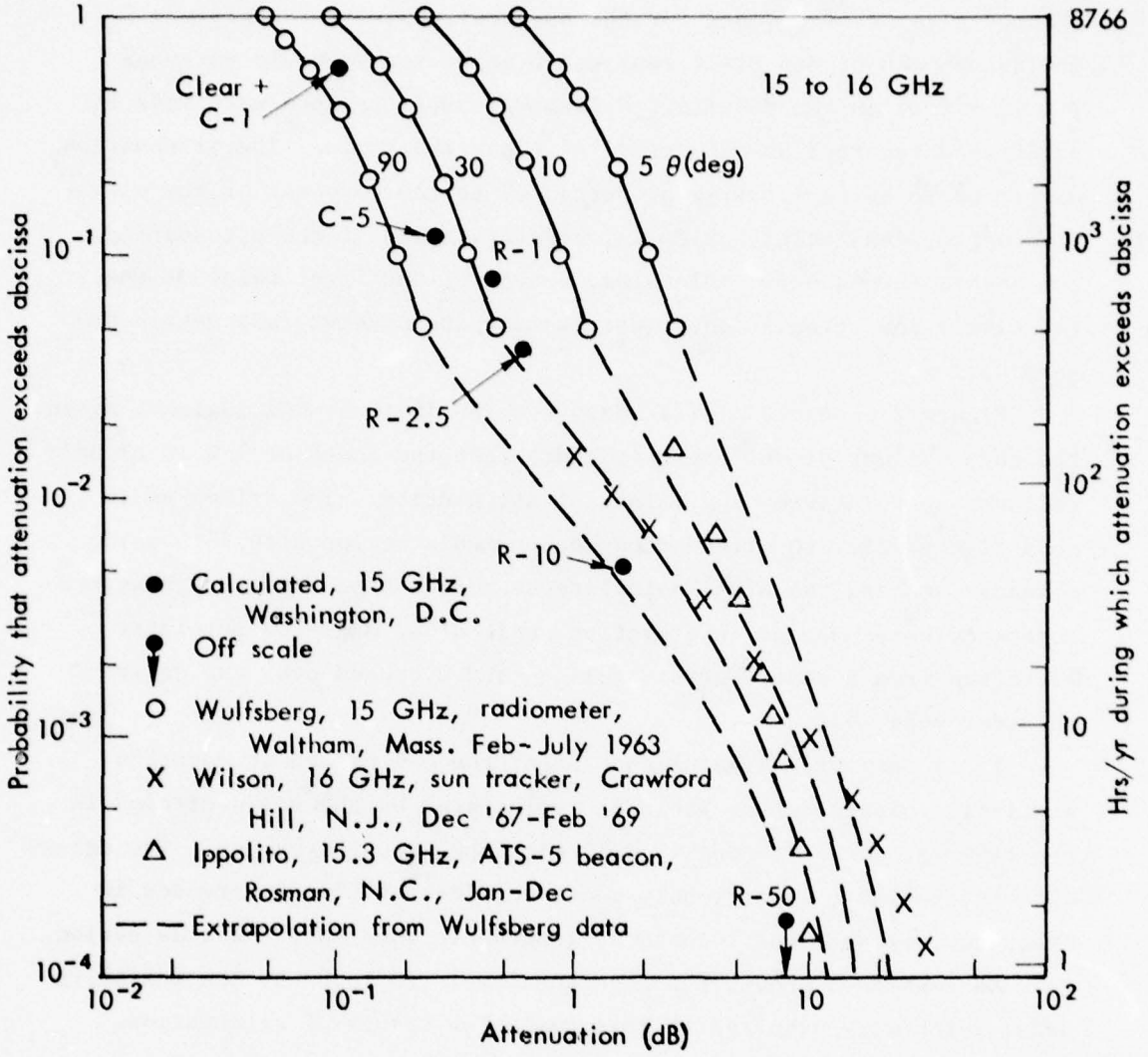

Fig. 2 — Comparison of calculated and measured cumulative probability distribution of attenuation through the entire atmosphere at 15 to 16 GHz

drawing the dashed lines in the figures, which represent a "best guess" extrapolation of the Wulfsberg curves to higher attenuations, with guidance being provided by the measurements of Wilson, Henry, and Ippolito, and the calculated points. The combination of the Wulfsberg curves and their extension represents the attenuation model for Washington, D.C. at 15 to 16 GHz and 30 to 35 GHz. No suitable measured data are available at higher frequencies; the attenuation estimates had to be made solely on the basis of the calculated values. Thus, the solid circles were first plotted for each frequency using the data in Table 3. Using these points and the known trends at lower frequencies from Figs. 1 and 2 as a guide, "best guess" curves were sketched in, representing the best estimate of the attenuation statistics at each elevation angle. These curves are shown as solid lines in Figs. 3 through 8. (The dashed curves in these figures, together with the associated notation "uncooled paramp 2000," will be discussed later in this section.) Table 4 gives the calculated values of A and T_{sky} for a few values of cumulative probability and for the values of frequency (f) and elevation angle (θ) at which link outage statistics are calculated in Sections III and IV.

The procedure used to build this model for estimating attenuation statistics is highly subjective and should be used with caution. Until more data become available, however, we must resort to procedures such as the one used here.* It is recommended that in the future statistical attenuation data be acquired as a function of frequency and elevation angle. The need for such data is so obvious that the neglect in acquiring it is quite surprising.

TOTAL PERFORMANCE DEGRADATION STATISTICS

In addition to attenuating the signal, the atmosphere degrades system performance by increasing the effective system noise temperature or operating temperature T_{op}. Measured at the input to the ground-based, low-noise amplifier, T_{op} can be expressed by the relation:[15]

*If the Bell Telephone Laboratories sun tracker data had been sorted into elevation bins, we would have a better validation of the model.

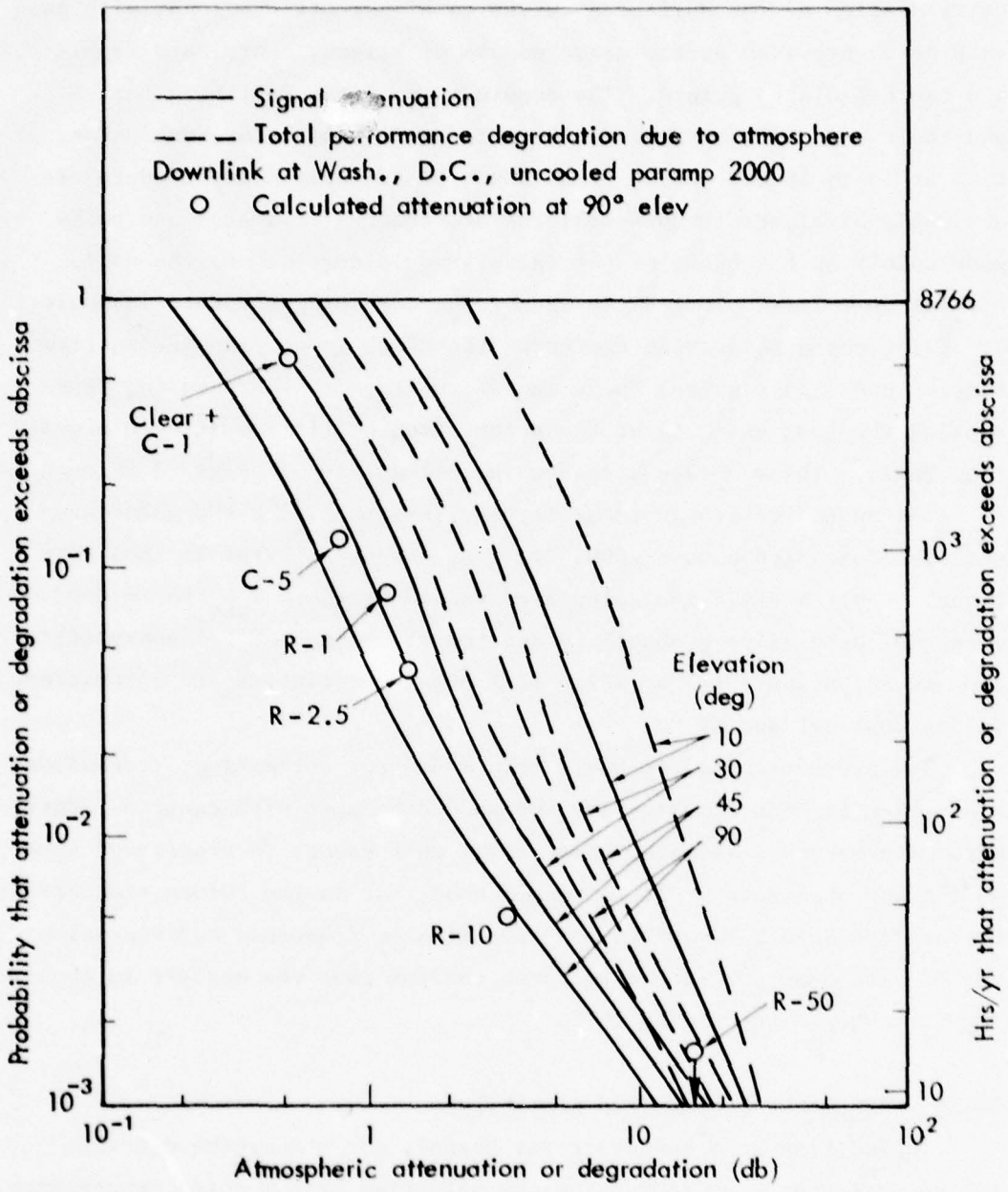

Fig. 3—Estimated cumulative probability distribution of attenuation and system performance degradation due to atmospheric effects at 21.2 GHz

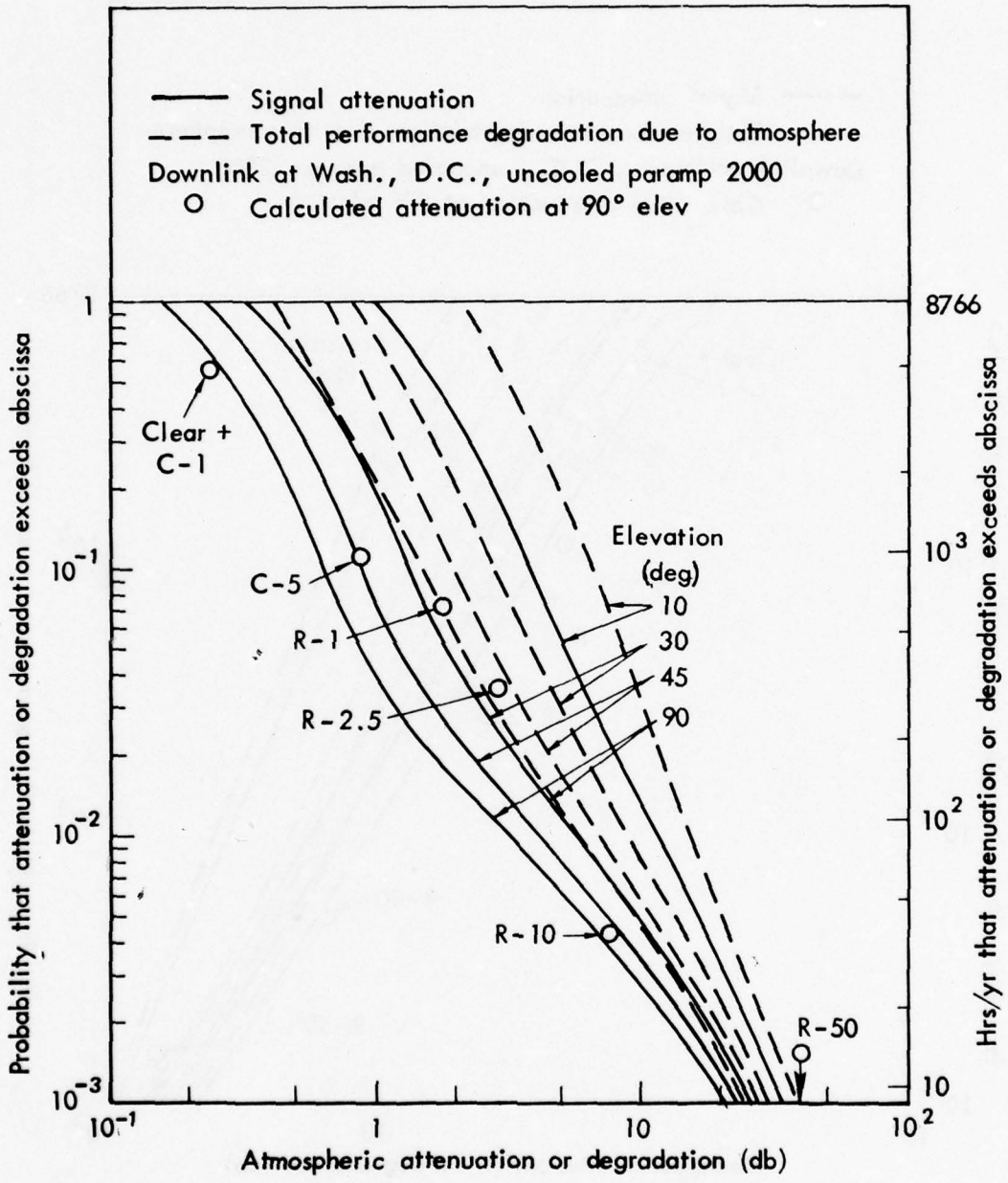

Fig. 4— Estimated cumulative probability distribution of attenuation and system performance degradation due to atmospheric effects at 31 GHz

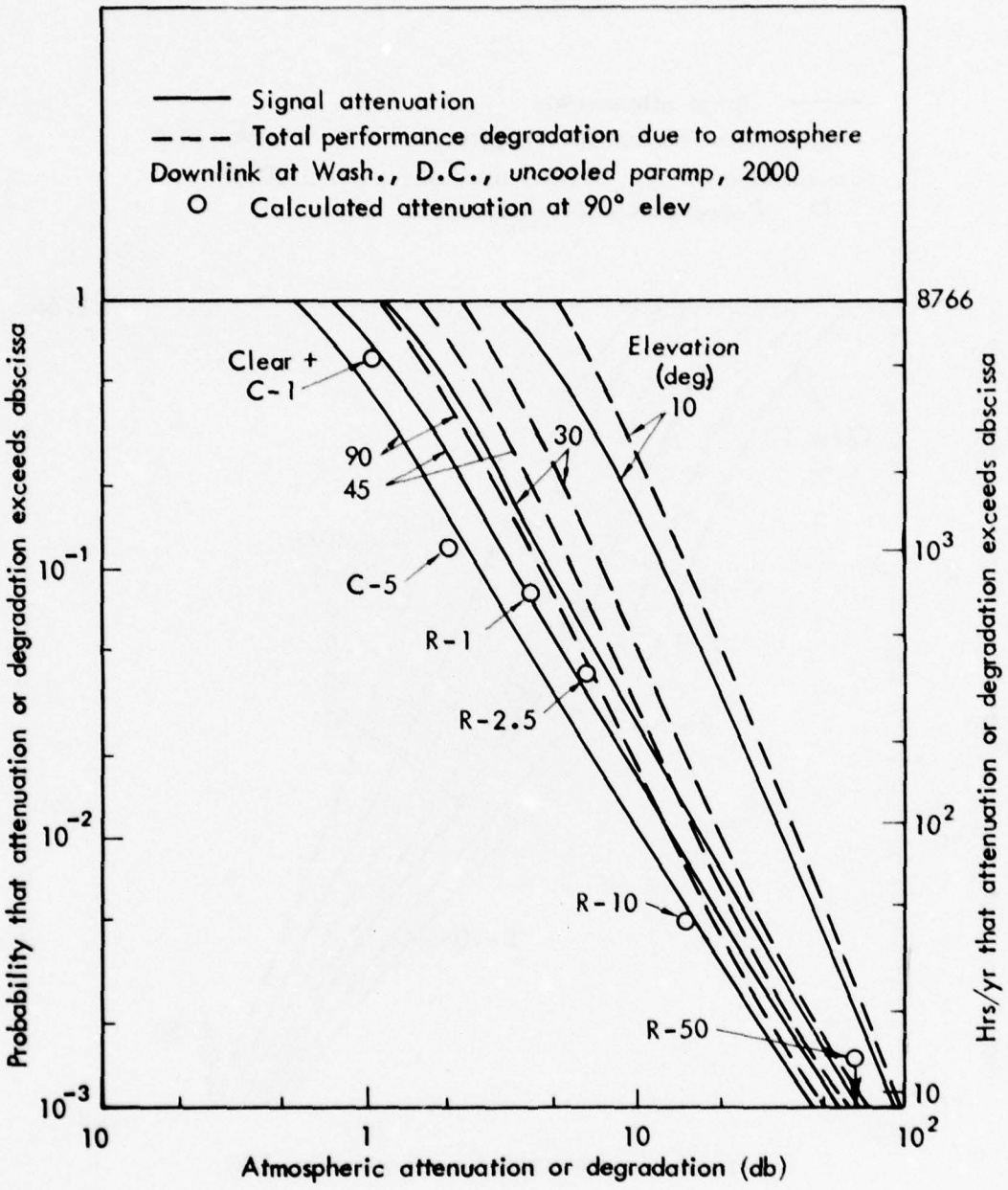

Fig. 5 — Estimated cumulative probability distribution of attenuation and system performance degradation due to atmospheric effects at 48 GHz

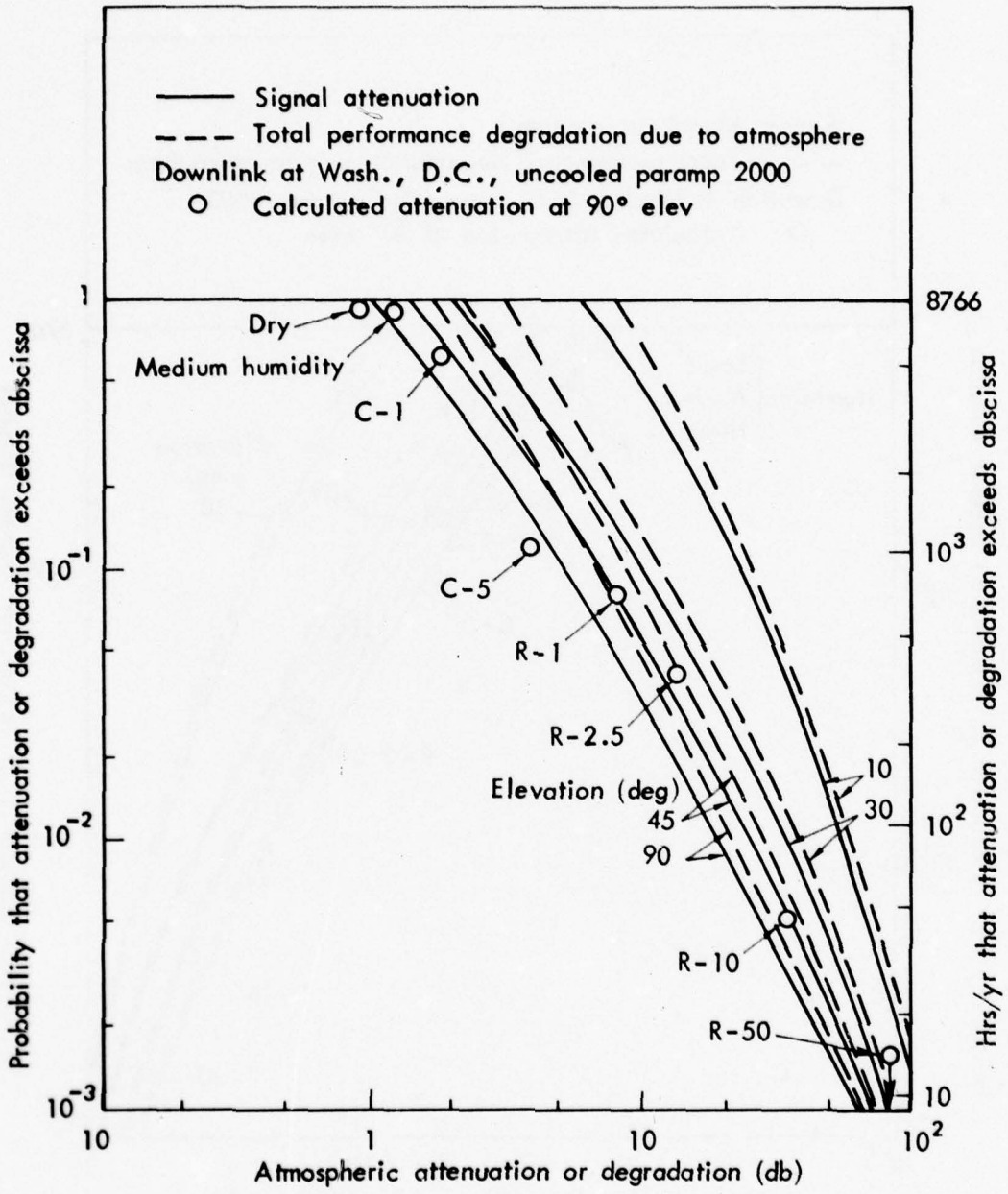

Fig. 6—Estimated cumulative probability distribution of attenuation and system performance degradation due to atmospheric effects at 101 GHz

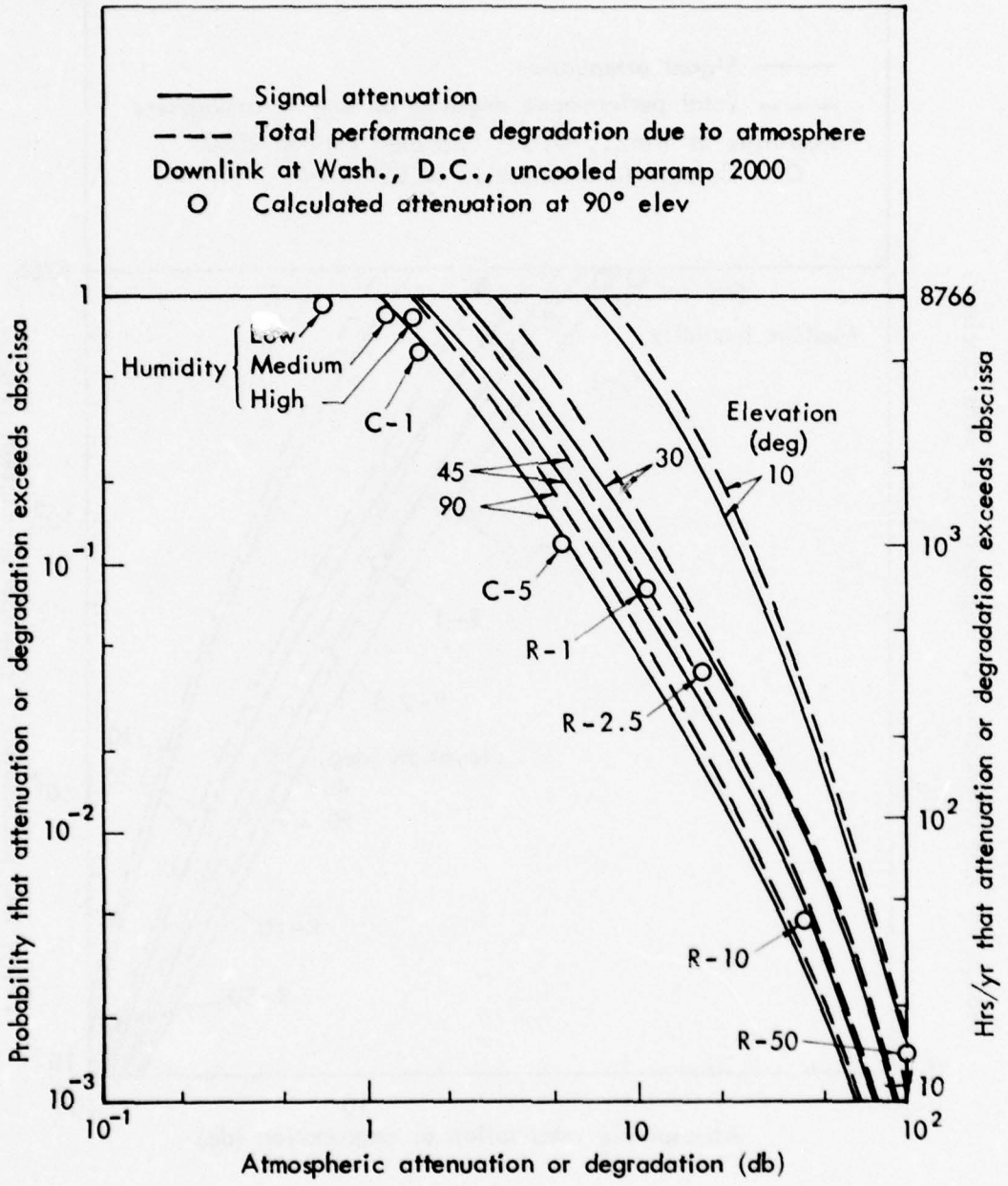

Fig. 7—Estimated cumulative probability distribution of attenuation and system performance degradation due to atmospheric effects at 152 GHz

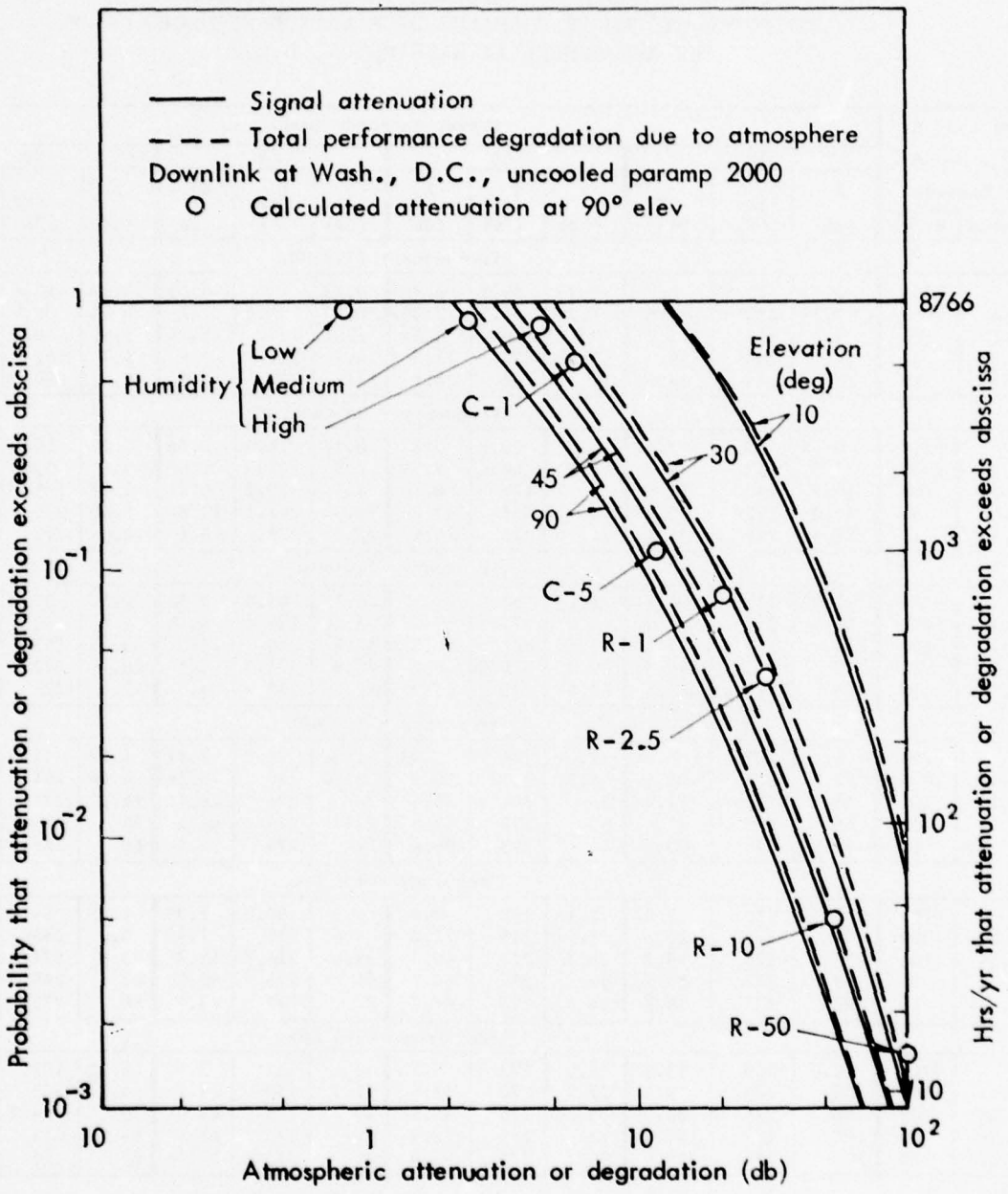

Fig. 8— Estimated cumulative probability distribution of attenuation and system performance degradation due to atmospheric effects at 265 GHz

Table 4

STATISTICS OF ATMOSPHERIC ATTENUATION, SKY TEMPERATURE, AND TOTAL SYSTEM PERFORMANCE DEGRADATION PRODUCED BY THE ATMOSPHERE AT WASHINGTON, D.C.[a]

Time that A, T_{sky}, and A_T are Exceeded		Elevation Angle (deg)											
		10			30			45			90		
Percent	hr/yr	A (dB)	T_{sky} (°K)	A_T (dB)	A (dB)	T_{sky} (°K)	A_T (dB)	A (dB)	T_{sky} (°K)	A_T (dB)	A (dB)	T_{sky} (°K)	A_T (dB)
Frequency = 21.2 GHz													
100	8766	0.92	52.5	2.24	0.33	20.1	0.88	0.23	14.2	0.63	0.17	10.6	0.54
11.4	1000	3.52	153	6.6	1.24	68.3	2.89	0.9	51.5	2.2	0.61	35.9	1.56
1.14	100	9	240	13.2	3.3	146	6.29	2.61	124	5.26	1.92	98.3	4.13
0.34	30	14.7	266	19.2	7.5	226	11.5	6.1	207	9.9	4.7	182	8.2
0.114	10	23	273	27.6	16	268	20.5	13.2	262	17.6	10.4	250	14.7
Frequency = 31 GHz													
100	8766	0.94	53.5	2.10	0.34	20.7	0.82	0.27	16.6	0.66	0.17	10.6	0.42
11.4	1000	3.5	152	6.2	1.2	66.4	2.59	0.8	46.3	1.82	0.6	35.5	1.4
1.14	100	10.5	250	14.4	5	188	8.16	3.5	152.2	6.21	2.80	131	5.22
0.34	30	19.0	272	23.1	13	261	17.0	10.0	247.5	13.8	8.40	235	12.1
0.114	10	32.0	275	36.1	24	273	28.1	22.0	273.2	26.1	19.0	272	23.1
Frequency = 48 GHz													
100	8766	3.05	139	5.17	1.1	61.5	2.17	0.75	43.6	1.53	0.53	31.6	1.11
11.4	1000	11.6	256	15.0	4.47	177	7.03	3.26	145	5.46	2.4	117	4.25
1.14	100	34	274.9	37.5	15.8	268	19.3	12.6	260	16.0	9.65	245	12.9
0.34	30	57	275	60.5	32.3	274.8	35.8	25.8	274.3	29.3	20.5	272.5	24.0
0.114	10	86	275	89.5	62.4	275	65.9	52	275	55.5	42.4	275	45.9
Frequency = 101 GHz													
100	8766	6.1	207.5	8.0	2.0	101	3.03	1.38	74.9	2.17	1.02	57.6	1.64
11.4	1000	22.2	273.3	24.6	8.8	239	10.9	6.24	210	8.16	4.64	181	6.34
1.14	100	55.5	275	57.9	34	274.9	36.4	24	274	26.4	18.2	271	20.5
0.34	30	81	275	83.4	55	275	57.4	43.8	275	46.2	36	274.9	38.4
0.114	10	97.6	275	100	84	275	86.4	72	275	72.4	60	275	62.4
Frequency = 152 GHz													
100	8766	6.3	211	7.62	2.16	108	2.89	1.5	80.3	2.05	1.05	59.1	1.46
11.4	1000	24.5	274	26.2	9.5	244	11.0	6.6	215	7.95	5.0	188	6.20
1.14	100	57.5	275	59.2	38.7	275	40.4	29.6	274.7	31.3	23.8	274	25.5
0.34	30	79	275	80.7	59	275	60.7	51	275	52.7	43.5	275	45.2
0.114	10	98	275	99.7	86	275	87.7	72	275	73.7	60	275	61.7
Frequency = 265 GHz													
100	8766	12.6	260	13.5	4.5	177	5.13	3	137	3.49	2.15	107	2.54
11.4	1000	45	275	45.9	17.7	270	18.6	12.3	259	13.2	9.3	243	10.14
1.14	100	88	275	88.9	53	275	53.9	40	275	40.9	30	274.7	30.9
0.34	30	105	275	105.9	72	275	72.9	62	275	62.9	46	275	46.9
0.114	10	125	275	125.9	95	275	95.9	82	275	82.9	65	275	65.9

[a]Assuming the "uncooled paramp 2000" amplifier noise temperature in Table 5.

$$T_{op} = \frac{T_{sky}}{L_c L_L} + \frac{T_g D_{SL}}{L_c L_L} + \frac{T'_{sky} D'_{SL}}{L_c L_L} + \frac{T_c\left(1 - 1/L_C\right)}{L_L}$$

$$+ T_L\left(1 - \frac{1}{L_L}\right) + T_F + \frac{T'_F}{G_F} , \qquad (2)$$

where

T_{sky} and T'_{sky} = effective sky temperatures inside and outside the main beam, respectively

T_g, T_c, and T_L = effective temperatures of ground, coupler, and line, respectively

L_c and L_L = losses in the coupler and line, respectively

D_{SL} and D'_{SL} = sidelobe acceptances, integrated over the sidelobes which are pointed toward the earth and toward the sky, respectively

T_F and T'_F = equivalent noise temperatures of the first- and second-stage amplifiers, respectively

G_F = gain of the first-stage amplifier.

In preparation for using T_{op} in the calculation of the communication data rate, this expression will be simplified by assigning "typical values" to some of its component parameters. Thus, a value of 290°K is assigned to T_g, the ground temperature. Since, for all mobile users, an uncooled parametric amplifier (paramp) is assumed, the coupler and line will not be cooled, and the same temperature will be assigned to T_c and T_L. The difference between T_{sky} and T'_{sky} will be neglected. The total acceptance of all sidelobes, D_{SL} and D'_{SL}, is often assumed to be unity. With proper design, however, one can easily achieve a value of 0.1. In fact, values lower than 10^{-4} have been realized.[16] In the present analysis, a "middle-ground" value of 0.1 is chosen. Assuming, further, that the sidelobes are isotropically distributed, we have $D_{SL} = D'_{SL} = 0.05$. A value of 1.12 (0.5 dB) is assigned to L_c, and 1.05 (0.2 dB) to L_L. The last term, T'_F/G_F, is assumed to be negligible relative to T_F. This will usually be the case when G_F exceeds 30 dB or so. Making these assumptions, Eq. (2) reduces to

$$T_{op} = 0.89\ T_{sky} + T_F + 56.3°K\ , \qquad (3)$$

where the first term is the "reduced" sky noise as viewed through the attenuating line and coupler; the second term is the front end noise; and the third term is the sidelobe, line, and coupler noise.

The noise temperature of the first-stage amplifier, T_F, depends on the frequency and is expected to decrease as electronic technology advances. Figure 9, adapted from Ref. 17, gives a summary of the performance of low-noise devices available in 1975, and an estimate of the performance which may be available in the year 2000. The devices represented include: bipolar transistors, tunnel diode amplifiers (TDA), field-effect transistors (FET), mixers followed by an IF amplifier (Mixer-IF), parametric amplifiers, and masers. Both uncooled and cooled (to 17°K) parametric amplifiers are included. In the present analysis, the amplifier performance indicated by the curve designated "Uncooled paramp 2000" is assumed for small mobile users. This assumption represents a compromise between the relatively poor performance of FETs, TDAs, and bipolar transistors, and the relatively costly cooled paramps and masers. Two choices are assumed for wide-band data relay users: "uncooled paramp 2000" or "cooled paramp 2000." The performance of the selected amplifiers has been extrapolated (from that in Ref. 17) to 265 GHz, as indicated by the dotted lines in Fig. 9. Table 5 indicates the specific amplifier noise temperatures assumed at the various frequencies in the present study; the values were obtained from Fig. 9.

Table 5

ASSUMED AMPLIFIER NOISE TEMPERATURES

Frequency (GHz)	Temperature (°K)	
	Uncooled	Cooled
8	49.2	13.5
21.2	75.4	17.5
31	100	20.6
48	140	24.6
101	280	35.9
152	470	48.0
265	960	75.7

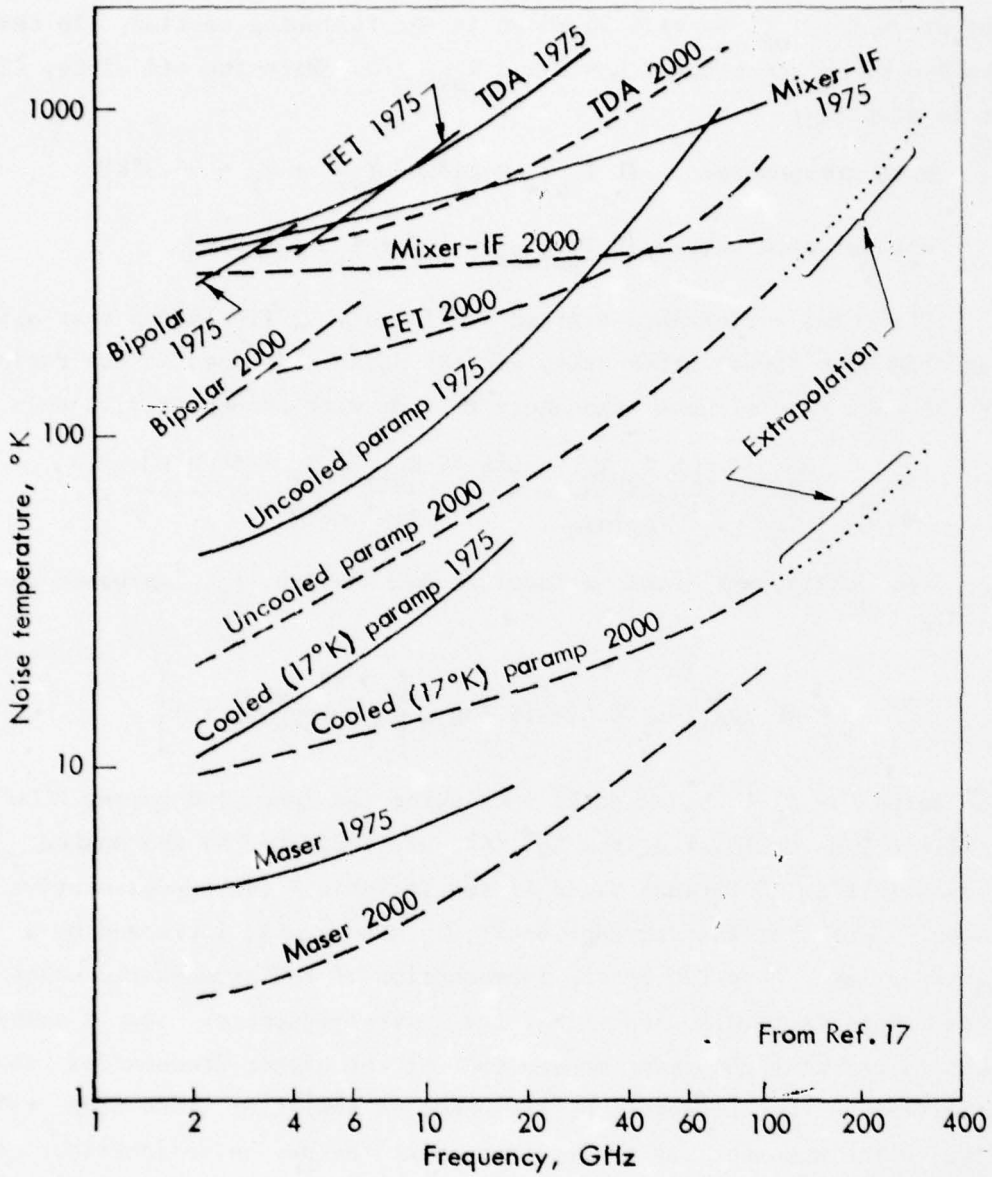

Fig. 9— Device noise temperature as a function of frequency (extrapolated above 100 GHz)

The communications data rate, R, is inversely proportional to the product $L\ T_{op}$, as will be shown in the following section. In the absence of an atmosphere, $L = 1$ and $T_{sky} = 0$. With the aid of Eq. (3), it is seen that

$$\text{with atmosphere:} \quad \left(L\ T_{op}\right)_w = L\left(0.89\ T_{sky} + T_F + 56.3°K\right)$$

$$\text{without atmosphere:} \quad \left(L\ T_{op}\right)_{w/o} = 1\left(0 + T_F + 56.3°K\right) .$$

The total performance degradation factor, L_T (including that arising from both signal attenuation and sky noise), defined as the ratio of the data rate without atmosphere to that with atmosphere, is then

$$L_T = \frac{R_{w/o}}{R_w} = \frac{\left(L\ T_{op}\right)_w}{\left(L\ T_{op}\right)_{w/o}} = \frac{L\left(0.89\ T_{sky} + T_F + 56.3°K\right)}{T_F + 56.3°K} .$$

Correspondingly, the total performance degradation, A_T, expressed in dB, is

$$A_T = 10\ \log_{10} L_T = A + 10\ \log_{10}\left[\frac{0.89\ T_{sky}}{T_F + 56.3°K} + 1\right] . \qquad (4)$$

The values of A_T to be expected when using the "uncooled paramp 2000" amplifier, as calculated from Eq. (4), are indicated by the dashed curves in Figs. 3 through 8 and listed in Table 4 for representative cases. Note that the degradation is, in some cases, increased by a factor greater than two by the introduction of the atmospheric noise term. This factor is greatest at the lower frequencies, and is somewhat larger at high elevation angles. At the higher frequencies, the amplifier noise temperature of the uncooled amplifier is so high, relative to the apparent sky temperature, that the sky noise contribution becomes much smaller. Knowing A_T, the value of $L\ T_{op}$ used in calculating the data rate, R, is conveniently given by

$$L\ T_{op} = 10^{A_T/10}\left(T_F + 56.3°K\right) , \qquad (5)$$

when the "uncooled paramp 2000" is used.

III. ESTIMATION OF LINK OUTAGE STATISTICS FOR SMALL MOBILE USERS

To assess the feasibility of employing higher frequencies, the cumulative probability of link outage is calculated as a function of data rate for a hypothetical digital satellite downlink. A link aimed at meeting the needs of the small mobile user will be considered first; a link to a wide-band data relay user is examined in the following section. An outage is assumed to occur when the ratio of E_b, the received energy per bit, to N_0, the average receiver noise power density, falls below the preselected value while the system is operating at the indicated data rate. In this calculation, the assumed value of the total downlink degradation due to atmospheric effects is represented by the dashed curves in Figs. 3 through 8; other parameters are assigned "typical" values to illustrate the performance of a link representative of future communications systems.

The link performance equation can be written:[15]

$$R = \frac{\pi^2 P_T \eta_T \eta_R D_T^2 D_R^2}{16\, k\, (E_b/N_0)\, \lambda^2\, M\, S^2\, T_{op}\, L\, L_c\, L_L}, \tag{6}$$

where the slant range, S, is given by

$$S = \left(R_e \sin^2 \theta + 2 R_e H + H^2\right)^{\frac{1}{2}} - R_e \sin \theta . \tag{7}$$

The atmospheric loss factor, L, is given by the relation

$$L = 10^{A/10},$$

where, as before, A is the atmospheric attenuation in dB. The definitions of the symbols, together with the values assigned to them, are presented in Table 6. These parameter values are subsequently used in estimating outage statistics.

Equation (4) applies equally well to the uplink. However, a number of the parameter values are likely to be quite different in the uplink case. For example, the transmitted power, P_T, of a small mobile terminal may be 10 to 100 times greater than that of the satellite (and

Table 6

DOWNLINK PARAMETERS FOR SMALL MOBILE USERS

Symbol	Definition	Units	Assumed Value
R	Data rate	bits/sec	(a)
P_T	Transmitted power	W	10
η_T, η_R	Efficiency of transmitting, receiving (parabolic) antennas	None	0.56
D_T	Diameter of transmitting antenna	m	4.4
D_R	Diameter of receiving antenna	m	0.1
k	Boltzmann's constant	$Wsec°K^{-1}$	1.38×10^{-23}
E_b/N_0	Ratio of energy per bit to noise power density	bit^{-1} [b]	10
λ	Carrier wavelength	cm	(c)
M	System margin	None	8 dB
S	Slant range from satellite to terminal	n mi	(d)
T_{op}	Effective system noise temperature	°K	(e)
L	Atmospheric attenuation loss factor	None	(f)
L_c	Coupler loss	None	0.5 dB
L_L	Line loss	None	0.2 dB
R_e	Radius of the earth	n mi	3441
H	Satellite altitude	n mi	30,000
θ	Elevation angle to satellite at terminal	deg	(g)

[a] Dependent variable.

[b] E_b/N_0 = (joules/bit)/(watts/Hz) = bit^{-1}.

[c] λ(cm) = 30/f, where f = 2i.2, 31, 48, 101, 150, and 256 GHz.

[d] See Eq. (7).

[e] See Eqs. (2) and (3).

[f] See Table 4, $L = 10^{A/10}$.

[g] 10, 30, 45, and 90 deg.

therefore the uplink system margin will be greater). If demodulation and remodulation are used in the satellite, the type of modulation, the modulation index, and the type of error correction coding can all differ on the up and down link. Even the data rate can be different due to onboard processing, such as multiplexing signal streams which originate on different uplink beams. In addition, on the uplink, T_{op} must be modified to reflect the fact that the main beam of the receiver is directed at the earth rather than at the sky. Thus, the first term in Eq. (3), $T_{sky}/L_c L_L$, must be replaced by $T_{earth}/L_c L_L$--a considerably larger quantity. Although the second term will be somewhat reduced, and the third term will be greatly reduced because the far sidelobes of the satellite antenna are directed at space, the increase in the first term will dominate, resulting in a net increase in T_{op}. The resulting degradation in performance is likely, however, to be more than offset by the increase in transmitted power. Accordingly, the uplink does not usually limit system performance, and only the downlink will be considered in the present analysis.

CONSTANT ANTENNA DIAMETER

A transmitting antenna diameter of 4.4 m is assumed. This is the largest size that can be accommodated by the space shuttle without folding. A mirror reflector of this size is being designed by Hughes Aircraft Company for NASA.[18] It is designed to operate at 193 GHz, have an rms surface roughness of 0.0017 in., and an overall aperture collection efficiency of 0.66. The calculated 3 dB beamwidth is 0.026 deg. The beamwidth and efficiency correspond to a gain of 77 dB.

The diameter of the mobile user's receiving antenna is assumed to be only 0.1 m (4 in.). This represents one extreme of interest--it minimizes the problems of the small mobile user at the cost of increased satellite complexity. Thus, the required pointing accuracy of the mobile user is moderate, since the beamwidth ranges from 13 deg at 21.2 GHz to 1 deg at 265 GHz. A margin, M, of 8 dB is allowed for all losses other than atmospheric absorption and scattering (which are included in L and T_{op}). The losses covered by the margin include, for example, those due to antenna boresight misalignment, degradation due to component aging, polarization losses, impedance mismatches, radome attenuation, and propagation anomalies (e.g., refractive index effects).

A value of 10 was selected for E_b/N_0 in the base case. Such a downlink will accommodate vocoded-voice with binary, PSK transmission using differentially coherent detection, and achieve an error probability of no more than 10^{-3}.*

The data rates, R, of interest for various users cover a wide range. Thus, for some small vehicles, teletype at 75 bps or message traffic at 150 bps may suffice; indeed, many present links are designed to supply just 75 bps.† Secure voice communication today typically requires a 16 to 32 kbps data rate using Continuously Variable Slope Delta (CVSD) modulation. Much higher data rates (10 to 100 Mbps) are usually required for sensor data, but raw sensor data requirements may extend to 1 Gbps.

As indicated in Table 6, a satellite altitude of 30,000 n mi was selected for the base case. The basis for this choice will become clear in Section V. Briefly, it is the lowest altitude at which a user at any point on the earth's surface has at least one satellite in view at an elevation angle of roughly 30 deg or higher when a constellation of only nine satellites is employed.

The transmitter output power of 10 W and antenna efficiencies (at both ends of the communication link) of 56 percent are typical of present systems at 8 GHz and are assumed to be reasonable goals throughout the millimeter-wave band.

Since the parameters all appear as linear or quadratic factors in the performance equation, Eq. (6), scaling to values different from those assigned in the base case is a straightforward task.

---

*A wide range of communication requirements can be satisfied by systems operating at the frequencies considered in this study. At one extreme, one might encounter a large number of users for whom economic and technological constraints might dictate the use of simple, noncoherent FSK at data rates of only 75 to 2400 bps. At the other extreme, a small number of sophisticated and demanding users might require the use of coherent PSK with convolutional coding and sequential decoding at data rates of 200 Mbps to 1 Gbps. Depending on the error rate required, the minimum value of E_b/N_0 could therefore be as much as 11 dB or as little as 5 dB. As noted above, the choice of 10 dB is representative of just one possible application.

†The volume of paper required to print out 150 bps for 24 hr is not insignificant. A data stream of 150 bps produces 12.95 gigabits in 24 hr for record traffic. Inasmuch as a typical double-spaced typed page has about $25 \times 72 \times 5 = 9000$ bits of information, this amounts to 1440 pages of printout per day.

The performance of a downlink to a mobile user was estimated with the aid of Eqs. (5) and (6) and the cumulative probability distributions for atmospheric degradation (A_T, shown in Figs. 3 through 8). Performance is presented as link outage statistics, calculated for the parameter values of Table 6.

Figure 10 (a through f) shows the results of these calculations at the six frequencies and four elevation angles considered. The outage (in hr/yr) is indicated as a function of data rate; the percentage of time during which the link is available for communication (not blocked out by weather) is indicated on the right-hand ordinate. These curves clearly show that higher data rates can be achieved only at the expense of increased outage.

The slope of the curves in Fig. 10 is a measure of the feasibility of "burning through" the atmosphere with higher power or larger antennas. Figure 10(a) shows that, at 21.2 GHz, the slope is relatively steep. Thus, at an elevation angle of 30 deg and a 100 hr/yr outage, a two-fold increase in satellite power will increase the data rate from 9.5×10^5 bits/sec (point A) to 1.9×10^6 bits/sec (point B). This represents a seven-fold decrease in outage time from the value of 700 hr (point C) experienced at the lower power level at the latter data rate. At 152 GHz, Fig. 10(e), however, the slope is lower. In this case, the same power increase (with the same value of θ and the same initial outage) would decrease the outage time by a factor of only 1.2 (points A, B, and C have the same significance in both figures). The curves similarly permit a determination of the decrease in outage time associated with any other system improvement, for example, a reduction in the required value of E_b/N_0 through improved signal processing techniques. The curves of Fig. 10 provide the essential background for Sections VIII through XII of this report.

Figure 11 is a cross-plot of the 30 deg elevation angle data from Fig. 10 (a through f), and emphasizes the variation of data rate with frequency. Figure 11 can be used in the initial selection of frequency for any specific application, while Fig. 10 provides more detail concerning performance. In good weather, the data rate increases with frequency, except at the highest frequency shown. When very low outages

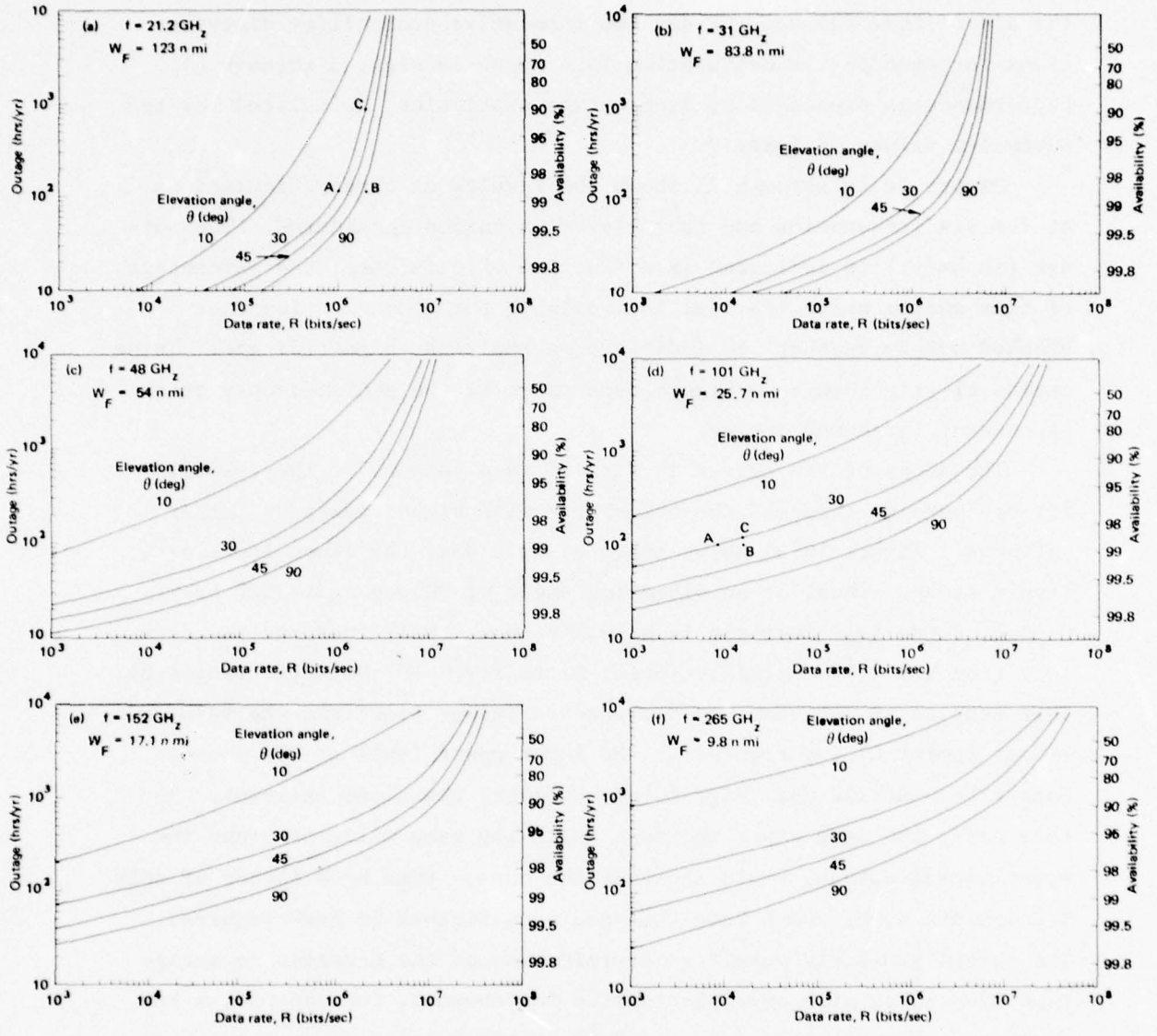

H = 30,000 n mi
Downlink
P_T = 10 W
D_T = 4.4 m
D_R = 0.1 m

$\eta_T = \eta_R = 0.56$
$E_b N_o = 10$
M = 8 dB
Uncooled paramp 2000
Washington, D.C.

Fig. 10—Outage as a function of data rate for small mobile users at various elevation angles and frequencies
(constant satellite antenna diameter = 4.4m)

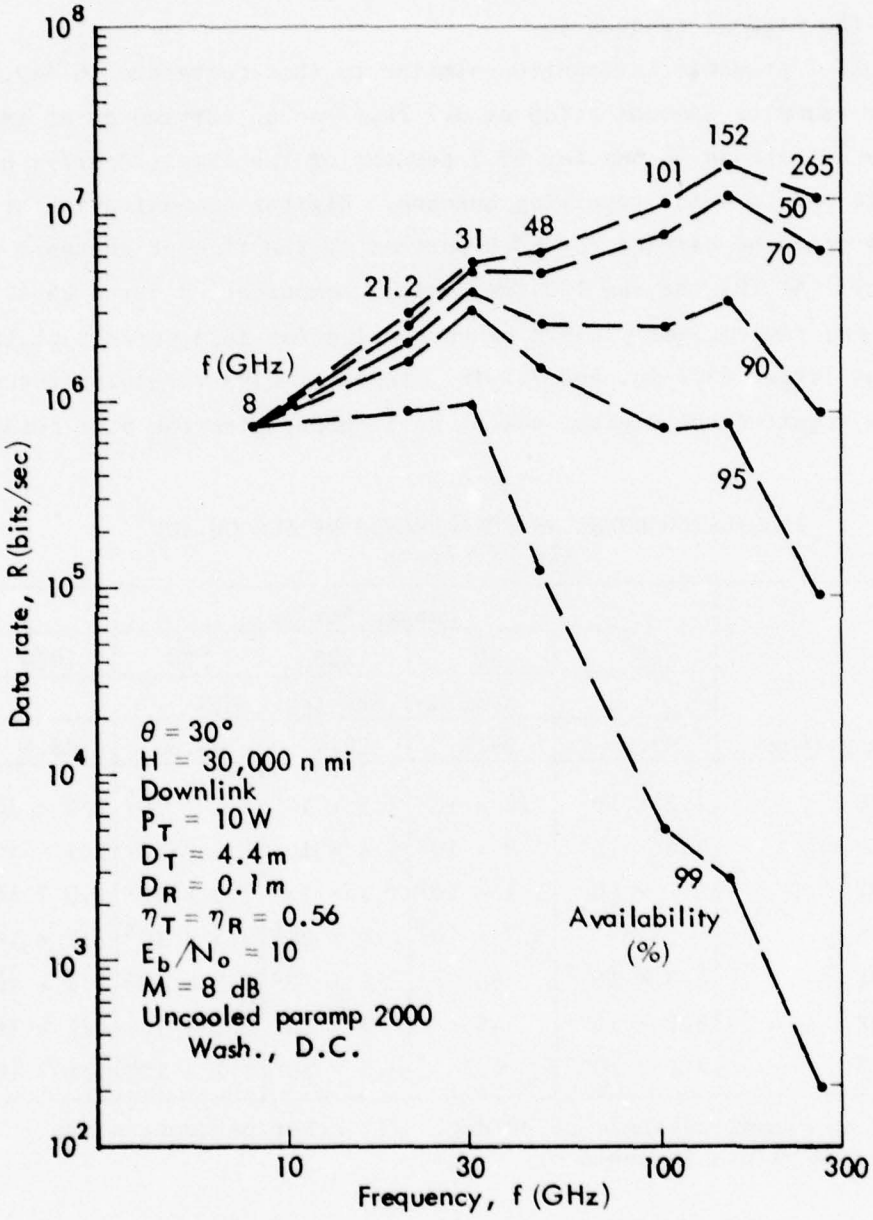

Fig. 11— Small terminal data rate as a function of frequency at various values of availability (constant antenna diameters)

are required, e.g., 1 percent or less, the achievable data rates are considerably lower at the higher frequencies. However, a single 75 bps data channel would be available more than 99 percent of the time even at the highest frequency.

Table 7 presents information similar to that contained in Fig. 11. For example, communication at 3.7 kbps can be carried on at frequencies as high as 48 GHz for 99.7 percent of the time (30 hr/yr outage) with only a 4-in. receiving antenna. Digital communication at 160 kbps could be carried for 98.9 percent of the time at the same frequency. At 101 GHz and 152 GHz, voice communication (at 8 kbps and 5 kbps, respectively) could be be carried for 98.9 percent of the time, but larger (5.7-in. and 7.2-in., respectively) receiving antennas would be required for digital voice, at 16 kbps, with the same outage.

Table 7

CALCULATED DOWNLINK PERFORMANCE VERSUS OUTAGE[a]
(In bits/sec)

	Outage (hr/yr)				
	10	30	100	300	1000
	Availability (percent)				
Frequency (GHz)	99.9	99.7	98.9	95.6	88.6
8	7.2×10^5	7.2×10^5	7.2×10^5	7.2×10^5	7.2×10^5
21.2	3.6×10^4	2.8×10^5	9.6×10^5	1.5×10^6	2.1×10^6
31	1.1×10^4	1.4×10^5	1.1×10^6	2.6×10^6	4.0×10^6
48	3.6	3.7×10^3	1.6×10^5	9.3×10^5	2.7×10^6
101	8.3×10^{-2}	66	8×10^3	2.6×10^5	2.9×10^6
152	8.9×10^{-2}	45	5×10^3	2.5×10^5	4.1×10^6
265	2.1×10^{-2}	4.2	3.3×10^2	2.2×10^4	1.1×10^6

[a]At an elevation angle of 30 deg. All other parameters are assigned the values in Table 6.

The total annual throughput increases materially with frequency, except at the highest frequency, as shown in Fig. 12. This figure shows the data rate averaged over 1 yr as a function of frequency. It is concluded that, if the outages can be tolerated, the efficiency (bits/dollar) will be materially higher at the higher frequencies.

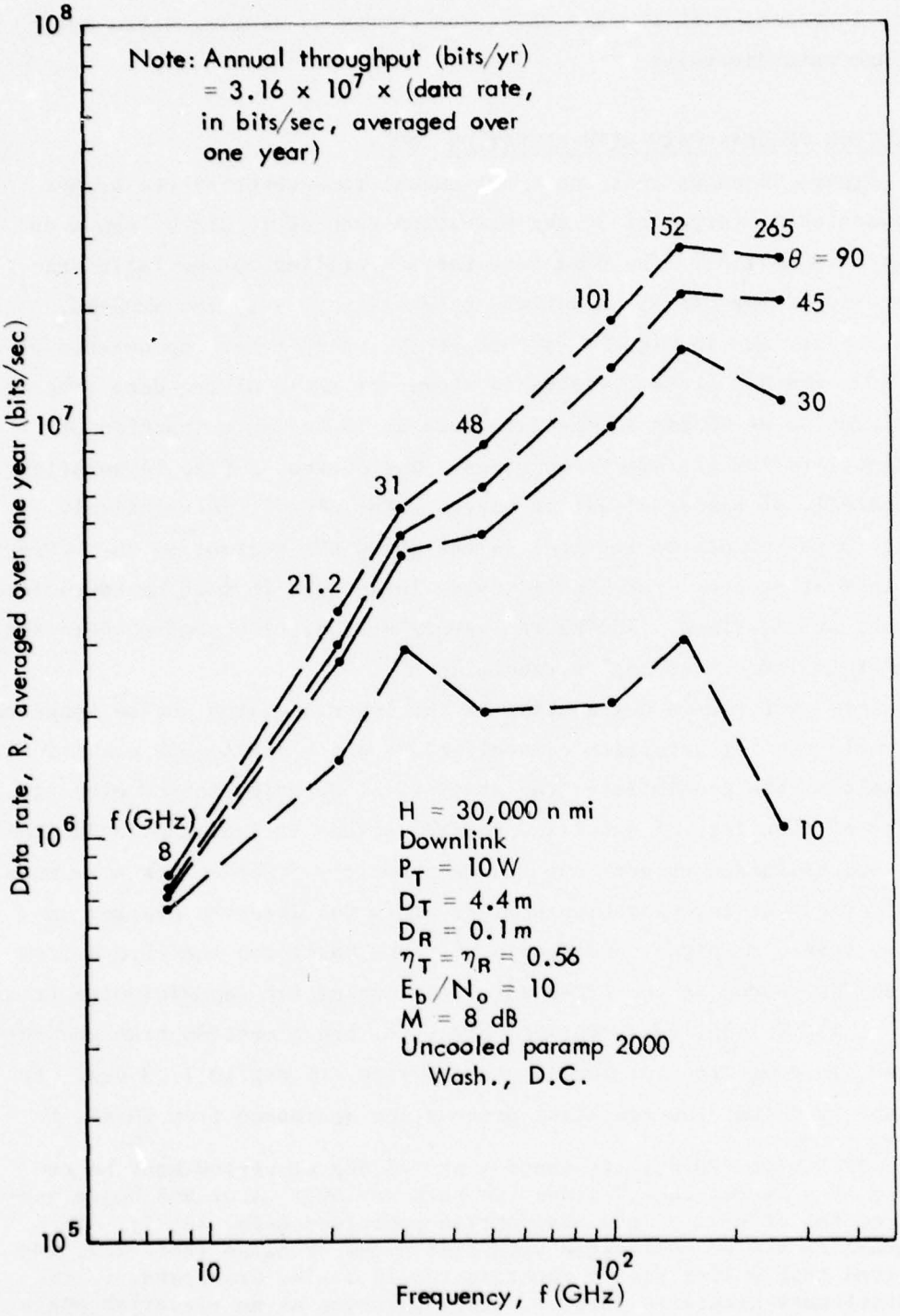

Fig. 12 — Data rate, averaged over one year, as a function of frequency and elevation angle (constant antenna diameters)

The outages may be reduced through such techniques as temporary power increases with the aid of stored energy or dodging storm cells through path diversity.

VARIATION OF DATA RATE WITH ELEVATION ANGLE

Figure 12 shows that the total annual throughput at the higher frequencies is larger at 30 deg elevation than at 10 deg by about an order of magnitude. The data rate for a specified outage falls dramatically at low elevation angles, especially at very low outages. This can be seen in Fig. 13 (a through c), which refers to outages of 10, 100, and 300 hr/yr. Figure 14 shows the ratio of the data rate at an elevation of 30 deg to the data rate at 10 deg as a function of availability for the six frequencies. The curves of Fig. 14 quantify the benefit of higher elevation angles. The benefit is relatively small (a factor of two to five) in the 20/30 GHz region; in the 100/300 GHz region, however, the benefit is so large that it must be taken into account at all times. 48 GHz represents a transition region where the benefit is large, but not overwhelming.

This performance degradation at the lower elevaton angles suggests the employment of satellite constellations which avoid such elevations. To explore this possibility, the statistical distribution of elevation angles of a variety of satellite constellations is examined in Section V.

Scintillation effects due to atmospheric refraction are also much more serious at low elevation angles. This was observed by, for example, Vogel, Straiton, and Fannin,[19] who monitored the return from the 30 GHz beacon on the ATS-6 satellite during its repositioning from 35°E to 130°W longitude. During this time, the elevation from the receiver, in Port Aransas, Texas, changed from 1.5 deg to 17.3 deg. It was observed that the resultant attenuation decreased from 20 dB* to

*This high (20 dB) attenuation at 1.5 deg elevation must be regarded as a "worst case," since the path was over water and hence subject to the effects of the evaporation duct (see Refs. 20-21). This attenuation may be contrasted with that noted by Allen (Ref. 22), who observed that a link from a mountain top in Thule, Greenland, to the geostationary satellite Anik II, also operating at an elevation angle of 1.5 deg, performed satisfactorily for three years with a 6.5 dB fade margin on the downlink. This margin, in fact, was considered to be larger than necessary based on the rarity of outages over the three-year period.

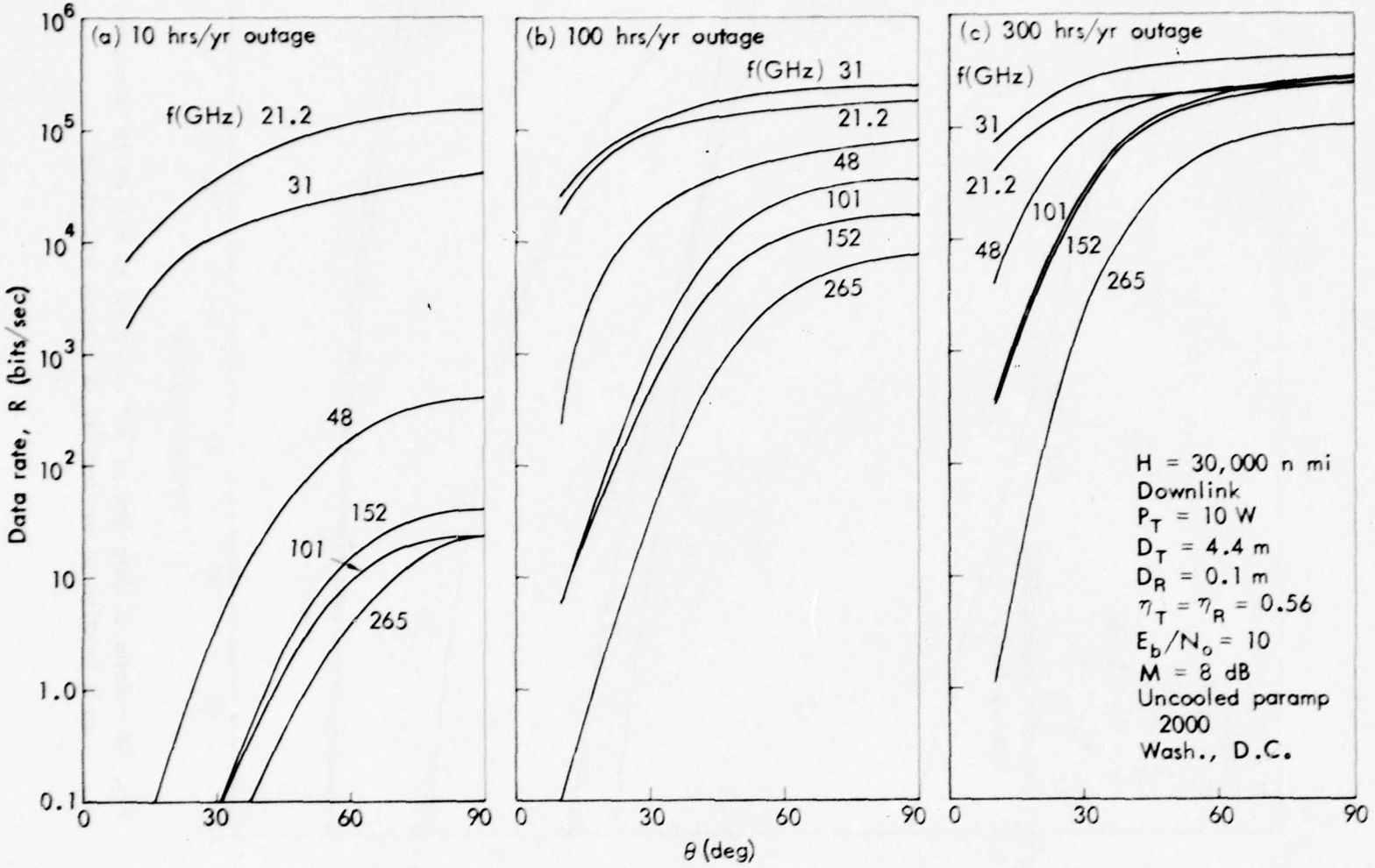

Fig. 13—Data rate versus elevation angle at various frequencies and outages (small mobile users, uncooled paramp)

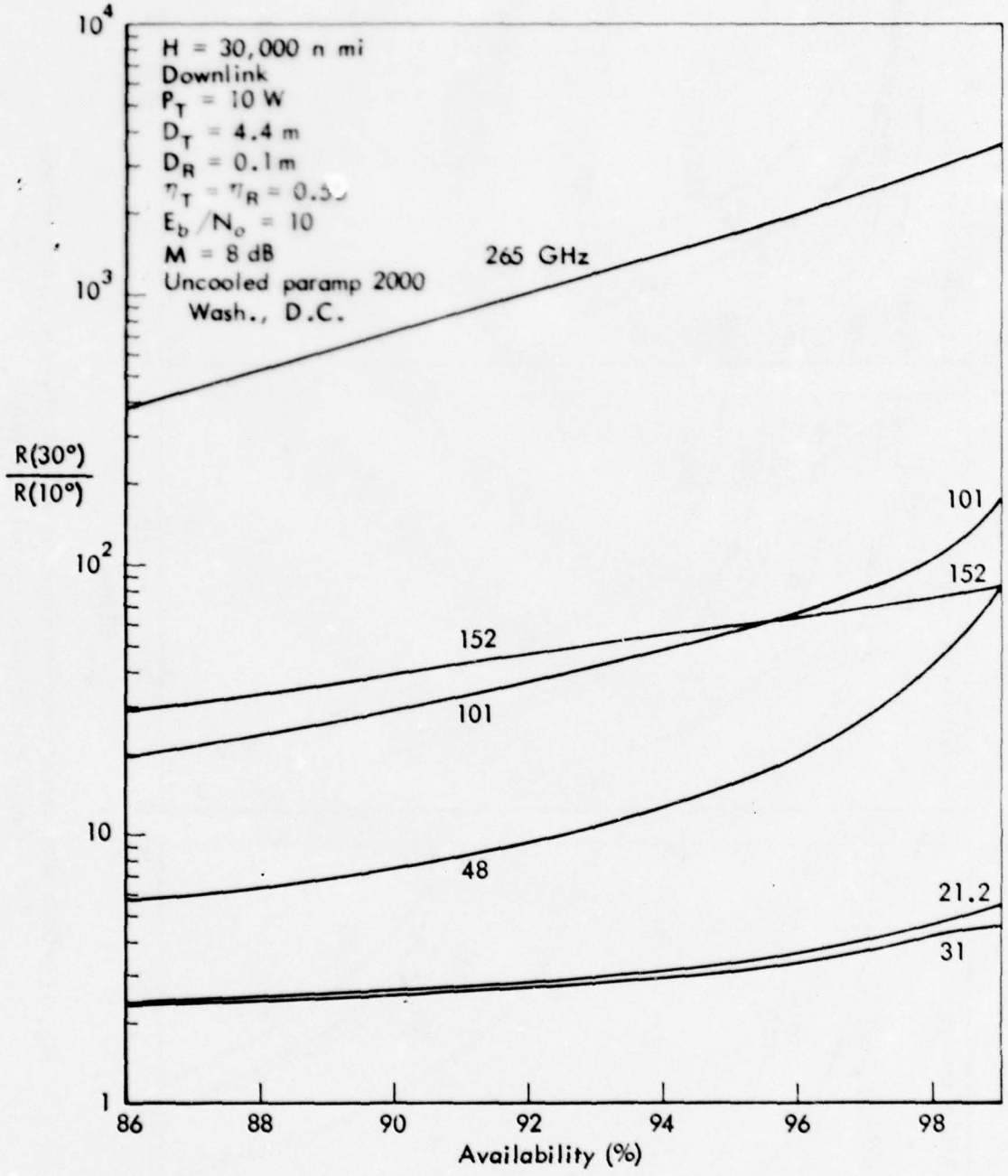

Fig. 14—Ratio of data rate at 30° elevation to that at 10° elevation as a function of availability at various frequencies

2 dB and the standard deviation decreased from over 6 dB to less than 0.2 dB.

CONSTANT SPOT SIZE

In the preceding analysis, the satellite antenna diameter was held constant (at 4.4 m) at all frequencies. The width of the beam footprint on the earth, correspondingly, decreased with increasing frequency. This is seen from Section VI and the Appendix, in which the shape and size of the footprint are examined in detail. It is assumed that the footprint width, W_F, is given by the relation

$$W_F = \frac{1.27\ \lambda\ S}{D_T}\ , \qquad (8)$$

where, as before, S is the slant path, and D_T is the diameter of the transmitting antenna.

The values of W_F, obtained from this equation at the various frequencies, are indicated in Fig. 10. They were calculated at an elevation angle of 90 deg, and are designated as W_F in the figure. The footprint width is seen to decrease from 123 n mi at 21.2 GHz to 9.8 n mi at 265 GHz. While the small spot size at high frequencies results in an increased data rate in good weather (Fig. 11), it complicates the problems of achieving adequate area coverage and of beam pointing. It is interesting to examine the variation of system performance with frequency in the alternative case, in which the footprint width is held constant as the frequency is increased by continually decreasing the satellite antenna diameter.

The results obtained in this alternative case are shown in Fig. 15 (a through f), and are similar to those shown in Fig. 10, except the footprint width is maintained at 123 n mi (its value at 21.2 GHz with a 4.4 m antenna) at all frequencies. The antenna diameter corresponding to this footprint width then decreases with increasing frequency, as indicated in the figure, so that, for example, 158 antennas operating at 265 GHz could be mounted in an aperture on the satellite that would be fully occupied by a single antenna operating at 21.2 GHz. The data rate, correspondingly, falls off rapidly with increasing frequency. This is shown in Fig. 16, which is a cross-plot of the 30 deg

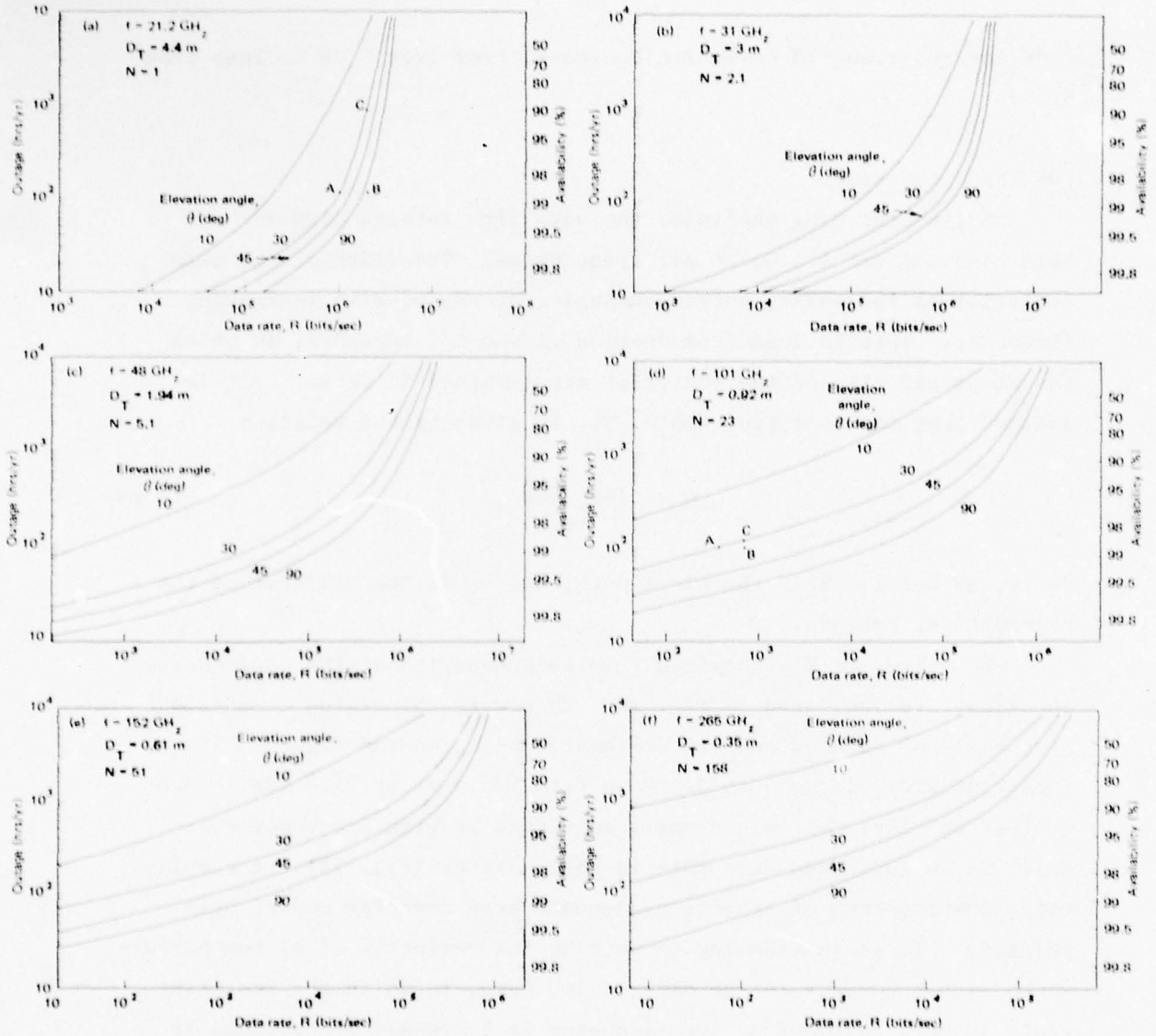

N = Relative number of antennas within a constant satellite aperture

Downlink	$\eta_T = \eta_R$
H = 30,000 n mi	E_b/N_o = 10
P_T = 10 W	M = 8 dB
D_R = 0.1 m	Uncooled paramp 2000
W_F = 142 n mi	Washington, D.C.

Fig. 15 — Outage as a function of data rate for small mobile users at various elevation angles and frequencies (constant nadir footprint width = 123 n mi)

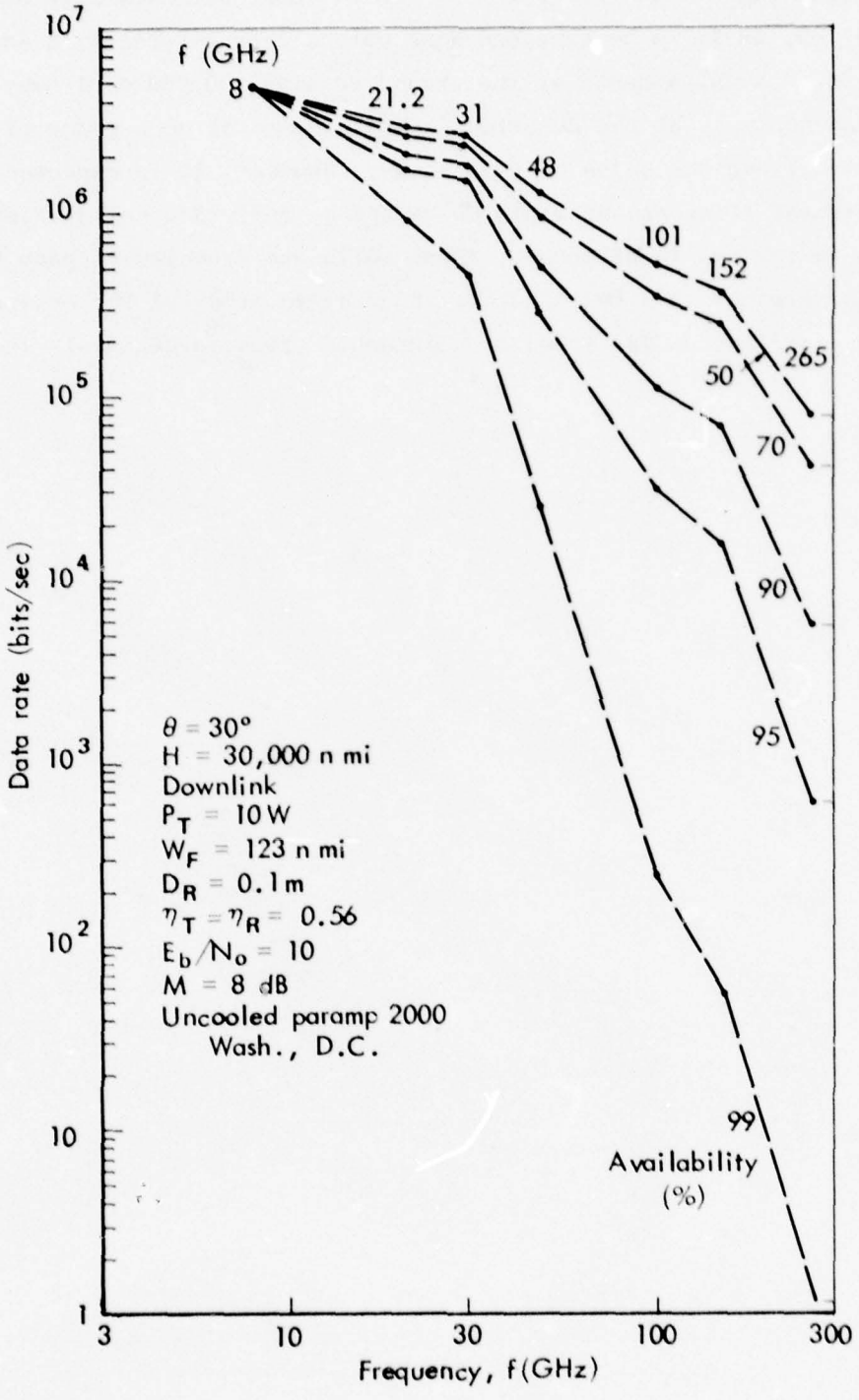

Fig. 16—Small terminal data rate as a function of frequency at various values of availability (spot width held constant at 123 n mi)

elevation angle data from Fig. 15. At 265 GHz, the data rate becomes quite low, as is to be expected with only a 1-ft antenna in a satellite and a 4-in. antenna at the ground terminal 30,000 n mi away.

An analysis of the durations and frequency of occurrence of outages is beyond the scope of this study. However, it is expected that the highest attenuations would be caused by tall rain cells which are small (a few km) in diameter. These cells are expected to pass over a ground terminal in a few minutes. A detailed study of the outage duration distribution in different geographic areas is certainly indicated.

IV. ESTIMATION OF LINK OUTAGE STATISTICS FOR WIDE-BAND DATA RELAY USERS

UNCOOLED RECEIVER

The wide-band data relay user requires a much higher data rate (e.g., 10^6 to 10^9 bps) than does the typical small mobile user (10^2 to 10^5 bps), but can employ a much larger diameter antenna. He is especially concerned about his interference with or from others because of his large bandwidth. The number of wide-band data relay users is quite small compared with the number of small mobile users. With these considerations in mind, we postulate a downlink for the wide-band data relay user that has a satellite antenna diameter of 1 m and a terminal antenna diameter of 10 m. The purpose of selecting so large an antenna diameter is to examine the other extreme, compared to the 0.1 m antenna of the small mobile user. (Other considerations may dictate the use of a 2 to 3 m antenna for this application rather than 10 m). The postulated downlink provides a 516-fold increase in data rate compared with the 0.1 m antenna in conjunction with a 4.4 m satellite antenna. The 1 m satellite antenna diameter permits the use of a number of independent, mechanically steerable antennas (an antenna "farm"), with each antenna dedicated to a single user or a group of closely spaced users. If these parabolic dishes are fed by an offset corrugated feed horn, properly loaded with a microwave absorber and shielded, very low (e.g., 80 dB down) sidelobe levels can be achieved.[16]

Figure 17 shows the data rate achievable with such a downlink at 30 deg elevation, estimated in the manner described in Section III. Note that a data rate of 10^9 bps can be obtained with availabilities ranging from 86 percent at 265 GHz to 97.7 percent at 31 GHz.

EFFECT OF USING IMPROVED RECEIVER

Large terminals, e.g., employing antennas 10 m in diameter, and high data rate terminals, e.g., 10^6 to 10^9 bps, represent such a large investment in antennas or modems that they justify a larger investment in other terminal components. Thus, a convolutional encoding modem

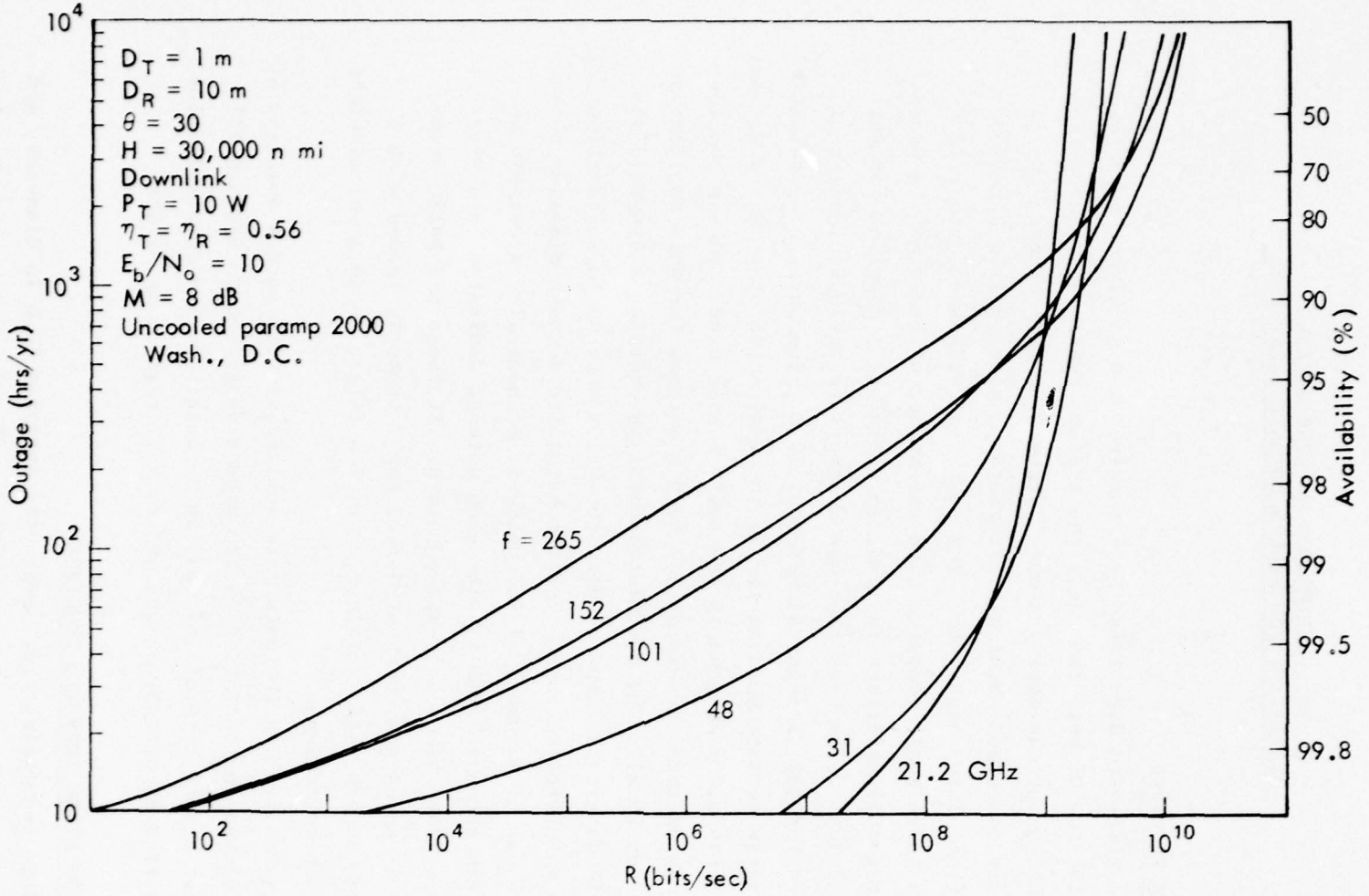

Fig. 17 — Outage as a function of data rate for wide-band data relay users at various frequencies

with coherent modulation may be justified, considering the total terminal investment. This would result in a 5 dB link improvement.[23] While the use of a cryogenic receiver can be justified on a proportionate cost basis, its effect in improving data rate is limited. Thus, for an atmospheric loss, L, of 10 to 20 dB or more, the system operating temperature, T_{op}, approaches 300°K regardless of how low the receiver first-stage noise temperature, T_F, is made.

In order to determine more accurately the benefits of coherent modulation and a cryogenic receiver, the calculation of data rate was repeated, assuming a 5 dB improvement (from 10 to 3.16) in E_b/N_0 and the use of a cooled amplifier. The amplifier was assumed to have the noise temperature characteristics indicated by the "cooled paramp 2000" curve in Fig. 9. The actual values of T_F used are indicated in Table 5. The coupler and line were both assumed to be at 50°K, so that the operating temperature obtained from Eq. (2) becomes

$$T_{op} \text{ (cooled amplifier)} = 0.89\ T_{sky} + T_F + 19.8\ . \qquad (9)$$

The total atmospheric degradation, A_T, in this case is included in Table 8. The results of this calculation are presented in Figs. 18-20. Figure 18, which is similar to Fig. 17, indicates the outages as a function of data rate at the various frequencies. Comparing Figs. 17 and 18, it is seen that, for example, at an elevation angle of 30 deg and an outage value of 100 hr/yr, the improved system increases the data rate by a factor ranging from 4.9 at 21.2 GHz to 11.7 at 265 GHz. Figures 19 and 20 show the performance of the improved system as a function of elevation angle. Comparing Fig. 20 with Fig. 14, it is seen that the performance improvement at 30 deg elevation relative to that at 10 deg is comparable in the two cases, although slightly greater with the improved system.

Table 8

STATISTICS OF ATMOSPHERIC ATTENUATION AND TOTAL SYSTEM PERFORMANCE DEGRADATION PRODUCED BY THE ATMOSPHERE AT WASHINGTON, D.C.[a]

Time that A, T_{sky}, and A_T Are Exceeded		Elevation Angle (deg)							
		10		30		45		90	
%	hr/yr	A (dB)	A_T (dB)	A (dB)	A_T (dB)	A (dB)	A_T (dB)	A (dB)	A_T (dB)
				Frequency = 21.2 GHz					
100	8766	0.92	4.44	0.33	2.03	0.23	1.49	0.17	1.14
11.4	1000	3.52	10.2	1.24	5.44	0.9	4.38	0.61	3.3
1.14	100	9	17.3	3.3	9.8	2.61	8.6	1.92	7.16
0.34	30	14.7	23.4	7.5	15.6	6.1	13.8	4.7	12.0
0.114	10	23	31.8	16	24.7	13.2	21.8	10.4	18.8
				Frequency = 31 GHz					
100	8766	0.94	4.32	0.34	1.97	0.27	1.62	0.17	1.08
11.4	1000	3.5	9.9	1.2	5.11	0.8	3.85	0.6	3.11
1.14	100	10.5	18.6	5.0	12.1	3.5	9.9	2.80	8.7
0.34	30	19.0	27.4	13.0	21.3	10.0	18.1	8.40	16.3
0.114	10	32.0	40.5	24.0	32.5	22.0	30.5	19.0	27.4
				Frequency = 48 GHz					
100	8766	3.05	8.8	1.1	4.59	0.75	3.48	0.53	2.66
11.4	1000	11.6	19.5	4.47	11.04	3.26	9.18	2.4	7.64
1.14	100	34	42.1	15.8	23.8	12.6	20.5	9.65	17.4
0.34	30	57	65.1	32.3	40.4	25.8	33.9	20.5	28.6
0.114	10	86	94.1	62.4	70.5	52	60.1	42.4	50.5
				Frequency = 101 GHz					
100	8766	6.1	12.4	2.0	6.18	1.38	4.79	1.02	3.85
11.4	1000	22.2	29.5	8.8	15.6	6.24	12.6	4.64	10.5
1.14	100	55.5	62.8	34	41.3	24	31.3	18.2	25.5
0.34	30	81	88.3	55	62.3	43.8	51.1	36	43.3
0.114	10	97.6	104.9	84	91.3	72	79.3	60	67.3
				Frequency = 152 GHz					
100	8766	6.3	12.1	2.16	6.0	1.5	4.63	1.05	3.54
11.4	1000	24.5	31.1	9.5	15.7	6.6	12.4	5.0	10.4
1.14	100	57.5	64.1	38.7	45.3	29.6	36.2	23.8	30.4
0.34	30	79	85.6	59	65.6	51	57.6	43.5	50.1
0.114	10	98	104.6	86	92.6	72	78.6	60	66.6
				Frequency = 265 GHz					
100	8766	12.6	17.9	4.5	8.74	3.0	6.57	2.15	5.16
11.4	1000	45	50.5	17.7	23.2	12.3	17.6	9.3	14.4
1.14	100	88	93.5	53	58.5	40	45.5	30	35.5
0.34	30	105	110.5	72	77.5	62	67.5	46	51.5
0.114	10	125	130.5	95	100.5	82	87.5	65	70.5

[a]Assuming the "cooled paramp 2000" amplifier noise temperature in Table 5.

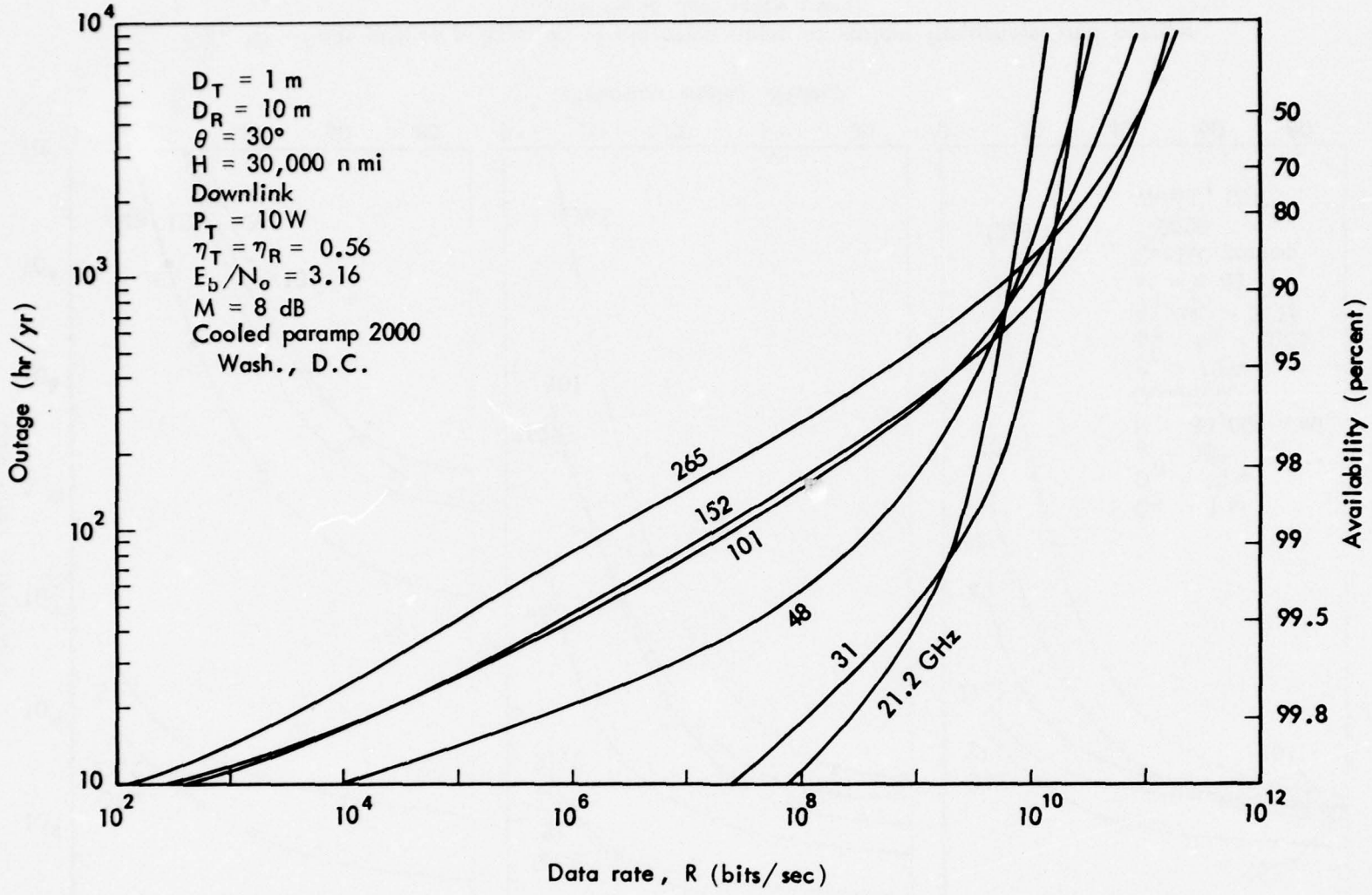

Fig.18 — Outage versus data rate for wide-band data relay users at various frequencies

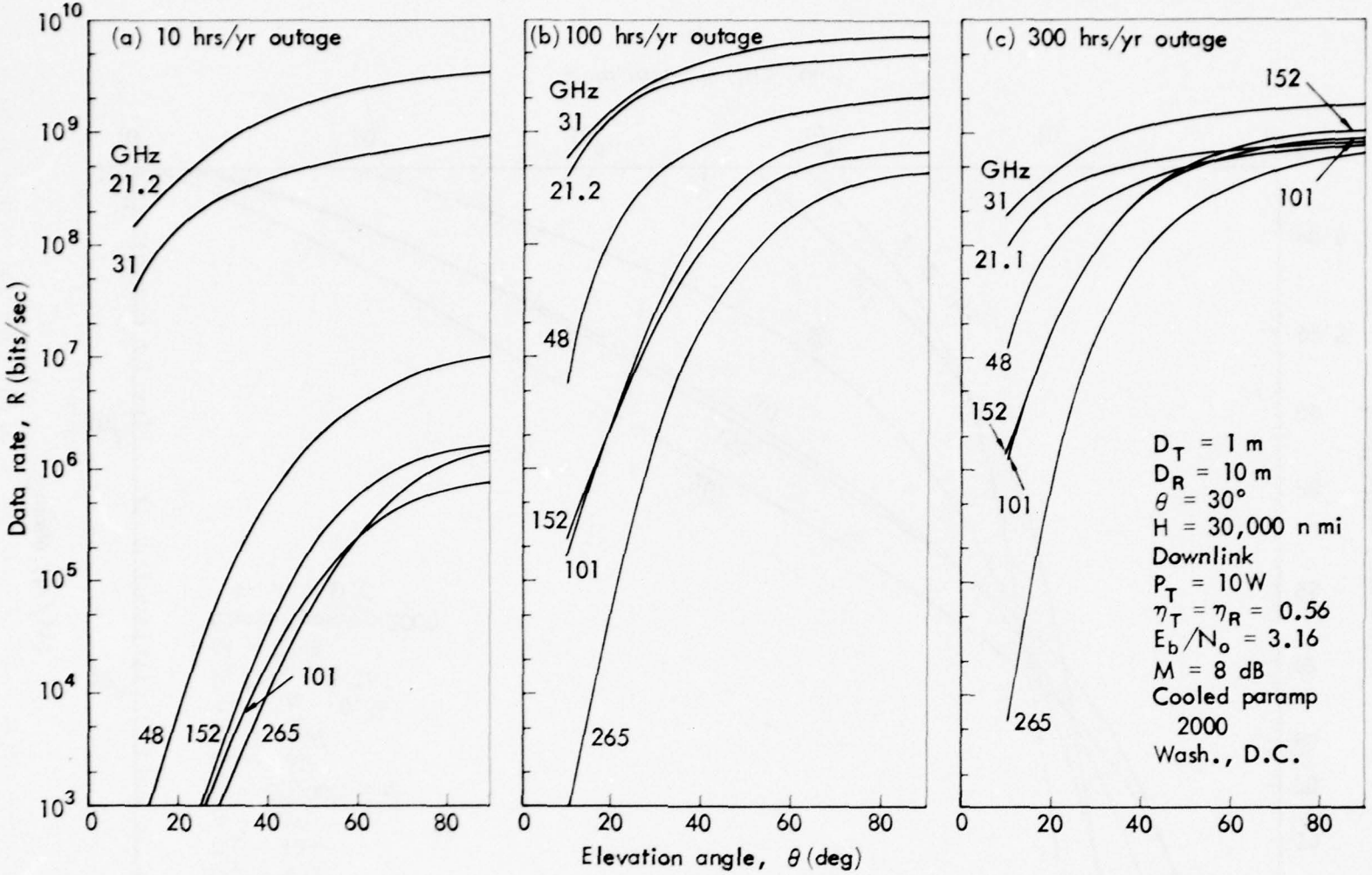

Fig. 19—Data rate as a function of elevation angle at various frequencies and outages (wide-band data relay users)

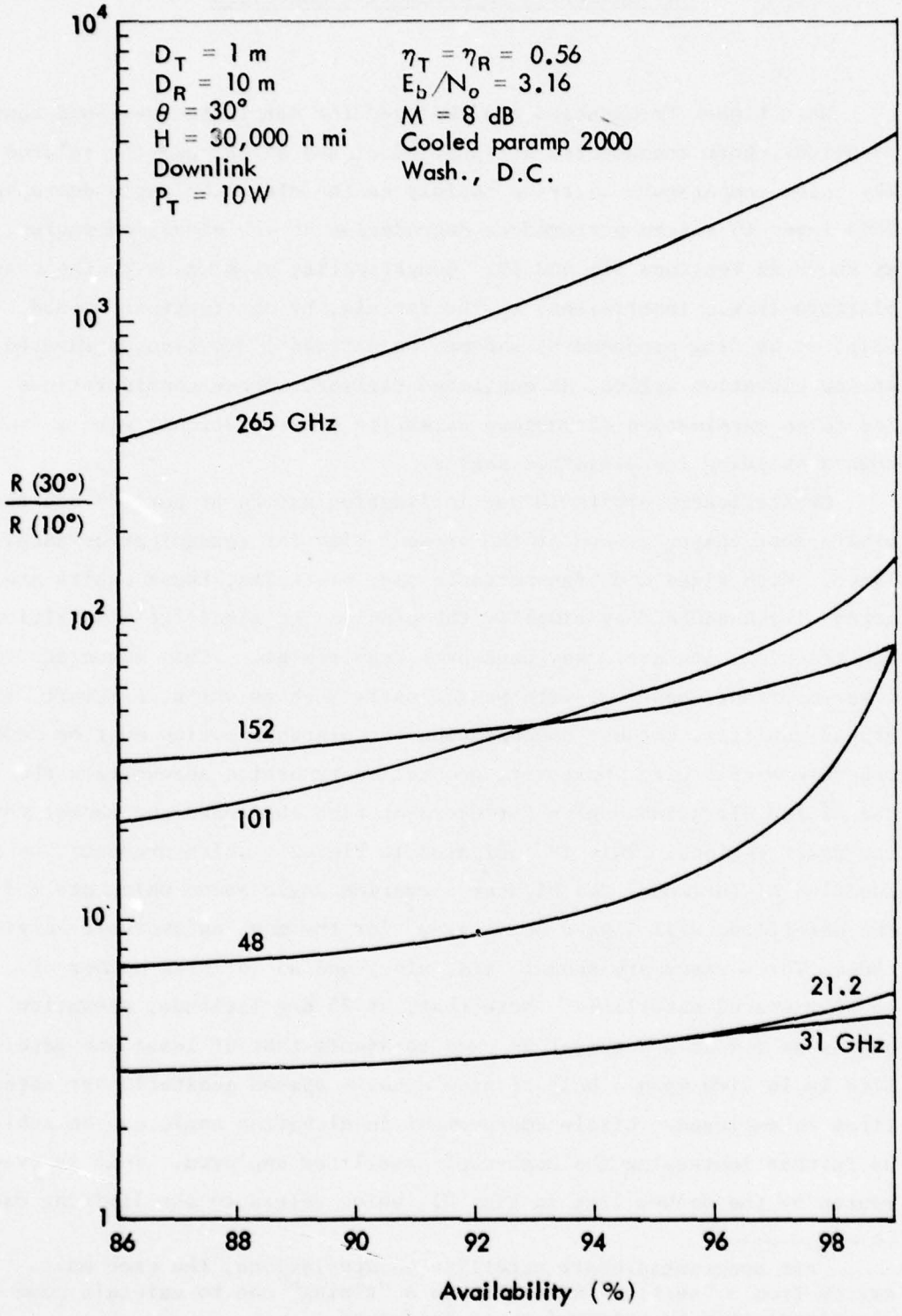

Fig. 20 — Ratio of data rate at 30 deg elevation to that at 10 deg versus availability (wide-band data relay users)

V. SATELLITE CONSTELLATION SELECTION

When higher frequencies are employed for satellite-to-ground communications, both atmospheric attenuation of the signal and the related sky noise temperature increase rapidly as the elevation angle decreases. This leads to severe performance degradation at low elevation angles, as shown in Sections III and IV. Compatibility problems with the user platform (e.g., interference by the terrain, by obstructions aboard ship, or by drag produced by radomes on aircraft) are also aggravated at low elevation angles, as mentioned earlier. These considerations led to an examination of various satellite constellations, with a view toward avoiding low elevation angles.

Geostationary orbits (0 deg inclination and 24 hr period) are the orbits most commonly used at the present time for communication satellites. With fixed and transportable user platforms, these orbits are attractive because they simplify the problems of satellite acquisition and tracking, and avoid any hand-over requirement.* This advantage is less important, however, with mobile users such as ships, aircraft, and ground vehicles, because compensation for platform motion must be made regardless of orbit. Moreover, geostationary orbits necessitate the use of low elevation angles for users at high latitudes and cannot cover the polar regions. This is indicated in Fig. 21, which presents, as a function of latitude, the highest elevation angle above which one and two satellites will always be in view† for the most unfavorable longitude. Three cases are shown: six, nine, and an infinite number of equally spaced satellites. Note that, at 75 deg latitude, elevation angles as low as 5 deg must be used to assure that at least one satellite is in view when a belt of nine equally spaced geostationary satellites is employed. Little improvement in elevation angle can be achieved by further increasing the number of satellites employed. This is evidenced by the dashed line in Fig. 21, which refers to the limiting case

*For nongeostationary satellite constellations, the user must switch from a "setting" satellite to a "rising" one to maintain communications; this is referred to as hand-over.

†Obviously more satellites may be seen as the elevation angle is lowered.

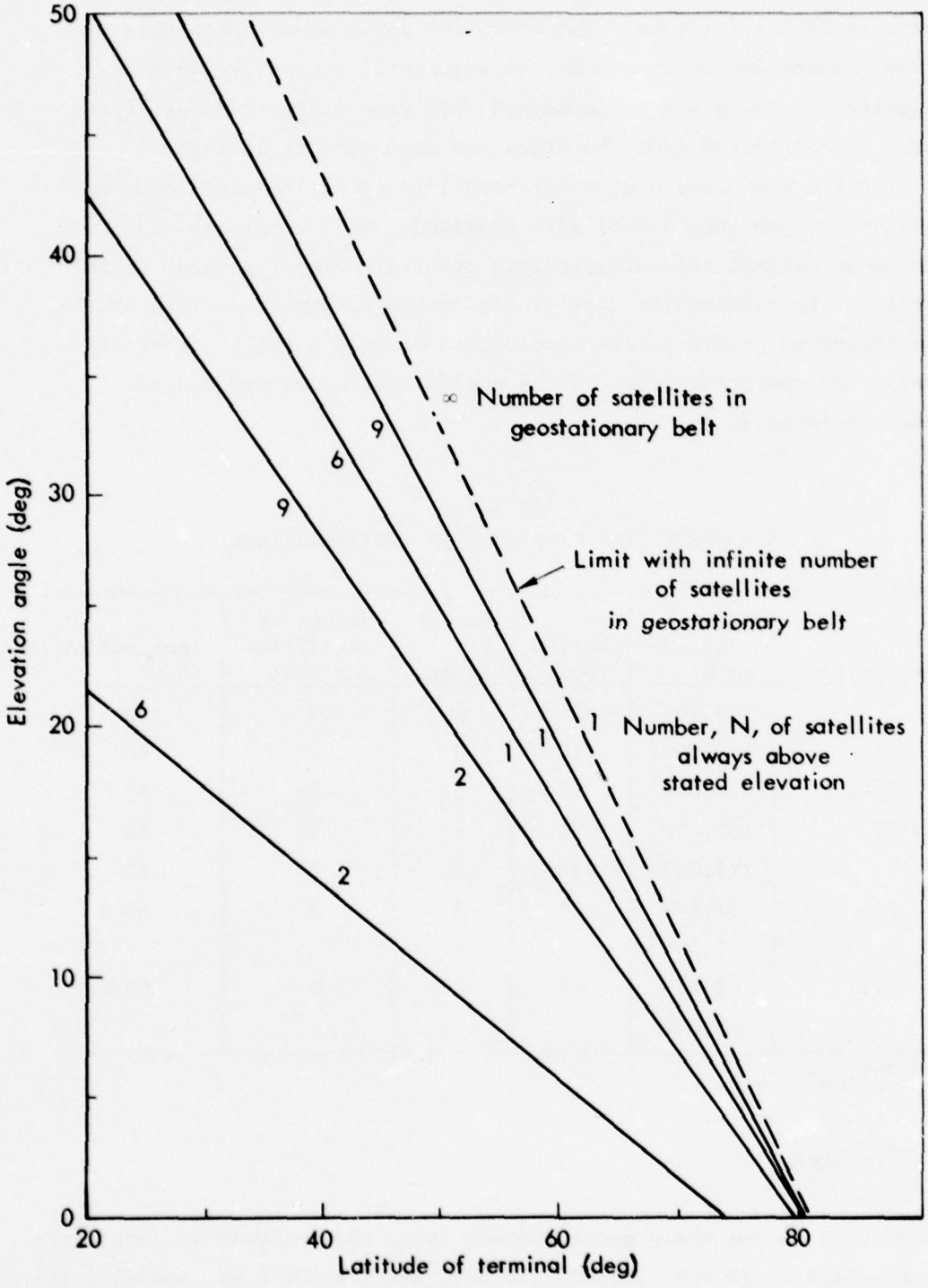

Fig. 21—Elevation angle above which N satellites are always in view as a function of terminal latitude

of an infinite number of satellites. Consider, for example, an observer at 75 deg latitude. The elevation angle above which this observer, regardless of longitude, is assured of having at least one satellite in view would be increased only from 5 deg to 6 deg if the number of satellites could be increased from nine to infinity.

For the above reasons, other satellite constellations assuring higher elevation angles were also examined. No attempt was made to develop an optimal constellation, to treat all limiting cases of interest, or to examine the sensitivity to key parameters, since available resources permitted the examination of only a small number of cases. The characteristics of the constellations considered are listed in Table 9.

Table 9

CHARACTERISTICS OF SATELLITE CONSTELLATIONS

Configuration	Altitude (n mi)	Period (hr)	Number of Belts	Number of Satellites per Belt	Inclination (deg)
I	19,360[a]	24	1	9	0
II	10,000[a]	10.9	3	3	60
III	30,000[a]	42.6	3	3	60
IV	100,000[a]	231.8	3	3	60
V	129,000[a]	335.8	3	2	60
VI	37,172[b] 5,000[c]	24	3	3	63.4
VII	103,059[b] 5,000[c]	96	3	2	63.4

[a]Circular orbit.

[b]Apogee.

[c]Perigee.

In addition to the basic geostationary case, the analysis includes circular orbits at 10,000, 30,000, 100,000, and 129,000 n mi, and elliptical orbits with 24 hr and 96 hr periods. The elliptical orbits are assigned an inclination of 63.4 deg to prevent rotation of the major

axis in the orbital plane as a consequence of the earth's bulge. Elliptical orbits have the advantage that the satellites spend 90 percent or more of their time in the Northern Hemisphere. During much of this time, the elevation is high--especially for users at high latitude.*

For each constellation configuration given in Table 9, Fig. 22 presents the probability that one or more satellites will be above 30 deg elevation as a function of latitude. Because of limited resources, only a small number of points were computed. To emphasize the coarseness of the data, these points were connected by straight lines. This is an average probability, i.e., the probability averaged over all longitudes and times. An important conclusion is that constellations involving nine properly phased satellites in circular orbits at 60 deg inclination (constellations II, III, and IV) provide worldwide coverage with a high probability of at least one satellite in view above 30 deg elevation. The probability increases with satellite altitude. For these three constellations, the smallest probability values occur around 30°N and 30°S latitude; the probability at the minima increases from about 0.8 at 10,000 n mi to 0.95 at 30,000 n mi, and to 0.97 at 100,000 n mi. For the two higher altitudes, it was found that at least one satellite is always in view above 20 deg elevation. Constellations which involve only six satellites are unsatisfactory even at 129,000 n mi, the highest "stable" cislunar altitude† (cislunar orbits above 130,000 n mi are unstable at 60 deg inclination because of lunar attraction). This is illustrated by constellation V, for which the probability of there being one satellite in view above 30 deg falls to 0.73 in the equatorial

---

*These advantages are obtained at the expense of communications capability in the Southern Hemisphere. Thus, for six to nine satellites, only 60 to 90 percent of the time is even a single satellite available in the entire Southern Hemisphere (10 percent of time × the number of satellites in the constellation).

†The word "stable" here means that the variation in altitude at 129,000 n mi can be held to ± 10,000 n mi over a period of 5 to 10 yr with less than 10 percent of the spacecraft weight devoted to orbital maintenance. Furthermore, the frequency and magnitude of thrust corrections would be compatible with current technology and thus compatible with long-life, reliable spacecraft. A more complete analysis of stable orbits and implications for the space vehicle design is beyond the scope of this study.

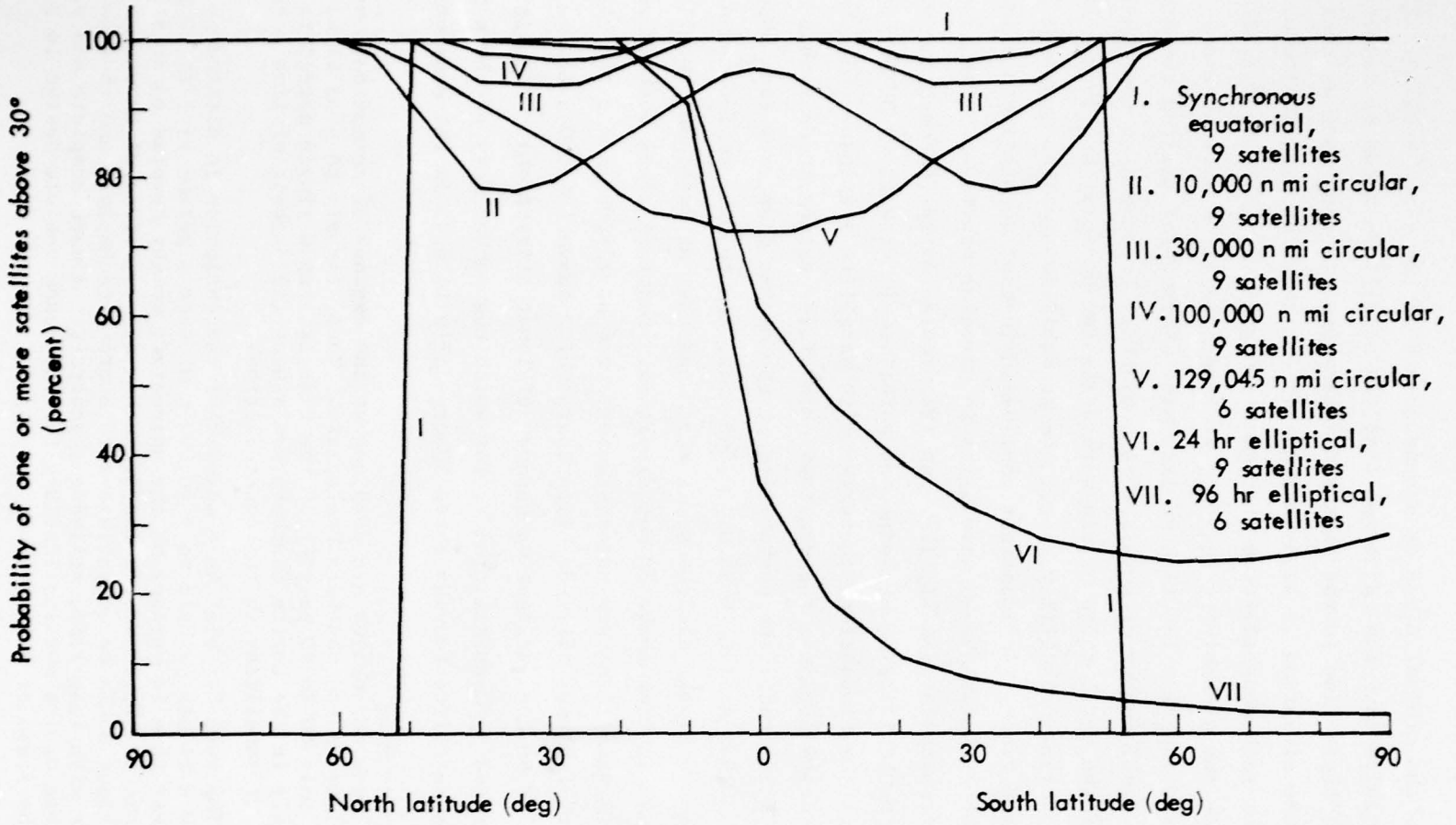

Fig. 22—Probability of one or more satellites above 30° elevation versus terminal latitude for seven satellite constellations

region. For Northern Hemisphere coverage at latitudes exceeding 20 deg, either of the elliptical orbits (constellations VI or VII) would be satisfactory.

VI. SHAPE AND SIZE OF THE BEAM FOOTPRINT ON THE EARTH

The satellite is designed to serve any user within the beam footprint formed by the intersection of the 3 dB contour of the main lobe of the satellite antenna pattern and the earth's surface. For a fixed antenna diameter, the size of the beam footprint or spot decreases as the frequency increases. The geometry of the spot is examined in the Appendix; it is shown that the spot is nearly elliptical if it does not approach the edge of the earth. To fourth powers of the beamwidth, it is shown that the length, width, and area of the footprint (L_F, W_F, and A_F, respectively) are given by Eqs. (A.9), (A.15), and (A.18), which, committed to our present symbology, become:*

$$L_F \simeq \frac{S\,\delta}{\sin\theta} + \frac{H\left(2R_e + H\right)\left(1 + 2\cos^2\theta\right)\left[\left(R_e + H\right)^2 - R_e^2\cos^2\theta\right]^{\frac{1}{2}}\delta^3}{24\,R_e^2\sin^5\theta} \tag{10}$$

$$W_F \simeq S\,\delta\left[1 + \frac{\delta^2}{4}\left\{\frac{S}{2R_e\sin\theta} + \frac{1}{2\sin^2\theta} + \frac{\left(R_e + H\right)^2 - R_e^2\cos^2\theta}{6R_e^2\cos^2\theta}\right\}\right] \tag{11}$$

$$A_F = \frac{\pi S^2\sin^2(\delta/2)}{\sin\theta} + \frac{\pi H^2\left(2R_e + H\right)^2\left(3 - \sin^2\theta\right)\delta^4}{128\,R_e^2\sin^5\theta} \tag{12}$$

$$\delta = 1.27\,\lambda/D \text{ for } \delta \leq 20 \text{ deg},^{\dagger} \tag{13}$$

---

*A different set of symbols is used in the Appendix. In the Appendix, the elevation angle is denoted by α rather than θ, the beamwidth by 2δ rather than δ, the earth radius by R rather than R_e, the slant range by r rather than S, and the length, width, and area of the footprint by $D_{\parallel}$, $D_{\perp}$, and A rather than L_F, W_F, and A_F.

†This beamwidth is obtained when the illumination of the antenna is tapered and has a distribution $(1 - r^2)$, where r is the normalized distance from the center $(0 \leq r \leq 1)$. With this illumination, the first sidelobe is, theoretically, 24.6 dB below the peak intensity of the main beam (Ref. 24). Approximately the same beamwidth is obtained with what is often referred to as "10 dB taper" illumination. Narrower beams can be obtained at the cost of higher sidelobes; it will be seen later (Section VI.), for example, that, for presently used terminals, δ is as small as $1.06\,\lambda/D$.

where S = slant range from satellite to center of footprint

δ = angular beamwidth in radians (between half-power points)

R_e = radius of earth

θ = angle of elevation

H = satellite altitude

D = antenna diameter.

In each case, the first term represents the value for an elliptical footprint and is obtained by assuming a flat earth. The succeeding terms represent the distortion induced by including earth curvature. The approximate values of L_F, W_F, and A_F are plotted in Figs. 23 and 24. Figure 23 presents the length and width of the footprint, obtained with a 4.4 m satellite antenna and a 30,000 n mi satellite altitude, as a function of frequency for elevation angles at the ground station of 10, 30, and 90 deg. Figure 24 illustrates the area of the footprint as a function of the same parameters. Note the break in the curve representing the footprint length at 10 deg elevation. The break occurs at the point where the edge of the beam falls off the earth (*i.e., is* above the horizon) at lower frequencies. In these cases, Eq. (10) does not apply, and the indicated value of L_F is an approximation. A similar estimation is made for A_F, and is indicated by the dashed line in Fig. 24.

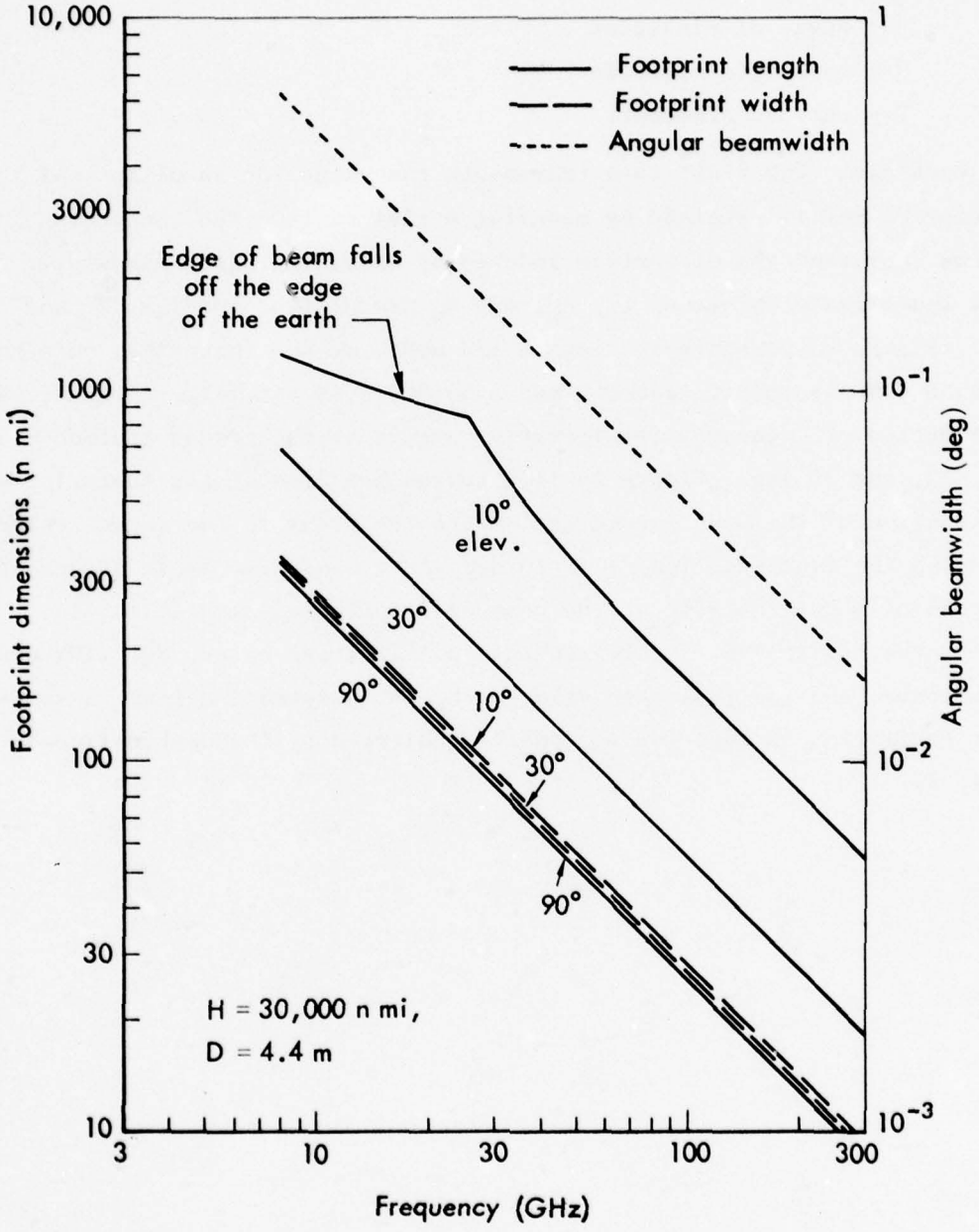

Fig. 23 — Dimensions of beam footprint and angular beamwidth of satellite antenna as a function of frequency and elevation at ground terminal

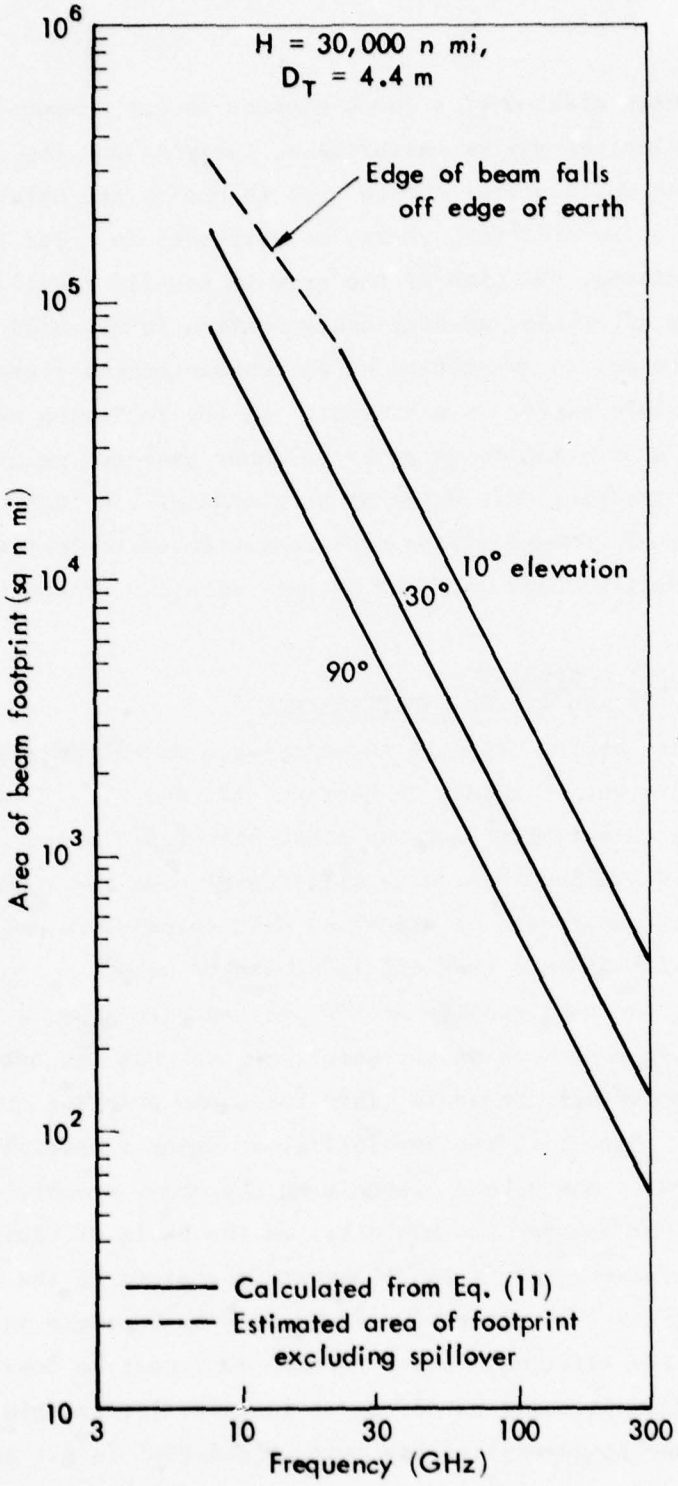

Fig. 24—Area of beam footprint as a function of frequency and elevation at ground terminal

VII. SOME SYSTEM ISSUES

The primary mission of a force element is not communication, although communication may be essential to carrying out its mission. Therefore, one would prefer not to have to modify the normal mission profile (e.g., the altitude, range, or attitude) in order to communicate. In addition, the time of the crew is usually tightly scheduled and, in times of crisis, greater concentration is demanded on mission-related functions, so automation of the communication operation to the greatest possible extent is essential. In the following sections of this report, consideration is given to those problems relating to pointing and tracking that arise at both ends of the link, and to the compatibility of communications equipment with user platforms, satellite configurations, and with the primary missions of the users.

TRADEOFF BETWEEN COMPLEXITY ON THE SATELLITE AND AT THE USER TERMINAL

Two points on the tradeoff curve between satellite and user antenna diameters were examined in Sections III and IV. These points, corresponding to satellite antenna diameters of 4.4 m and 1 m and terminals of 0.1 m and 10 m, were selected to meet the requirements of small mobile users and of wide-band data relay users. A more complete discussion of this tradeoff is presented here.

Clearly, the small mobile user's problems are greatly alleviated by using a larger antenna on the satellite, so that the user's beam can be correspondingly broader. This eases his pointing and tracking requirements. Moreover, the feasibility of using a satellite communications service may depend strongly on the size, weight, or cost of the required antenna and its gimbals. On the basis of equipment cost alone, the optimum tradeoff point between the sizes of the two antennas depends on the number of users served by a single satellite antenna over its lifetime. Other factors that must be considered in determining the optimum tradeoff point include, for example, the ability of the user to accomplish his primary function (e.g., as measured by the probability of mission success)--a factor which may well push

the optimum tradeoff point toward smaller user antennas than are dictated by relative antenna cost alone.

The performance tradeoff between the antenna sizes at the two ends of the communications link, under the conditions specified in Table 6, is illustrated by the solid sloping lines in Fig. 25. In this figure, the required satellite diameter, D_T, is plotted against the terminal antenna diameter, D_R, for a data rate of 10^6 bps (e.g., 60 Time Division Multiple Access (TDMA) users, each using digital voice at 16 kbps) with an availability of 99 percent. Note that, with a constant satellite antenna diameter of 4.4 m, these conditions can be met at frequencies up to 31 GHz with a terminal antenna diameter of 0.1 m. At 48 GHz, the required terminal antenna diameter increases to 0.28 m, while, at 101 GHz, it jumps to 13.9 m. At the higher frequencies, lower availability must therefore be tolerated if the receiver antenna size is to remain constant. Thus, with constant 4.4 m and 0.1 m antennas, availability falls to 96.3 percent at 48 GHz and to 94.1 percent at 101 GHz (see Fig. 10 (c and d)).

At smaller values of satellite antenna diameter, the terminal antenna diameter must be increased in the manner depicted in order to maintain the specified data rate and outage values. Thus, with a 1 m satellite antenna (the value selected for wide-band data relay users in Section IV), the 10^6 bps data rate would require a receiver antenna diameter of 0.46 m in the 20 to 30 GHz frequency region. This increases to 14.5 m when a data rate of 10^9 bps is required with the same availability.

The dashed lines in Fig. 25 join points of constant footprint width, W_F. The footprint width, and the corresponding values of the 3 dB beamwidth, δ_T, of the angular resolution of the transmitting antenna, are indicated in each case.

To improve system performance, the satellite EIRP per beam may be increased beyond the assumed value. This provides excess margin, which can be used to obtain higher availability or a multiple-user capability within the same footprint, rather than to decrease the user antenna diameter. In the multiple-user case, there is a multiple access problem. TDMA is more efficient than FDMA (Frequency Division

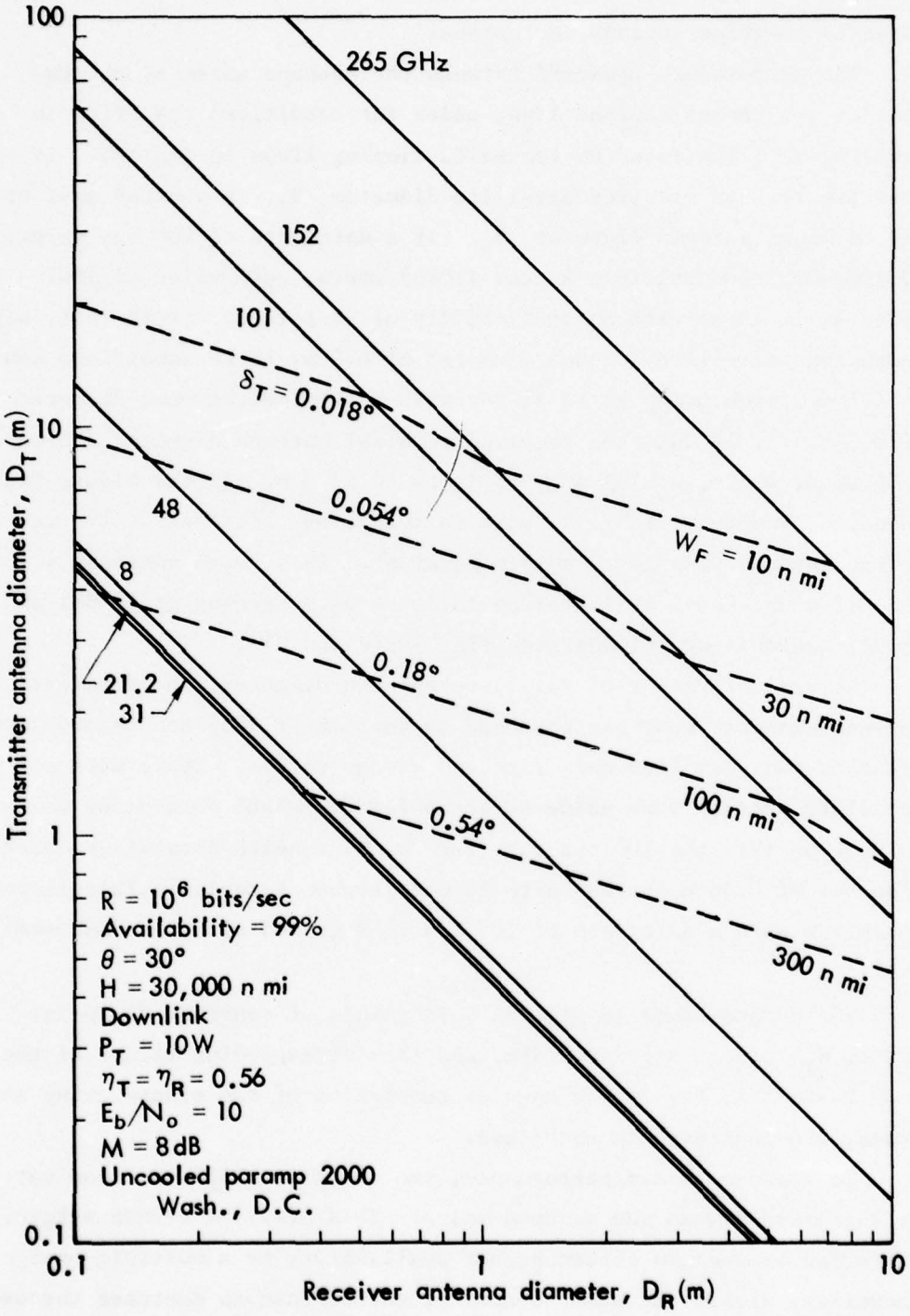

Fig. 25— Tradeoff between antenna diameters on satellite and at terminal

Multiple Access); but in both cases, the equipment complexity and time required for doppler search and frequency correction may be appreciably greater in the millimeter-wave band than at lower frequencies. The multiple access problem, including frequency, code, and phase synchronization, has not been examined in this study.

The employment of small terminal antennas greatly eases certain problems encountered by small mobile users, as discussed in Sections VIII through XII. At the same time, the correspondingly large size (4.4 m) of the satellite antenna results in very narrow beams, especially at the higher frequencies (see Fig. 23). These narrow satellite beams significantly decrease vulnerability to interference by friendly or unfriendly sources. At the same time, the small footprints obtained from these beams permit increased frequency reuse from the same satellite. The advantages associated with narrow satellite beams are obtained at the cost of increased pointing and tracking accuracy requirements at both ends of the link and a need for a more complex acquisition system, multiple beam antennas, and an autonomous computer-controlled assignment system for serving large numbers of widely spread, small mobile users. The pointing and tracking problem is discussed in Section VIII. The acquisition problem is a major one; while a detailed treatment is beyond the scope of this study, a few comments are in order.

THE ACQUISITION PROBLEM

Two generic antenna arrangements can be employed on the satellite: electronically scanned or steered multiple-feed or multiple-beam antennas (including phased arrays), and mechanically scanned single-beam antennas. Each type has its advantages and its problems.

Multiple-beam antennas have received much attention during recent years.[25] They usually involve an array of feed elements, e.g., horns which illuminate a lens antenna, or a parabolic or spherical reflector in either an offset or Cassegrainian arrangement. Their greatest advantage is that the beam can be stepped quickly (in nanoseconds to microseconds) from one position to another by switching among the feed elements. They are, however, limited in the degree to which sidelobes can be suppressed, especially when large angles are scanned. This

characteristic renders them more vulnerable to jamming, and so limits their usefulness in military systems.

Mechanically scanned antennas can maintain very low (e.g., 80 dB down)[16] sidelobes through essentially unlimited scan angles. The time required to scan from user to user, settle down, and begin information transfer (after frequency, code, and symbol and phase synchronization) is, however, long (usually a few seconds). They are generally limited in the number of users they can serve without employing a very large number of independent antennas (antenna "farms"). However, when only short messages are involved, they might be delivered without stepping the antenna--e.g., during the course of a continuous raster scan. While this essentially removes the limit on the number of users who can be served, it is efficient only if the density of users (average number per spot) is high over the area scanned.

With either type of antenna arrangement, a communications link can be established in one of two basic ways. In one approach, the user first directs his antenna beam at the satellite and transmits a brief acquisition message informing the satellite of his location, his identity, precedence level, and type of message (e.g., length); this transmission is received by the satellite either through a wide beam, e.g., an earth- or theater-coverage antenna, or through a scanned spot beam. The satellite then directs a beam at the user's location and goes into a search pattern surrounding the user's position until contact is made and a two-way communications link is established. In the second approach, the satellite continuously scans the entire area served, in either a continuous or stepped scan, receiving and transmitting messages as it moves along. While considerably less efficient, this second method may be adequate for low data rate communications in a dense user environment.

VIII. POINTING AND TRACKING AT HIGH MICROWAVE FREQUENCIES

When higher frequencies are employed with a given antenna diameter, narrower beams result. An extreme example is a laser communications system, where the beamwidths are measured in microradians. With narrower beams, the acquisition problem is aggravated and, after acquisition, more accurate tracking is required.

We first examine in this section the general pointing and tracking accuracy requirements and limitations as they relate to other system parameters. We then consider the pointing and tracking problems peculiar to wide-band data relay users, small mobile users, and the satellite station--with emphasis on the adaptation to higher frequencies.

OPEN-LOOP POINTING AND ACQUISITION

Techniques for the initiation of communications between a satellite and a user terminal (acquisition techniques) were mentioned in Section VII. In all cases, the user--knowing his own location and the satellite ephemeris--may begin by pointing a beam at the satellite in an open-loop (autonomous) manner. This initial pointing must be sufficiently accurate (usually to a few beamwidths) to ensure illumination of the satellite after only a nominal search. Searching may be accomplished by mechanically scanning or by electronically stepping the beam (with the aid of multiple feeds), or by a combination of both. After learning the location (latitude and longitude) of a valid user by means of the acquisition beam, the satellite may point a narrow communications beam toward the user (again in an open-loop manner), with sufficient accuracy to avoid excessive search time.

The solid angle which must be searched is determined by the location errors in the transmitter and receiver in conjunction with the slant range. Pointing errors will further increase the number of search positions. Assuming all errors to be random and independent, the resultant angular dimension of the field of view to be searched is the root-sum-square of the individual angular errors. Assume the satellite to be at the zenith and that the search field is small. Then:

$$\Delta\theta_x = \sqrt{\left(\frac{\Delta x_T}{H}\right)^2 + \left(\frac{\Delta x_R}{H}\right)^2 + \left(\Delta\theta_{xp}\right)^2} \tag{14}$$

and

$$\Delta\Omega = \Delta\theta_x \, \Delta\theta_y \ , \tag{15}$$

where Δx_T, Δx_R = x-components of the error in the location of the transmitter and receiver, respectively

$\Delta\theta_{xp}$ = x-components of the angular pointing error introduced by errors in attitude reference, mechanical linkage, etc.

H = satellite altitude

$\Delta\Omega$ = solid angle which must be searched

$\Delta\theta_x$, $\Delta\theta_y$ = angular dimensions of the field of view which must be searched, measured in the x- and y-directions, respectively.

Equations (14) and (15) show the relation between the required solid-angular search area, $\Delta\Omega$, and the errors in location and pointing. The search area is also related to the search time, T_s, by

$$T_s = \frac{\Delta\Omega \ t_d}{\Omega_b} \ , \tag{16}$$

where t_d = stepping time of the beam from one search position to the next, including the dwell, transit, and settling times

$\Delta\Omega$ = solid angle subtended by the main lobe of the search beam.

Equations (14) and (15) may be combined to yield

$$\Delta\theta_{xp}^2 = \frac{T_s \ \Omega_b}{t_d} - \left(\frac{\Delta x_T}{H}\right)^2 - \left(\frac{\Delta x_R}{H}\right)^2 \ . \tag{17}$$

Errors in satellite location are determined by errors in the ephemeris and timing. The error in the ephemeris is a function of the length of time the satellite has been tracked and the tracking system accuracy. Similarly, the error in the position of the small mobile user depends on the accuracy of the navigation system employed. With the deployment

of the Global Positioning System (GPS) after 1985, both the user and the satellite locations may be determinable to 10 to 20 m.[26] With a satellite altitude, H, of 30,000 n mi,* both $\Delta x_T/H$ and $\Delta x_R/H$ would then become negligible, in which case the required pointing accuracy would depend only on the time allowed for search, the beamwidth, and the stepping time.

To illustrate the application of Eq. (16) in this case, consider a 0.1 deg beam for which the stepping time, t_d, is 0.1 sec. If 100 sec are available for search, the open-loop pointing error may then be as large as 3 deg.

The pointing accuracy, in the case of mobile users, is limited by the accuracy of the attitude reference system employed. This performance will be discussed later in this section for the three stations of interest.

Tracking may be accomplished using either a satellite-borne beacon signal or the communication signal itself. Monopulse techniques† are usually employed to generate the error signal, but a conical scan‡ is used in some systems. Present tracking techniques may be extended to higher frequencies without change. The tracking accuracy is limited by the shape of the main lobe and the signal-to-noise ratio. The narrower beams obtained at higher frequencies generate usable error signals with small displacements, and so permit higher tracking accuracy--with other parameters remaining unchanged. In Sections III and IV, a value of 10 has been assumed for E_b/N_0, which is an adequate signal-to-noise ratio for most tracking purposes.

ANTENNA BEAMWIDTHS AND DSCS TERMINAL CHARACTERISTICS

As noted above, both the pointing and tracking requirements are closely related to the antenna beamwidth, δ, which decreases at higher

---

*It was found in Section V that a constellation involving nine satellites at 30,000 n mi altitude and 60 deg inclination provided worldwide coverage above 30 deg elevation about 97.5 percent of the time. This altitude is selected as a reference altitude in the remainder of this report.

†See Ref. 27, pp. 175-184.

‡See Ref. 27, pp. 166-175.

frequencies. The actual values of this quantity, obtained from Eq. (13), are presented in Fig. 26. For convenience, the values of δ for the frequencies and diameters of special interest here are shown in Table 10.

Table 10

BEAMWIDTHS FOR SELECTED
ANTENNA DIAMETERS AND FREQUENCIES
(Degrees)

Frequency (GHz)	Diameter (m)			
	0.1	1	4.4	10
21.2	10.3	1.03	0.234	0.103
31	7.04	0.704	0.160	0.0704
48	4.5	0.455	0.103	0.0455
101	2.16	0.216	0.049	0.0216
152	1.44	0.144	0.033	0.0144
265	0.82	0.082	0.019	0.0082

The various Defense Satellite Communications System (DSCS) terminals, which operate around 8 GHz, provide a convenient reference point for a discussion of the use of higher frequencies. The electronic characteristics of representative DSCS terminals are presented in Table 11. Included are the Fixed Satellite Communication terminal (FSC-78), the Mobile Satellite Communication terminal (MSC-61), the Transportable Satellite Communication terminal (TSC-86), a Ground Mobile Forces (GMF) terminal, two Water-borne (shipboard) Satellite Communication terminals (WSC-2/(V)1 and (V)2), and an Airborne Satellite Communication terminal (ASC-24). Note that the 3-σ tracking error ranges from 0.04 to 0.27 beamwidth. The antenna illumination appears to be chosen to yield narrow, high-gain beams with high efficiency, judging from the smallness of the reported values (averaging 1.16) of the constant k in the following equation:

$$\sigma = k\,\lambda/D\ . \tag{18}$$

(This constant usually ranges from 1.27 to 1.47.)

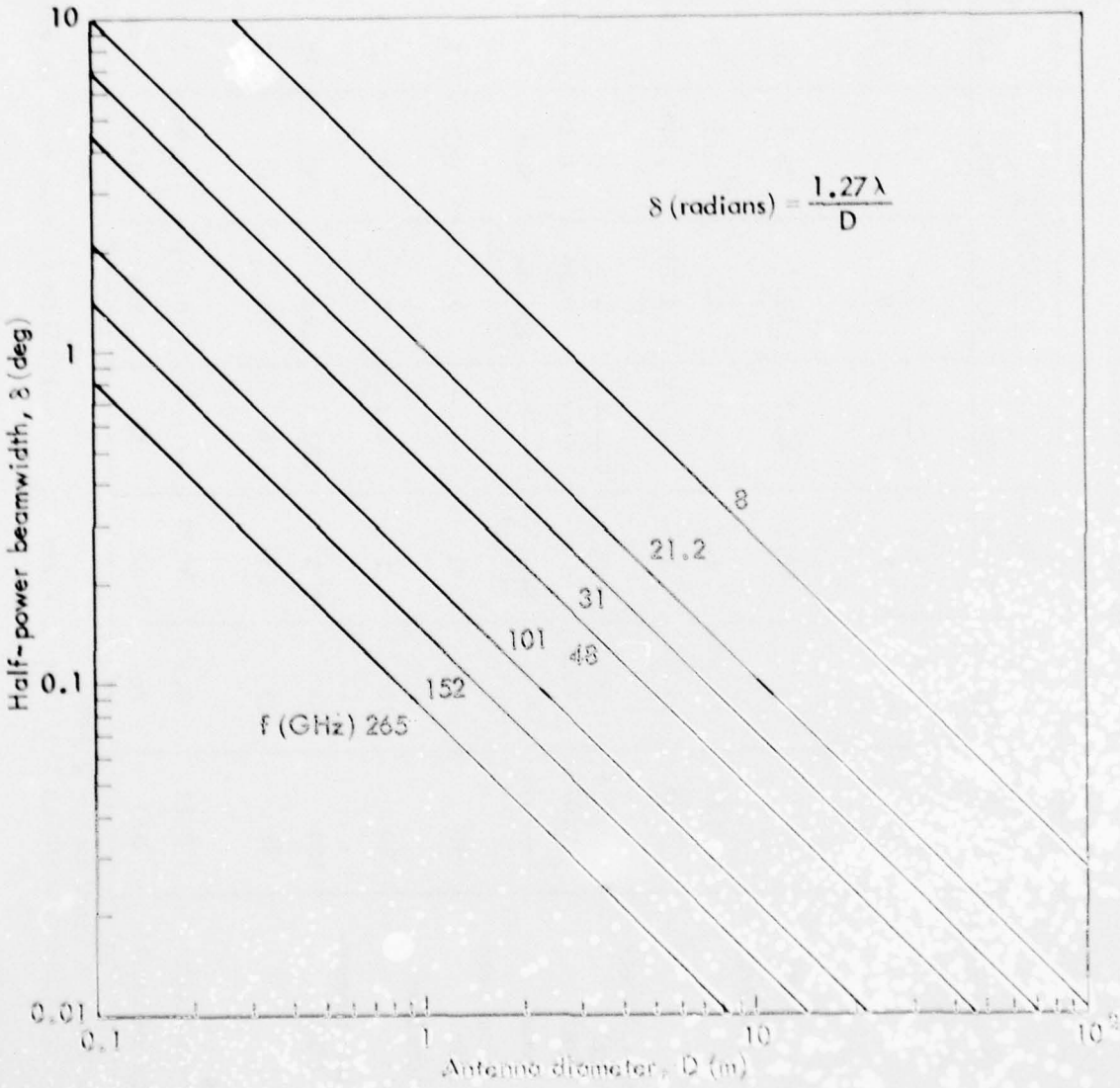

Fig. 26 — Half-power beamwidth as a function of antenna diameter and frequency

Table 11

DSCS TERMINAL CHARACTERISTICS

Characteristic	(28) FSC-78	(29) MSC-61	(30) TSC-86	(31) CMF	WSC-2 (32) (V)1	WSC-2 (32) (V)2	(33) ASC-24
Antenna diameter, D (m)	18.3	11.6	2.4	2.4	2.4	1.2	0.84
(ft)	60	38	8	8	8	4	2.75
Peak gain, G_r, at 7.25 GHz (λ = 0.0414 m)(dB)	62	56	42.5	42.5	42.7	36.7	32
Half-power beamwidth, δ (deg)	0.14	0.26	1.1	1.1	1.1	2.5	3
Constant, k[a]	1.08	1.27	1.13	1.13	1.13	1.29	1.06
3-σ tracking accuracy antenna (deg)	0.015	0.03	0.3	------	0.1	0.1	0.5
readout[b] (deg)	0.07	0.2	------	------	0.16	0.16	------
Acquisition mode	-------	------	Search 15°×4°	------	Spiral	Scan	Raster 20°
Acquisition time from turn-on[c] (min)	90	------	30	------	0.5	0.5	5
Maximum transmitter power (kW)	10	10	1	0.5	10	10	12.5
Receiver noise temperature, T_p (°K)	200	158	300	282	260	260	92
G_R/T_p (dB)[d]	39	34	18	18	18	12	12
3-σ tracking accuracy/beamwidth	0.11	0.12	0.27	------	0.091	0.04	0.017
Operates with radome?	No	No	No	No	Yes	Yes	Yes

[a] In the equation: δ (radians) = k λ/D.
[b] This is the accuracy with which the line of sight to the satellite is read out, in earth coordinates.
[c] Includes warm-up time.
[d] This ratio of the gain to the noise temperature of the receiver is the standard measure of its performance.

WIDE-BAND DATA RELAY USERS

Wide-band data relay users may require data rates as high as 10^9 bps, and therefore employ larger antennas than small mobile users. In Section IV, the availability of a downlink with a 10 m terminal antenna in conjunction with a 1 m satellite antenna was estimated as a function of data rate. When a cooled parametric amplifier is used in such a link, in conjunction with coherent modulation, the estimated availability at data rates of 10^8 and 10^9 bps, respectively, at 30 deg elevation (obtained from Fig. 18) is shown below:

Frequency (GHz)	Estimated Availability (percent)	
	At 10^8 bps	At 10^9 bps
21.2	99.9	99.5
31	99.8	99.4
48	99.3	98
101	98	97
152	98	96
265	97	94

No fundamental problems are anticipated in developing terminals with antennas as large as even 20 m for operation at 30 GHz. Higher tracking accuracy would be required at the higher frequency; expressed as a fraction of a beamwidth, however, the required tracking accuracy is independent of frequency, so no fundamental tracking problems are anticipated. To illustrate the tracking accuracy achievable with equipment of this nature, it is noted that the AN/FPS-16 radar, with a 12 ft antenna and a beamwidth of 1.1 deg, has systematic and random tracking errors of 0.0057 deg each when the signal-to-noise ratio is at least 20 dB.[34] The AN/TPQ-18 SN-5 radar, with a 0.4 deg beam, has a random tracking error of 0.00287 deg. The RCA Mobile Medium-Range Tracking Radar System has a tracking accuracy of 0.002 deg, with a beamwidth of 1.2 deg.[35] Note that the tracking errors of these systems are well under one-hundredth of a beamwidth.

Wide-band data relay users may be able to devote considerable time to the search process, since they seldom need to perform this task with geostationary satellites. Thus, 90 min is allowed for

acquisition (including warm-up) in the case of the FSC-78 terminal. It can be seen from Eq. (17) that, in this case, the permitted open-loop pointing error may greatly exceed the beamwidth.

On the other hand, astronomical telescopes have demonstrated open-loop pointing errors which are much smaller than the narrowest beamwidth listed in Table 10 (0.0082 deg). Thus, for example, the millimeter-wave radio telescope at Onsala, Sweden,[36] has an aperture of 20 m and can be pointed with an rms accuracy of 2 sec of arc (0.00056 deg), which is less than one-fifteenth of the narrowest beamwidth considered here. The task of astronomical telescopes is somewhat simplified, of course, by the fact that the target location is accurately known, and the only tracking required is that needed to overcome the effect of the earth's rotation. This is usually accomplished by uniform drive of an equatorial mount.

Pointing an antenna at a moving satellite from a stationary platform is a more difficult task than that faced by astronomers, but is still relatively straightforward. The ephemerides of the satellites should preferably be stored in a computer, together with the location and attitude of the platform. This information, together with the time of day, permits calculation of the line of sight to the satellite. With geostationary satellites, the pointing and tracking problems are minimal. With satellites in high-altitude inclined orbits, however, the pointing and tracking operations must extend over the entire sky above 30 deg elevation. This may lead to considerable added cost and inconvenience, but the angular rates involved are so low that little loss in accuracy should result. This can be seen from Fig. 27, which presents the maximum (overhead) angular rates for the orbits discussed in Section V. Handover from one satellite to the next will be required; this adds to system complexity, but should have little impact on pointing or tracking accuracy.

SMALL MOBILE USERS

Mobile DSCS terminals include the shipboard WSC-2/(V)1 and (V)2, and the airborne ASC-24 terminal, which has a 33 in. antenna (Table 11). Antennas of this size can only be accommodated on larger ships and aircraft, as discussed in Section IX. When larger satellite

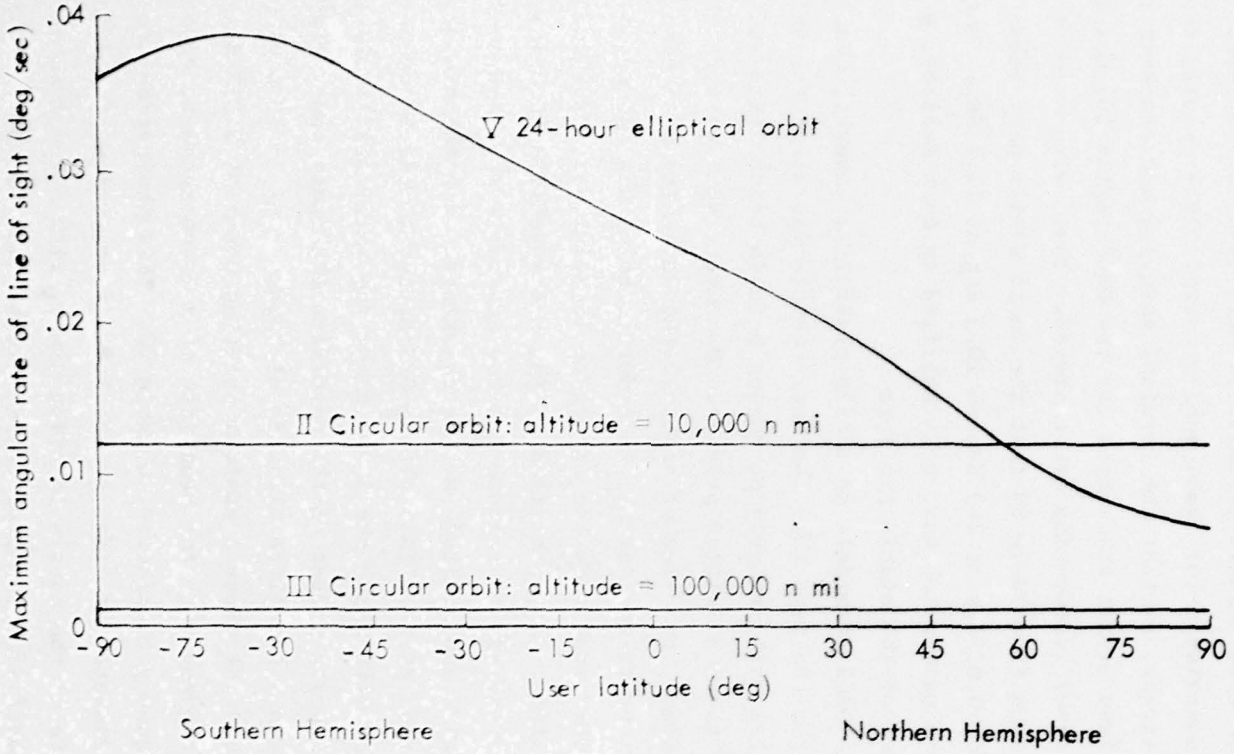

Fig. 27—Maximum angular rate of the line of sight to satellites in various orbits

antennas are employed at higher frequencies, smaller user antennas will suffice, in which case the satellite communication service can be extended to smaller vehicles. Thus, in the baseline system discussed in Section III, relatively small (4 in., or 10 cm) antenna diameters were postulated for small mobile users. As a result, the beamwidths are larger, so that the terminal pointing and tracking requirements are less strict than those for the DSCS terminals, despite the fact that higher frequencies are employed. Thus, with a 10 cm antenna, it is seen from Table 10 that the small mobile user beamwidth ranges from 0.82 deg at 265 GHz to 10.3 deg at 21.2 GHz. Moreover, the antenna mass which must be stabilized is much smaller, greatly reducing the cost of the stable platform.

As with the DSCS terminals on mobile platforms, however, complications arise from the fact that the user vehicle (an aircraft, ship, or ground vehicle) will probably be moving both in translation and rotation during the acquisition process. Moreover, when geostationary orbits are abandoned, the line of sight to the satellite will also be moving with respect to the earth. In order to point his antenna at the satellite, the user must know the satellite location, his own location, and his own attitude. As with fixed users, the satellite location may be obtained with the aid of computer-stored ephemeris data and a clock. The user's location and attitude may be determined with the aid of an Inertial Navigation System (INS) or the GPS system mentioned above.

The accuracy with which the location of the small mobile platform must be known is quite modest at the satellite altitudes considered above. Thus, with a satellite altitude of 30,000 n mi, a 30 n mi navigation error would introduce a maximum pointing error of 0.057 deg. This is small compared with the beamwidth of a 10 cm antenna, even at the highest frequency considered in Table 10. This navigation accuracy would also be adequate, at least at the lower frequencies, for informing the satellite of the user's location since, with a 4.4 m antenna, the width, or small dimension, of the satellite beam footprint ranges from 123 n mi at 21.2 GHz to 25.7 n mi at 101 GHz (see Fig. 23) at 90 deg elevation.

The accuracy with which the attitude of the user platform must be known is determined by the user beamwidth and the size of the angular

field which can be searched in the time available. Ideally, the attitude error should be smaller than the beamwidth which, as seen from Table 10, ranges from 0.82 deg at 265 GHz to 10.3 deg at 21.2 GHz when a 0.1 m terminal antenna is employed. Attitude accuracies of this magnitude present little challenge to most attitude reference systems.

Navy carriers, cruisers, and submarines have Shipboard Inertial Navigation Systems (SINS) whose accuracy greatly exceeds that needed for communication when a 0.1 m antenna is employed. Small Navy ships and ground vehicles provided with pendulous gyros and magnetic compasses could provide attitude information with an accuracy of 1 to 2 deg at a cost of $6,000 to $8,000. A strapped-down heading and reference system, with an accuracy of 0.1 to 0.25 deg, could be provided at a cost of $25,000 to $30,000.* This accuracy is more than adequate for communications systems employing 10 cm antennas. At a cost of $40,000 to $50,000, an accuracy of about 0.03 deg could be achieved. This would suffice if considerably larger communications antennas were employed (assuming that space could be found for them on small vehicles).

The angular rates of roll, pitch, and yaw of small mobile terminals greatly exceed the angular rates of the line of sight to the satellite. This can be seen, in the case of Navy ships, by comparing the data presented in Fig. 27 with that in Table 12. Thus, the roll rates of ships in heavy seas range from 8 to 21 deg/sec, whereas the maximum angular rate of the line of sight to a satellite in any of the orbits considered in Section IV is 0.04 deg/sec. (This worst case is for a 24 hr elliptical orbit observed overhead at perigee.) The roll rate thus exceeds the maximum line-of-sight rate by a factor ranging from 200 to 500. The angular rates of ground vehicles and aircraft can be higher than that of ships, so they also considerably exceed the angular rates of the satellites considered. We conclude that no additional hardship due to tracking is imposed on mobile users by abandoning geostationary orbits in order to avoid low elevation angles, for the reasons discussed in Section III.

*Private communication from personnel of the Kearfott Division of Singer-General Precision, Inc., Little Falls, New Jersey.

Table 12

ANGULAR MOTION OF SHIPS[a]

	Major Ships		Medium Ships	
	Sea State[b]			
	5	7	5	7
Roll				
Period, sec	12	12	9	9
Amplitude, deg	16	16	25	31
Maximum roll rate, deg/sec	8.4	8.4	17.5	21.6
Pitch				
Period, sec	7	7	6	6
Amplitude, deg	5	5	6.5	12
Maximum pitch rate, deg/sec	4.5	4.5	6.8	12.6
Yaw				
Period, sec	> 60	> 60	> 60	> 60
Amplitude, deg	2	5	4	7.5
Maximum yaw rate, deg/sec	< 0.21	< 0.79	< 0.42	< 0.79

[a]"Major" ships here exceed 10,000 tons; "medium" ships range from 1,000 to 10,000 tons.

[b]The wave height at Sea State 5 ranges from 9 to 15 ft; at Sea State 7, it ranges from 24 to 36 ft. Wave heights exceeding 12 ft are encountered 40 percent of the time in a large portion of the North Atlantic Ocean in winter.

THE SATELLITE PLATFORM

In the "base case" of small mobile users discussed in Section III, the complexity was shifted from the user terminal to the satellite in order to simplify the terminal. A 4.4 m diameter was thus assigned to the satellite antenna. The associated beamwidths are so narrow (Table 10) that very precise pointing and tracking are needed. This places a great premium on accuracy in the satellite attitude reference system. Fortunately, systems which meet--and some which considerably exceed--the requirements are either in use or in development.

Most of the satellite attitude reference systems considered use some combination of sensors to update a gyro-stabilized reference platform, usually with the aid of statistically optimal filtering. Kalman filtering,[37,38] for example, is widely used. Some characteristics of the main types of satellite attitude reference systems are presented in Fig. 28.

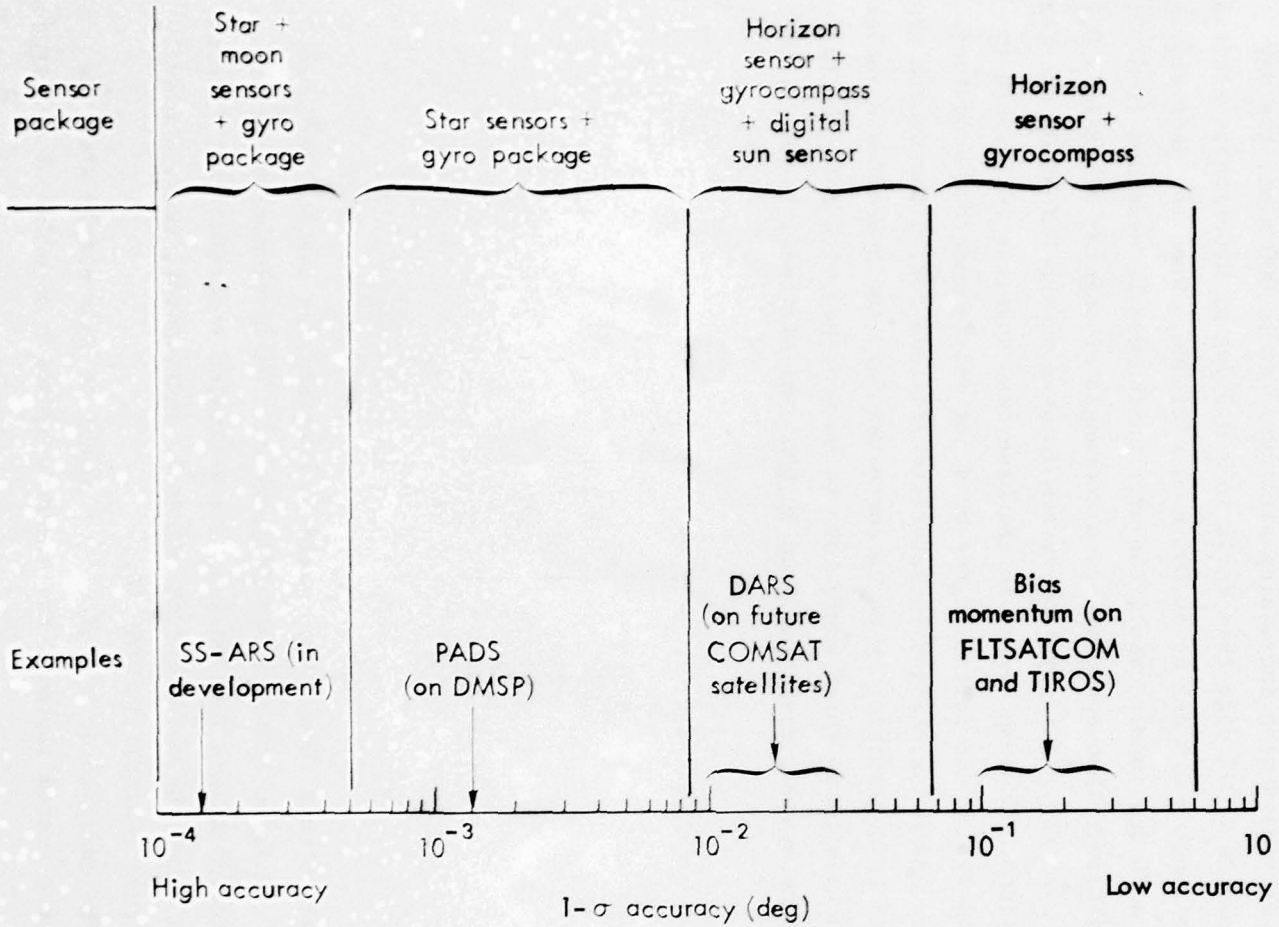

Fig. 28 — Satellite attitude reference systems

The simplest, but least accurate system (designated as "bias momentum" in Fig. 28) combines a horizon sensor and a gyrocompass. The horizon sensor provides roll and pitch information with a 3-σ accuracy of about $\pm$ 0.1 deg. The gyrocompass indicates yaw with an accuracy which decreases with increasing altitude. At 10,000 n mi, the 3-σ accuracy is $\pm$ 0.2 deg; this falls to $\pm$ 0.3 deg at synchronous altitude, and to about $\pm$ 0.5 deg at 30,000 n mi altitude. When the user elevation is 30 deg (worst case), the area which must be searched from 30,000 n mi altitude then approximates a rectangle of angular dimensions 0.2 deg $\times$ 0.21 deg. This type of system is used on the FLTSATCOM and TIROS satellites. Its employment in the base case downlink (discussed in Section III) would introduce the need for only a moderate amount of search. Assuming changes in satellite attitude during the search process to be negligible, or to be corrected for, the approximate number of beam positions which would have to be searched with this attitude reference system, operating from 30,000 n mi altitude, is as follows:

Frequency (GHz)	δ (deg)	Number of Positions
21.2	0.234	1
31	0.160	4
48	0.103	9
101	0.049	18
152	0.033	39
265	0.019	116

It appears that this system would be adequate for use in the "base case," at least at the lower frequencies. While simple in concept, this system is not inexpensive; the estimated recurring cost (future models after the nonrecurring research, development, test, and evaluation cost (RDT&E)) is $800,000.*

The addition of a digital sun sensor to this simple attitude reference system improves the accuracy by about an order of magnitude,

*Private communication with personnel of the Avionics Division, Honeywell Corporation, St. Petersburg, Florida.

yielding a 1-σ error of 0.01 deg in roll and pitch, and 0.03 deg in yaw. An arrangement of this type is used in the Digital Attitude Reference System (DARS), which is planned for future use by COMSAT. This system would be suitable for use with the downlink employing the 4.4 m mirror reflector discussed in Section III. The estimated cost of a system of this type with a 7 to 10 yr life is about $1 million.

The addition of stellar sensors to the DARS system can improve the accuracy by another one to two orders of magnitude. An example of this is the Precision Attitude Determination System (PADS,)* which is used on the Defense Meteorological Support System (DMSP) satellite. This device achieves a 1-σ accuracy of 0.0014 deg in all three axes at a cost of approximately $2 million.

A second example of stellar-inertial systems is the Space Sectant-Attitude Reference System (SS-ARS), which is presently under development.(39) Since this system promises to yield very high accuracy at a reasonable cost, it bears special mention. The SS-ARC employs two sensors to measure the angle between the moon and selected stars. On the basis of this information, plus information on the moon's ephemeris and time, an onboard computer reads out attitude with a 1-σ accuracy of 0.6 sec of arc (0.00017 deg) within 15 min. (Satellite position is also determined with an error of less than 1 mi.) This accuracy far exceeds that required for any presently contemplated microwave communications system, since the stated accuracy represents only one-tenth of a beamwidth for a 50 m antenna at 265 GHz. Attractive features of the SS-ARS include the fact that it is completely autonomous, small (2.92 ft^3), low power (45 W), and light weight (43 lb). It is immune to radio frequency interference and jamming, and to severe nuclear environments. It contains no high-risk components and is expected to have a 5 yr life in the space environment. It also will operate satisfactorily on a maneuvering spacecraft. The Air Force plans to implement this system in the near future with an on-orbit demonstration planned for 1979 or 1980. The estimated cost is three-quarters of a million dollars.

Attitude accuracy always can be traded for increased search time. This is a profitable approach when rapid search is possible, as with

*Private communication with personnel of the Avionics Division, Honeywell Corporation, St. Petersburg, Florida.

an electronically stepped beam or when a small reflector does the scanning. The search rate can be increased by broadening the receiver search beam while simultaneously decreasing the post-detection bandwidth in order to preserve signal-to-noise ratio. This approach has been proposed for use with laser communications systems.*

Many of the preceding attitude reference systems have considerably more accuracy than is required for the present application, and one might hope to design a simpler, less costly system. It appears, however, that significant cost reductions are difficult because, in order to meet the requirement for a 5 to 10 yr lifetime, all of the systems require at least three (preferably four) gas-bearing gyros, each of which costs $50,000. In addition, horizon sensors of the scanning type cost approximately $175,000, while those of the "staring" type cost twice as much. The staring horizon sensors have no moving parts, and so promise a very long lifetime; they also have an estimated accuracy of a few hundredths of a degree when operating from 30,000 n mi.

It is concluded that long-lived satellite attitude reference systems are very expensive (more than half a million dollars) even when the accuracy is "nominal" (a few tenths of a degree). The extra cost needed for the ten-fold improvement in accuracy associated with operation at the higher frequencies appears to be relatively small. The digital sun sensor, for example, costs only about $70,000.

---

*Private communication with personnel of the Barnes Engineering Corporation.

IX. COMPATIBILITY OF HIGHER FREQUENCY TERMINALS WITH USER AND SATELLITE PLATFORMS

In examining the feasibility of employing the higher frequencies in satellite communications systems, an important consideration is the compatibility of the communications equipment with the satellite and user platforms. This factor is particularly important when consideration is given to extending the communications service to large numbers of such users as small ships, small aircraft, and ground vehicles. Such platforms impose tight constraints on the weight, size, power, and location of the communications equipment. These constraints are examined in this section. The availability and performance of radomes and antennas suitable for the higher frequencies are also discussed. The weight and size of the satellite station must be considered in relation to the space shuttle, which has a cylindrical payload chamber 15 ft in inside diameter and 60 ft long and can carry 6000 to 7000 lb to either geostationary orbit or into a circular orbit with an altitude of 30,000 n mi and an inclination of 60 deg. (The latter orbit is attractive because it provides worldwide coverage with elevation angles at the user which nearly always exceed 30 deg, as shown in Section V.)

SIZE AND LOCATION CONSTRAINTS

Presently planned (DSCS) SHF mobile ground terminals are costly and bulky--hence, they are limited to the larger vehicles. Four- and eight-ft antennas are employed on ships, and 33-in. antennas on aircraft (see Table 11). Emphasis is on geostationary satellite orbits, which dictate the use of low elevation angles for high latitude users. In such cases, obstruction of the antenna beam by other components and structural members (e.g., the superstructure on a ship) is a serious problem, often demanding dual antennas.

Many of these compatibility problems are alleviated in the "base case" downlink discussed in Section III. The "base case" antenna is 4.4 m in diameter--the largest diameter compatible with the space shuttle. This large satellite antenna permits the use of very small (10 cm) terminal antennas. Elevation angles below 30 deg are avoided

AD-A056 100 RAND CORP SANTA MONICA CALIF F/G 17/2.1
THE FEASIBILITY OF EMPLOYING FREQUENCIES BETWEEN 20 AND 300 GHZ--ETC(U)
MAY 78 L MUNDIE, N FELDMAN

UNCLASSIFIED RAND/R-2275/DCA NL

2 OF 2
AD
A056 100

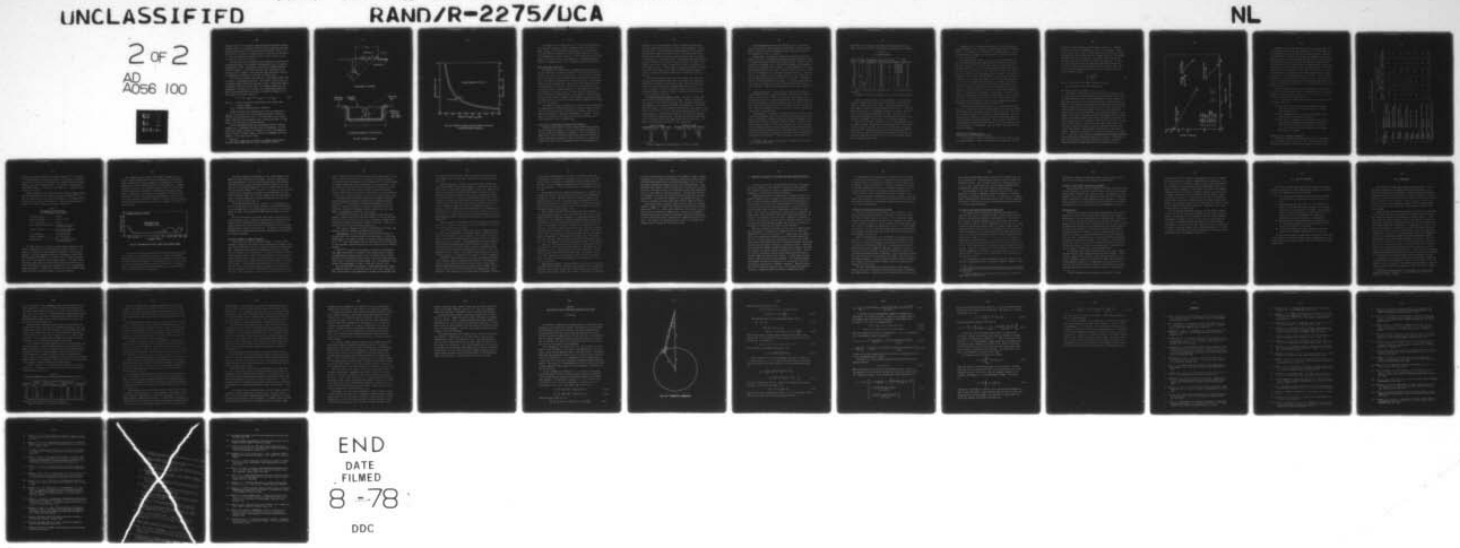

END
DATE
FILMED
8-78
DDC

through selection of a satellite constellation involving high-altitude inclined orbits. It was shown in Section III that adequate performance for many applications can be achieved with this system. Thus, it is seen from Fig. 10 that, at 30 deg elevation, a data rate of 10^6 bps* is possible with estimated availabilities which range from 98.9 percent at 31 GHz to 89 percent at 265 GHz.

The small size of the terminal antennas employed in this base case system permits their use on smaller user platforms than are presently contemplated for SHF. Considerable flexibility in antenna placement would be available, so that obstruction by other components of the platform could be avoided. Even with small ships and ground vehicles, no compatibility problem due to antenna size should arise.

With aircraft platforms, the drag due to a projecting radome would be reduced to negligible proportions. The "radome" could, in fact, be a conformal window, flush with the aircraft skin. Figure 29(a) depicts the geometry involved, and Fig. 29(b) is a schematic diagram of the arrangement. Allowing for a clearance of one wavelength between the edge of the beam and the aircraft skin, the required diameter, W, of the opening in the skin is given by

$$W = 2\,B \cot \theta_{min} + D \csc \theta_{min} + 2\,\lambda \csc \theta_{min}\,, \qquad (19)$$

where B = depth of beam pivot point beneath the aircraft skin

D = antenna diameter

θ_{min} = minimum allowable angle of elevation.

Figure 30 presents the calculated value of W as a function of θ_{min} for the case in which a 10 cm antenna is mounted as close as possible to the surface (B = D/2). It is seen that a 40 cm (16-in.) window would then permit operation down to 30 deg elevation; at lower angles, the required size increases rapidly.

Such an arrangement would avoid the problems faced by external radomes, e.g., aerodynamic drag and erosion by raindrops. The cost would also be small relative, for example, to that of the AN/ASC-24 radome on the E-4 aircraft, which, in order to accommodate its 33-in. antenna, is 6 ft wide and 18 ft long.

---

*10^6 bps is sufficient to provide, for example, Time Division Multiple Access (TDMA) digital voice at 16 kbps to 60 users.

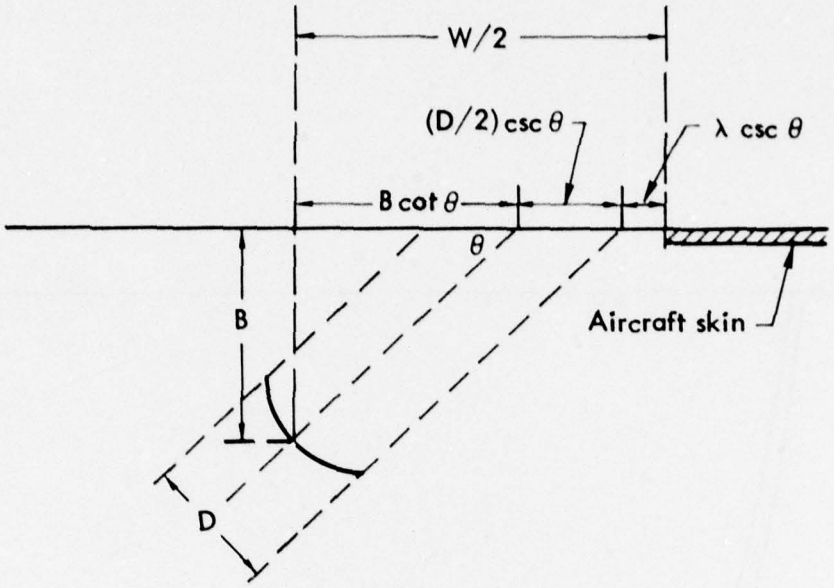

(a) Calculation of diameter

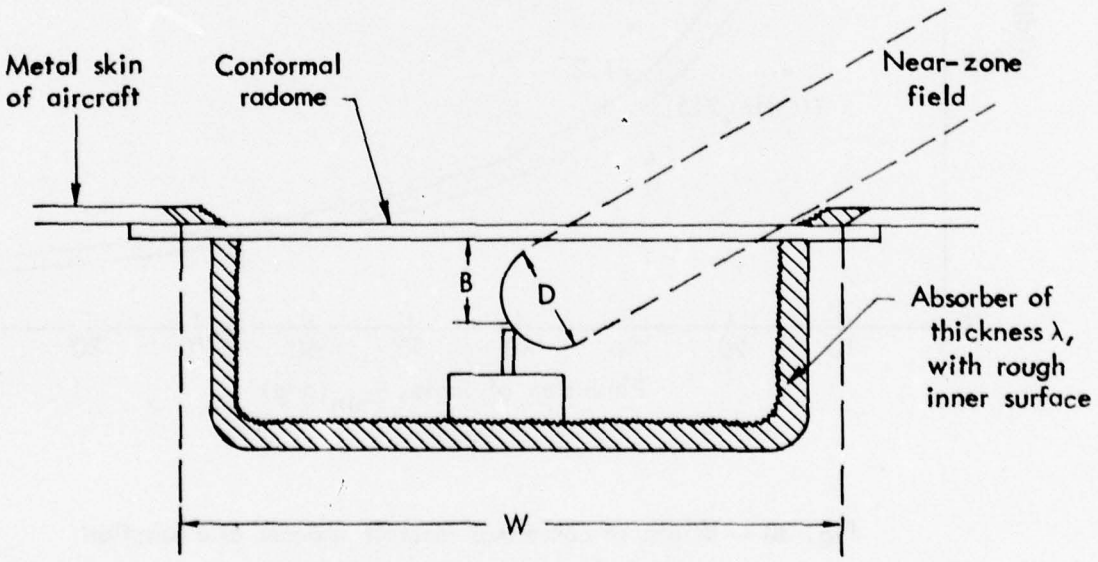

(b) Schematic diagram of aircraft antenna

Fig. 29— Conformal radome

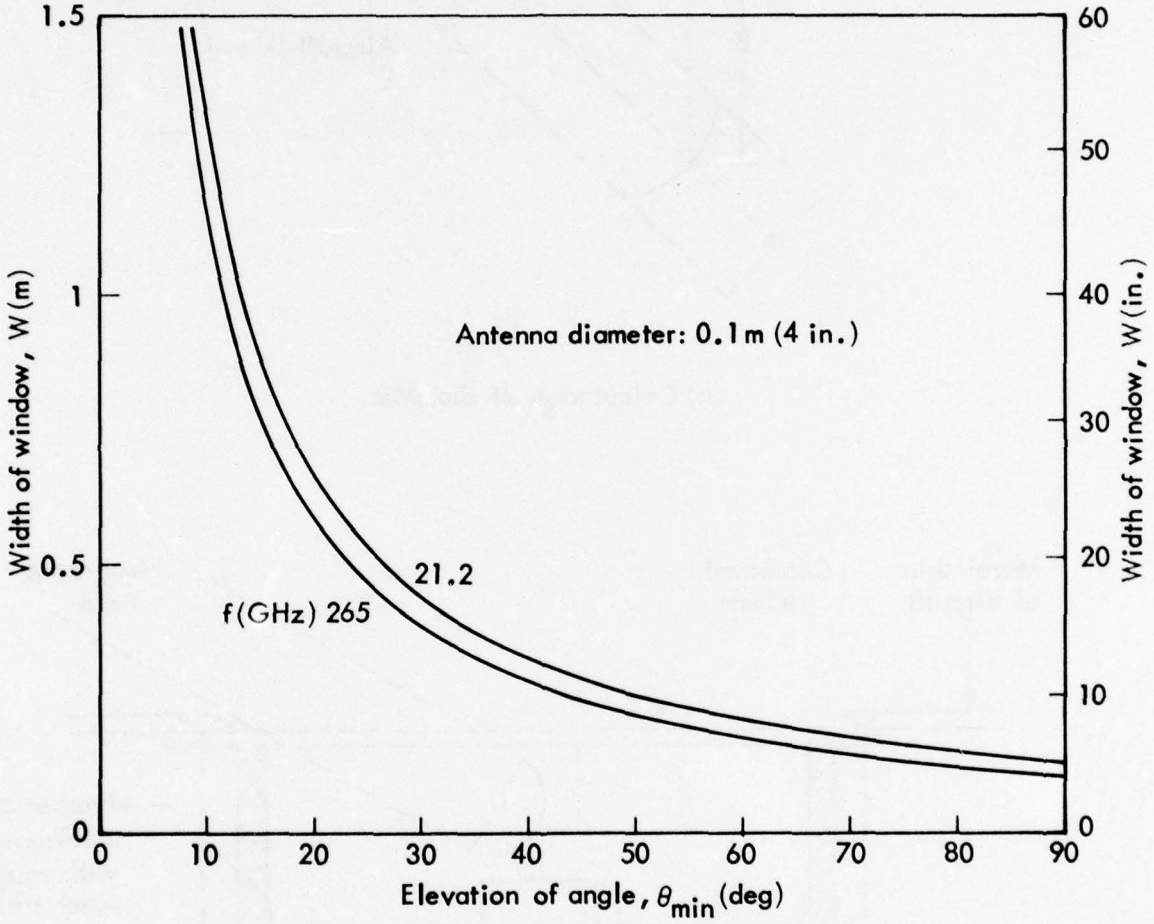

Fig. 30 — Width of conformal aircraft radome as a function of elevation angle and frequency

We conclude that no significant size or location constraints are introduced by operating at higher frequencies up to data rates of 1 Mbps. Indeed, if a sufficiently large antenna can be used in the satellite, the user problems are eased so that a wider use of satellite communications becomes feasible. If the required data rate corresponds to only one to three voice channels, a 1 m diameter satellite antenna, in combination with a 0.1 m terminal antenna, would suffice.

WEIGHT AND POWER CONSTRAINTS

In examining the compatibility of communications stations with the user platforms, two generic components of the former must be considered: the antenna and the electronics. In the systems postulated above, the antenna poses no weight problems for the small mobile user since the diameter considered for it was small (0.1 m). The antennas employed by the wide-band data relay user are fixed and require only limited mobility; in any event, no increase in size would be associated with a switch to higher frequencies. The diameter of the satellite antenna (4.4 m) was chosen to fit into the space shuttle and should introduce no weight problems. The assembly of antenna "farms" in space could, however, present a fairly complex engineering problem. The characteristics of various satellite antenna systems are discussed later in this section.

The weight and power compatibility of the electronics package with the communications stations would become a problem at higher frequencies if the efficiency were to degrade too seriously, since the required output power is reasonably independent of frequency. Accordingly, the variation of efficiency with operating frequency is of crucial importance, and is examined next.

Efficiencies of High-Power Millimeter-Wave Amplifiers

Packaged power amplifiers involve power-conditioning equipment and output amplifier stages. The power-conditioning equipment efficiency is high and independent of frequency. Over a large range of power levels, current technology permits high efficiency whether one or many independent voltages are supplied, whether the voltages and currents are high or low, and whether coarse or fine regulation is

provided. The only requirement is that the normal operating power levels be high enough to make the no-load losses negligible. Because the efficiency of the power-conditioning equipment is high, the output amplifier becomes the dominant factor. The output power device, which forms the heart of the power amplifier output stage, is either a vacuum tube or a solid-state device. Although vacuum tubes generally are being replaced by solid-state devices, this does not apply at the highest power levels. Thus, at high power levels in the millimeter-wave band, only one or a small number of vacuum tube devices are likely to be used, rather than a large number of lower-powered solid-state devices. Vacuum tube amplifier efficiency is therefore a matter of concern.

Traditional microwave amplifiers--particularly those using the klystron and traveling wave tube (TWT)--are suitable for generating high power at frequencies below about 30 GHz. Above that frequency, the circuit losses and voltage breakdown problems are severe. As a result, a number of new tube types have evolved; these include the extended-interaction amplifier (EIA), the ubitron tube, the coupled-cavity TWT, and the gyrotron.

Extended-Interaction Amplifier (EIA). The EIA is a linear beam klystron with an extended interaction cavity. Varian of Canada has tested an EIA at 94 GHz which delivered 100 W peak power (30 dB gain).* The bandwidth of this device was 40 MHz. Development of a 94 GHz EIA which will operate at 1 kW peak power and 100 W CW is anticipated. This EIA will be the size of a 5-in. cube and will weigh less than 15 lb (including magnets). Varian predicts that the EIA can produce CW power levels similar to the power levels achieved with their extended-interaction oscillator (EIO); these power levels, and the peak powers estimated to be achievable with the EIA, are listed below:

VARIAN OF CANADA DEMONSTRATED EIO CW POWER LEVELS		VARIAN OF CANADA ESTIMATED EIA PEAK POWER CAPABILITY	
Frequency (GHz)	*Power (W)*	*Frequency (GHz)*	*Power (W)*
18	1100	35	14,000
30	650	94	4,000
70	150	140	200
140	30	270	40
155	10		
280	1		

*Private communication with personnel of Varian of Canada.

The CW amplifiers will have an efficiency of 10 to 15 percent and the pulsed power amplifiers have an efficiency of about 7 percent. These efficiencies could be doubled by using a depressed collector. The bandwidth is about 0.4 percent.

Ubitron Tube. The ubitron (undulating beam interactions) tube employs a DC electron beam moving through an undulating magnetic field to provide high-power millimeter-wave amplification. This tube has the advantage of requiring only a relatively weak magnetic field (approximately seven kilogauss) and is capable of large bandwidths.[40] It has the disadvantage of low efficiency. Several years ago, General Electric built a 150 kW ubitron at 54 GHz with 6 percent efficiency. One solution to the problem of low efficiency would be to use a depressed collector, which would raise the efficiency to 30 percent. Although it has not yet been experimentally verified, it is believed that ubitrons can be used at frequencies as high as 100 GHz and at power levels of 50 to 100 kW CW. These power levels require voltages of from 60 to 70 kV.

Coupled-Cavity TWT. A power level of 1 kW at 94 GHz has been demonstrated with the coupled-cavity TWT.* This device is limited to power levels of from 6 to 8 kW. An efficiency of 30 percent can be obtained with the use of depressed collectors. The coupled-cavity TWT has a gun convergence (ratio of cathode area to cross-section area of the electron beam) which ranges from 150 to 200--it can be as high as 600. Such high convergence ratios can be used to achieve either high power output or long lifetime.

Gyrotron Tube. The highest recorded millimeter-wave power levels, both peak and average, have been achieved with the electron cyclotron maser--or gyrotron. This tube represents a major breakthrough for frequencies above 30 GHz, extending to 300 GHz or more. A group at the Gork'ii State University in the Soviet Union was the first to develop practical high-efficiency gyrotrons, and that success has stimulated parallel work in the United States. Under Department of Energy sponsorship, Varian Associates is currently developing a tube at 28 GHz with a CW power level of 200 kW.[41] Work in progress covers 200 kW tubes

*Private communication with personnel of Hughes Research Laboratories, Malibu, California.

operating in CW, long-pulse, and high-pulse-repetition-rate modes. Table 13 is a list of CW cyclotron masers, operational or in design.

Table 13

CW GYROTRON DEVICES

Frequency (GHz)	Power (kW)	Gain (dB)	Harmonic Number	Tube Type[a]	Efficiency (percent)	Magnet[b]	See Reference
10		10	2	GK		Standard	42
15	4	--	1	GM	50	Standard	43
25	4.5	--	2	GM	16	Standard	43
28		20	1	GK		Standard	44
33.7	9	--	2	GM	40	Standard	45
37.5		20	1	GT		S.C.	46
37.5	200	--	1	GM		S.C.	47
107	12	--	1	GM	31	S.C.	48
150	7	--	2	GM	15	S.C.	48
150	22	--	1	GT		S.C.	49
158	0.002	--	2	GM	10	S.C.	48
230	1 to 10	--	2-4	GM		S.C.	46
333	1.5	--	2	GM	6	S.C.	48

[a]GK = gyroklystron; GM = gyromonotron; GT = gyro-traveling-wave amplifier.

[b]Standard = normal electromagnet; S.C. = superconducting magnet.

There are three variations of the gyrotrons. The gyromonotron oscillator (GM), which is the type incorporated in Soviet devices, involves a single oscillatory cavity. The gyroklystron (GK) oscillator employs resonant cavities separated by drift spaces. These two designs are limited to a bandwidth of about 0.1 percent. The third type is a gyro-traveling-wave amplifier (GT). In this device, a traveling electromagnetic wave and an electron beam interact as they traverse a waveguide. The GT has a 3 to 10 percent bandwidth.

While the efficiency of gyrotrons in U.S. experiments has been less than 1 percent, the Soviets have obtained 12 kW at 100 GHz with an efficiency of 31 percent, and 1.5 kW at 333 GHz with 6 percent efficiency.[50] Recent theoretical work by Sprangle and Drobot[51] at NRL has made the Soviet efficiency claims quite credible and, indeed, has shown that efficiences of 30 to 40 percent should extend into the megawatt power range.

Tunability may be a useful characteristic if sufficient instantaneous bandwidth is not achievable. Assuming that stable GT configurations can be built, it is estimated that a tuning range of 5 to 10 percent should be achieved with relative ease, and that 20 to 30 percent may be possible.[46]

For higher powered systems, i.e., 5 to 10 kW average power, the size and weight of the power supply and output amplifier stage will dominate the total.[46] In such cases, system size and weight estimates are similar to those for lower frequency systems of the same output power and tube efficiency. For lower power systems, e.g., 100 W, the size of the gyrotron electromagnet may be dominant. One method for reducing the size of the required magnet is to operate the gyrotron at a harmonic. This reduces the magnetic field and therefore the magnet size--but need not impair the efficiency. For example, the highest reported efficiency (CW operation) at millimeter wavelengths, 40 percent at 33.7 GHz, was obtained using the second harmonic. Another method for reducing magnet size is to use a superconducting magnet instead of a conventional electromagnet. Development of compact cooling units is required before these superconducting magnets can be packaged efficiently. With magnetic fields in the 50 to 100 kilogauss range using superconducting magnets, compact gyrotron amplifier packages at frequencies up to 300 GHz should be practicable.[46]

Comparing the ubitron and gyrotron for use in the millimeter-wave band, it is noted that the gyrotron has a higher efficiency and requires less voltage (about two-thirds) than the ubitron, while the ubitron requires a smaller magnetic field and has a larger bandwidth. The gyrotron may not be suitable for space or airborne applications unless it can be operated at its fourth harmonic. This is because operation at a high frequency fundamental would require a large superconducting magnet (approximately 35 kilogauss). Both the ubitron and gyrotron have stability problems.

Variation With Frequency of the Efficiencies of Various Amplifier Types

It is generally accepted that amplifier efficiency decreases with increasing frequency. This is true within any one tube type, but the

decrease is slow and measures can be taken to offset it. Changing tube type can entirely eliminate the fall-off of efficiency. These factors can be seen in Fig. 31, which shows the efficiencies of eight representative tubes, operating over a frequency range of five decades. The eight tubes plotted represent four generic types--triodes and tetrodes, klystrons, traveling wave tubes, and gyrotrons. Two tubes of each type, each made by the same manufacturer but optimized for operation at widely separated frequencies, are included. The slope, -n, of the line joining the members of each pair indicates the frequency dependence, where

$$\frac{\eta_H}{\eta_L} = \left(\frac{f_H}{f_L}\right)^{-n} , \tag{20}$$

and η_H = efficiency at the higher frequency, f_H, and

η_L = efficiency at the lower frequency, f_L.

Note that n tends to be small, i.e., $0 < n < 0.3$.

The decrease in efficiency in going from tube A to tube B is due to such factors as skin loss, dielectric loss, and transit time effects. At higher frequencies, the current distribution over the internal element cross sections is less uniform (skin effect) and the physical dimensions of the internal tube structure are larger with respect to wavelength. Higher losses in the insulation result because the dielectric is no longer at the voltage minimum. There is also an appreciable length of lossy structure before the wave reaches the external circuit. Despite these effects, operating tube B at the maximum allowable screen voltage (to minimize transit time effects) and using a very narrow conduction angle (in Class C operation) could raise the efficiency of tube B up to that of tube A. In this case, the power output may be only one-tenth as much as the tube is rated for, but the efficiency could be more than doubled. This tradeoff of complexity for efficiency is common. Compared to the triode, the tetrode is precisely such a tradeoff. In the multi-cavity klystron, maximum gain (and minimum bandwidth) can be obtained by synchronous tuning of all cavities. Alternatively, gain can be traded for increased efficiency by simply retuning the klystron cavities (in some tubes this can be done in the field).

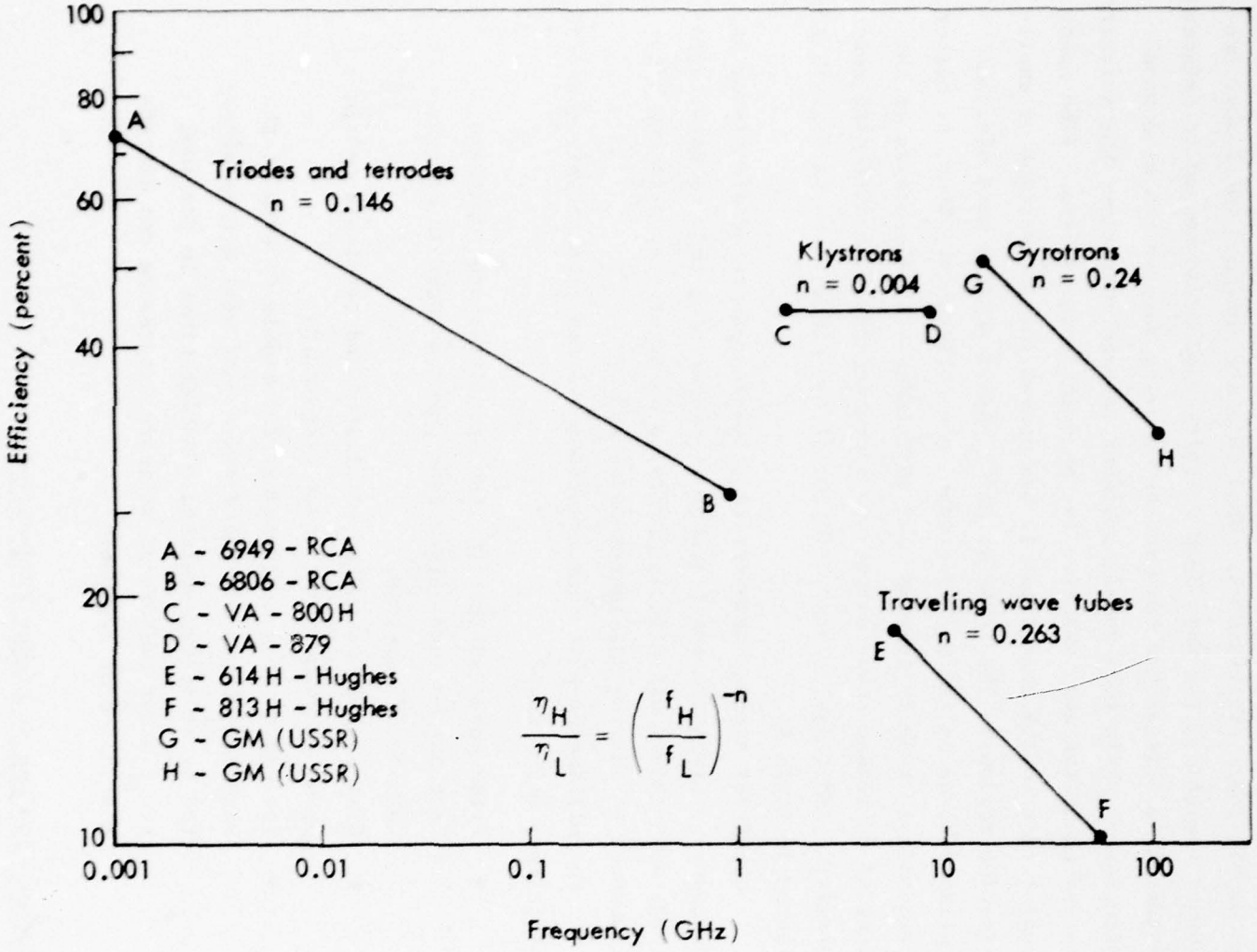

Fig. 31 — Efficiency of vacuum tube power amplifiers

Although the traveling wave tubes selected have much lower efficiencies than the other tube types shown in Fig. 31, these TWTs can be redesigned using voltage jumps and multiple depressed collectors to double their efficiencies. When TWTs are designed for higher frequency operation, the mean beam velocity must be increased to maintain synchronism between the beam and the growing wave on the slow wave structure. While this requires higher voltage operation, the velocity spread about the mean velocity in the spent beam is less. (The spent beam refers to the beam after it has passed the interaction or amplification region.) The lower velocity spread permits more efficient collection, as do the multiple depressed collectors. Thus, at higher frequencies, roughly constant TWT efficiency can be achieved at the cost of decreased power output and increased power conditioning complexity. Additional characteristics of the eight tubes in Fig. 31 are listed in Table 14.

Gyrotrons already demonstrate a low dependence of efficiency on frequency. Given the small amount of research on them to date, gyrotrons may achieve efficiencies of 25 to 50 percent even at the high-frequency end of the millimeter-wave band.

For millimeter-wave communications systems, the roughly constant efficiency means that:

- Prime power sources for the satellites and terminals need not be much larger than power sources in current UHF and SHF systems.
- Heat exchangers in the satellites and terminals remain about the same as at lower frequencies.
- The choice of a frequency at the middle or even at the high end of the millimeter-wave band will not be affected by efficiency-related considerations in the long run. Other factors of military importance can dictate the choice of frequency.

Radomes for Use at Higher Frequencies

Radomes of essentially standard construction are available for use at frequencies up to at least 40 GHz. The Electronics Space Structures Corporation (ESSCO) has, for example, designed such a

Table 14

SELECTED VACUUM TUBE POWER AMPLIFIERS

Tube[a]	Type	Description	Frequency (GHz)	CW Power Output (kW)	DC Plate or Beam Voltage (kV)	DC Plate or Beam Current (A)	Efficiency (percent)	See Reference
A	6949-RCA	Super-power, shielded-grid beam triode, in continuous commercial service	0.001	500	17.5	40	71	52
B	6806-RCA	RF amplifier beam power tetrode, Class C operation	0.9	13.5	7.5	6.8	27	53
C	VA-800H (Varian)	Four-cavity klystron amplifier, tuned for high efficiency	1.8	13	16	1.85	44	54
D	VA-879 (Varian)	Multicavity klystron, tuned for high efficiency	8.5	103	39	6.05	44	55
E	614H (Hughes)	Traveling wave tube	5.9	10	18.5	3	18	56
F	813H (Hughes)	Traveling wave tube	55.5	1	25	0.4	10	56
G	Gyromonotron (USSR)	Cyclotron resonance maser, gyrotron	15	4	----	-----	50	43
H	Gyromonotron (USSR)	Cyclotron resonance maser, gyrotron	107	12	----	-----	31	48

[a]Designated as tubes A through H in Fig. 31.

radome for use with shipboard (or ground) terminals.[57] This radome is a truncated sphere molded in one piece; it can be made of either a glass-fabric-reinforced solid laminate or a sandwich with glass-fabric-laminate skins over a honeycomb core. The outside is finished with a high-quality enamel. At 34.9 GHz, this radome has a transmission efficiency of 90 percent.

Radomes composed of thin membrane panels supported by metal frames have been developed, also by ESSCO, for use up to 300 GHz.[57] This type of radome relies on the spatial distribution of the members of the frame for its electrical characteristics. The environmental specifications of this type of radome are presented in Table 15.

Table 15

ENVIRONMENTAL SPECIFICATIONS
OF A METAL-FRAME FACETED RADOME

Operating winds	150 mph
Operating ambient	-65°F to 160°F
Ice or snow loads	70 psf
Solar radiation rejection	90 percent or greater (white exterior)
Actinic radiation	Must retain properties in tropical sun
Salt atmosphere	Coastal/seagoing
Relative humidity	0 to 100 percent
Sand and dust	Must retain performance in arid regions

The ESSCO radome is a faceted, truncated sphere composed of individual, triangular panels bolted together to form the structure. The panels are arranged in a quasi-random triangulation of the spherical geometry. The panel membrane material is a reinforced plastics laminate trademarked "ESSCOLAM VI." A Tedlar film is integrally bonded to both sides of the panels to insure against erosion. The white Tedlar film rejects more than 90 percent of the incident solar radiation, inhibits the formation of water film, prolongs panel life, and minimizes radome maintenance. Each panel is enclosed in a frame of 6061-T6 aluminum; the frames are bolted together to form the structure.

The transmission loss through this radome is dependent on the amount of metal framework and the type and thickness of the membranes. Figure 32 shows both of these components of transmission loss versus frequency for a 68-ft diameter metal space frame radome with a membrane thickness of 0.030 in. At frequencies above 0.4 GHz, it is seen that the metal framework contribution to transmission loss remains essentially constant, while the membrane's contribution increases at higher frequencies. The loss associated with the membrane is a direct function of its thickness, uniformity, dielectric constant, and loss tangent. The "ESSCOLAM VI" membranes have a dielectric constant of 2.8 and a loss tangent of 0.01.

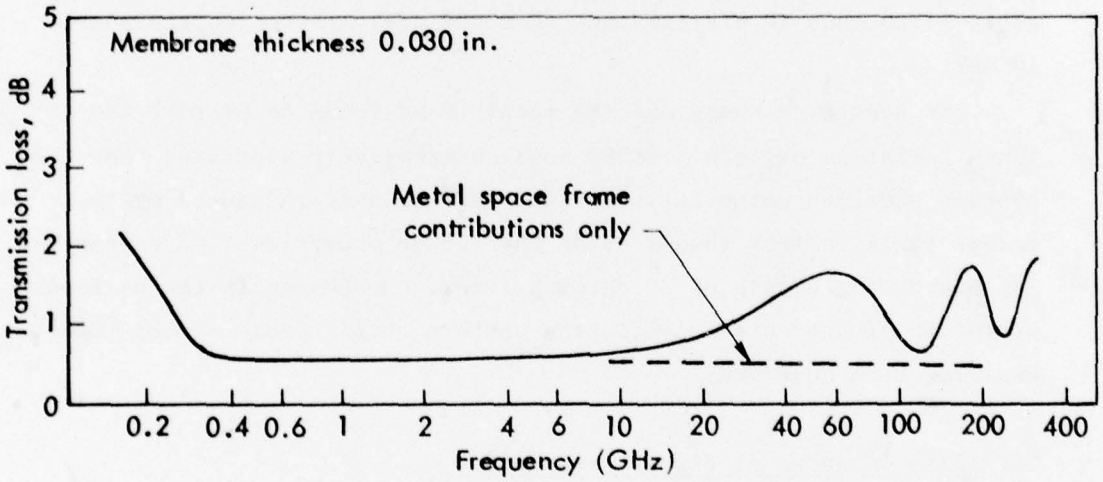

Fig. 32—Transmission loss due to metal-frame faceted radome

It can be seen that the transmission exhibits the maxima and minima characteristics of an interference effect; as a result, the membrane thickness can be selected so that a resonant minimum will coincide with the desired operating frequency. The transmission loss due to the radome is negligible compared with other losses in the system. A 1-mm thick film of sea water on the radome would introduce about 1 dB of attenuation, but only 0.1 dB for a 0.1-mm film.

The noise temperature contribution of the radome depends on the amount of energy dissipated by the radome. The noise temperature of the radome referred to in Fig. 32 would be expected to vary between 33°K and 111°K as the loss fluctuates between 0.5 dB and 2 dB. The increase in noise temperature due to rain is claimed to be less than 10°K over the dry radomes.[57] The effect of sea water would be greater; a uniform film, 1-mm thick, would have a noise temperature of about 100°K at 400 MHz. While this is small compared with the noise temperature of uncooled amplifiers, it would be important with cooled receivers (as can be seen in Fig. 9).

The radome boresight shift is a function of the randomness, as well as the openness, of the radome framework. Extensive measurements of the boresight shift of the ESSCO faceted radome show it to be negligible--less than 10 microradians (0.00058 deg) at frequencies above 10 GHz.

The scattered energy of the metal frame tends to perturb the antenna radiation pattern. ESSCO has conservatively specified that the average sidelobe perturbation of the antenna pattern caused by the radome shall be less than 1 dB at the -25 dB power level of an exposed antenna having a gain of 35 dB or greater. No change in the half-power beamwidth of the antenna radiation pattern attributable to this radome has ever been observed.

Satellite Antennas at Higher Frequencies

Early satellites used the turnstile antenna to provide roughly isotropic coverage so that control of the satellite and telemetry readout could be maintained even if the satellite developed an unanticipated spin. Omni-directional antennas providing continuous earth coverage from an equatorial orbit evolved next, followed by mechanically despun earth-coverage antennas. Next came spot-beam antennas, which provided narrow coverage areas. However, satellites with spot beams for high-information-rate users retained their earth-coverage beams to serve the bulk of users. Over the entire spectrum from 20 to 300 GHz, this pattern of at least two different kinds of antennas can be expected to persist--although there may be significant differences in the way they are used. At 20 and 30 GHz, one earth-coverage antenna may do for the

bulk of users, while a few narrow-coverage antennas may provide for the bulk of traffic and involve only a few users. At higher frequencies, the broad-coverage antennas may provide somewhat less than earth coverage to minimize interference and be used only to access the system. This may require only 100 to 300 bits of information, transmitted over 1 to 30 sec. After a bona fide access is made, the satellite commits a narrow-coverage beam to the new user. The benefits of such an approach increase with increasing frequency, because of the higher antenna gains.

The highest gain-to-sidelobe ratios (70 to 80 dB) are obtained from offset, horn-fed parabolic reflectors with microwave absorber shielding.[16] The problems of packaging large numbers of such antennas on a launch vehicle such as the space shuttle need to be examined as a function of frequency, orbital constellation, spot size, number, and geographic distribution of the users.

An alternative approach is to form a number of beams from each antenna. Although the ratio of the main beam gain to the average sidelobe level will be much less in this case, a variety of schemes may be feasible for reducing interference through the sidelobe. There is extensive activity in the multi-beam antenna area.

Three types of antennas are used to form multiple spot beams: lens antennas, reflector antennas, and phased-array antennas.

Lens Antennas. For a 30 dB sidelobe specification (relative to the main lobe), the refractive index of the dielectric in a solid-lens antenna must be controlled to within 0.8 percent around a nominal value of 2.0.[58] Since light-weight, low-loss materials with this uniformity are not available, refractive lenses are not practical for low sidelobe antennas.

Scott[59] has analyzed a 400-element, transverse electromagnetic wave (TEM) constrained, or "bootlace," lens antenna which is capable of simultaneously generating any 6 out of 61 possible dual polarized beams over a 17 deg field of view, at both 4 and 6 GHz, while maintaining at least 27 dB isolation between beams. The 3 dB beamwidths of this antenna are approximately 4.2 deg at 4 GHz and 2.8 deg at 6 GHz.

Binz and Wainer[60] have analyzed a 2000-element TEM lens capable of forming 64 beams over its 18 deg field of view. With a single-horn feed, the calculated 3 dB beamwidth was 1.99 deg and the sidelobe level

was 20 dB below the main beam. With a seven-horn cluster feed, the 3 dB beamwidth was 2.31 deg with a sidelobe level of 30 dB below the main beam.

Reflector Antennas. Reflector-type multiple beam antennas are attractive because of their design simplicity, inherently large bandwidth, ease of construction, light weight, and low cost. However, the large feed structures of multiple beam antennas can cause excessive blockage and thus high sidelobe levels in all configurations except the offset-fed types. Offset-type paraboloidal antennas have the disadvantage of having rapid deterioration of sidelobes and cross-polarization properties for off-axis beams, although techniques such as reflector shaping and dual-focus design can compensate partially. A spherical reflector permits off-axis pointing with less degradation in performance than a paraboloid, but it has higher sidelobe levels and is less efficient. A spherical reflector will provide adequate protection between adjacent beams if the beams are separated by four or more beamwidths.[61]

Rigid, as opposed to deployable, reflector antennas are presently preferred at frequencies above 8 GHz due to the difficulties in obtaining accurate folding and deployment.

Turrin[61] has developed a spherical-reflector satellite antenna for the 20 and 30 GHz bands. This antenna employs a spherical reflector 60 in. in diameter, a plane reflector, and a cluster of six feed horns. The gain of a laboratory model was measured to be 47 dB at 19 GHz and 49.2 dB at 30.2 GHz. The minimum physical separation between feeds limited the minimum angular beam separation to about 1.2 deg. Isolation between the beams was about -20 dB at the minimum angular separation, and the half-power beamwidth was less than 0.7 deg. The maximum error was 0.38 deg. The coupling between ports was less than -40 dB in all cases. Blockage by the feeds was of little consequence.

Semplak[62] proposed the use of an offset Cassegrainian antenna fed by separate, small corrugated horns at 100 GHz. The antenna consists of a 61-cm diameter parabolic reflector and a confocal hyperboloidal subreflector which is 38.1 cm wide by 10.2 cm high. The antenna is fed by an offset collector which is illuminated by a dual-mode horn. The current state of the art needs to be pushed to produce

a satisfactory corrugated horn at 100 GHz. The ratio of the prime focal length to the diameter of the reflector is 1.9; hence, the feed should be able to scan tens of beamwidths by lateral displacement of the feed. The 3 dB beamwidth was measured to be less than 0.5 deg at all scanning angles. A scan of 8 deg results in a degradation in gain of 5 dB.

The Kokasuka Electrical Communication Laboratory in Japan[63] has designed and tested a seven-beam dual reflector antenna with multiple feed horns at 50 GHz. The main reflector is 198 cm in diameter and the subreflector is 17 cm. The antenna gain was measured to be 57.8 dB when the primary horn is on the focal point. If the horn is pointed 1 deg off axis, a decrease in gain of 0.55 dB is measured. The isolation between beams is better than -24 dB.

Meier, Rudish, and Taub[64] have demonstrated the feasibility of receiving multiple beams at 60 GHz over an 18 deg field of view. Their antenna consists of available components, or components within current technology. A "pin cushion" of narrow overlapping beams, covering the required field of view, is generated by an array of feeds in the focal plane of the antenna. Each feed is connected to a separate receiver front end. Based on the outputs of the front ends, only those channels containing active signals are combined in a common output. An antenna of this type with an aperture of one square meter could produce approximately 50 beams with a 3 dB beamwidth of one-third deg. The antenna used was a spherical reflector with a planar mirror, which has a gain of 52 dB. This antenna can be scaled to operate between 20 and 100 GHz.

Tang et al.[65] have analyzed and tested an antenna which, operating in the 9 to 10 GHz region, produces multiple 1 deg beams over a 10 deg half-angle cone. The antenna gain is over 40 dB and the sidelobe levels are more than 20 dB below the main beam. The antenna consists of an offset parabolic reflector which is fed by a space-fed spherical lens. The space-fed lens provides multiple overlapping beams on the reflector aperture.

Phased-Array Antennas. A planar phased array consists of identical uniformly spaced radiators. Multiple steerable beams can be obtained by providing separate beam forming and steering networks for each beam and combining their outputs at each array element. The weight and complexity

of such a system increase in proportion to the number of beams. Another disadvantage of the phased-array transmit antenna is the need to provide individual power amplifiers at each radiating element, each of which must handle simultaneous signals from all of the multiple beams. These amplifiers must operate in their low-efficiency linear regions to avoid saturation (saturation results in intermodulation and signal suppression effects in the presence of multiple signals). This penalizes the overall transmitter efficiency and further increases weight and prime power requirements. The weight and complexity of the phased array tend to limit its usefulness in applications where multiple beams are desired.

Multi-beam antennas are quite limited in their ability to suppress sidelobes relative to a single-beam offset-horn antenna which has 80 dB suppression.[16] As a result, their usefulness is restricted to acquisition and to low-data-rate communications. However, with adapative antenna patterns (null steering on interfering sources) and cancelling of strong interfering signals, high-data-rate communications may be feasible. The choice of an optimum satellite antenna for high-data-rate communications is beyond the scope of this study.

X. COMPLEXITY, RELIABILITY, LIFETIME, AND INTEROPERABILITY EFFECTS

In this section, we are concerned with the effects of increased operating frequency on the complexity, reliability, and lifetime of the satellite, and with the effect, on interoperability among user communities, of adding still another frequency.

Communications satellites operating at the higher microwave frequencies should be about as complex as lower microwave frequency systems. Critical satellite components are the null-forming adaptive lens antennas, the pointing and tracking subsystems for multiple reflector antennas, and the high-power amplifiers. Multiple reflector antennas require drive trains to continuously track the users from space. The reliability and lifetime of these satellite components are treated here. High reliability and long lifetime are particularly important for the satellite end of the link. Operational lifetimes of 5 to 10 yr are typical of current satellite systems, and are a reasonable goal for higher frequency systems. What are the philosophy and procedures for achieving such long satellite lifetimes?

Historical studies of the useful on-orbit life of communications and other types of satellites were conducted in 1975 by Buehl and Hammerand,[66] and in 1977 by Levine.[2] Levine noted, for example, that of 63 representative military spacecraft launched between 1962 and 1977, 75 percent were still operational four years after launch. Both studies found surprisingly little correlation between the observed lifetime and the complexity, weight, or predicted lifetime. There was high correlation, however, between lifetime and the degree of reliability analysis and testing that was performed prior to launch. The use of a type of reliability analysis termed Failure Modes and Effects Analysis (FMEA) was particularly effective. It identified the major effects caused by failure of each component. This knowledge permits the designer to reduce the probability of a catastrophic failure by providing alternate paths or redundant components. FMEA was found to be most effective when conducted early in the design phase and when there was a combined design and reliability engineering effort.

A comprehensive test program was also found to be very valuable in achieving long operational life. Highest success was achieved by testing all levels of components and subsystems from the lowest level of assembly to the whole spacecraft. Power-on environmental testing at both the subsystem level and for the complete spacecraft proved to be exceptionally effective in culling out marginal components and assemblies, whether due to manufacturing defects or design errors.

In higher frequency communications satellite programs, as in those using lower frequencies, it is therefore important that sufficient time and funding be allowed for reliability analyses and testing procedures of the types mentioned above.

LIFETIME OF POINTING AND TRACKING SUBSYSTEMS

No special problems in the lifetime or the reliability of the pointing and tracking subsystems are expected to be associated with the change to higher frequency operation. In the "base case" communications system discussed in Section III, the complexity was shifted to the satellite in order to ease the problems of the small mobile user, with a view to extending the communications service to a larger number of such users. The users thus have smaller antennas and broader beams at the higher frequencies than current SHF users, so that high subsystem reliability is expected.

The only remaining area to be considered is associated with the satellite. A 4.4-m diameter satellite antenna was postulated in the base case, for which the beamwidth ranged from 0.234 deg at 21.2 GHz to 0.019 deg at 265 GHz (see Table 10). Tracking with such narrow beams involves little fundamental additional complexity, since the required error signal amplitude is generated with smaller angular displacements when sharper beams are employed. Satellite open-loop pointing associated with initial acquisition is, however, more difficult at the higher frequencies. Thus, as higher pointing accuracy is required, more complex satellite attitude reference systems are indicated, as discussed in Section VIII.

The basic "Bias Momentum" attitude reference system (simply a horizon sensor and a gyrocompass) presented few problems on FLTSATCOM and TIROS satellites. However, both the reliability and accuracy could

be increased by employing a horizon sensor of the "staring" type that has no moving parts. Gas-bearing gyros appear to have an essentially unlimited lifetime. Such a system, having a 1-σ pointing accuracy of 0.1 to 0.3 deg, could be used with a 4.4-m diameter millimeter-wave communications antenna with only a limited search required.

The performance of this basic attitude reference system can be improved by an order of magnitude through the addition of a digital sun sensor, as discussed in Section VIII. The sun sensor is a simple, highly reliable device, which should detract little from the subsystem reliability. With such an accurate attitude reference system, little or no search would be required.

LIFETIME OF HIGH-POWER MILLIMETER-WAVE AMPLIFIERS

The dominant failure mechanism in high-power millimeter-wave amplifiers (klystrons, traveling wave tubes, extended interaction amplifiers, and gyrotrons) should be cathode depletion. This need not be a frequency-dependent phenomenon; the cathode area must be made large enough so that the cathode temperature does not have to be raised to increase the emission current density in higher frequency tubes. A higher-convergence electron gun or a tube whose cross section does not scale with frequency, e.g., the gyrotron traveling wave amplifier, alters the conventional relationship between lifetime (and power output) and frequency. NASA's *A Forecast of Space Technology*,[17] makes no allowance for these alternatives. It predicts that the lifetime* of future 100 W tubes will fall from a value of 9.9 yr for frequencies in the 2 to 10 GHz range to about 1 yr at 64 GHz based on simple frequency scaling. Designers of such devices† believe that long lifetimes can be achieved independent of frequency. We conclude that 5 to 10 yr lifetimes should be achievable at 10 to 100 W power levels throughout the millimeter-wave band.

As an example, note that an Extended Interaction Amplifier (EIA) klystron is guaranteed to have a lifetime of 1000 hr. However, actual

*For practical purposes, the lifetime of space tubes is defined as the time required for a 3 dB fall-off in power output below the nominal or rated value.

†Private communication with personnel from Varian of Canada and Hughes Research Laboratories.

lifetimes are expected to range from 5000 to 15,000 hr, since operation in excess of 6000 hr has already been demonstrated.*

LIFETIME OF DRIVE TRAINS FOR SATELLITE ANTENNAS

When geostationary orbits are abandoned in favor of inclined orbits to avoid operation at low user elevation angles, the satellite antennas must be driven continuously to track the user. This situation is quite analogous to the case of spin-stabilized satellites with "de-spun" antennas. While DSCS II, which employed such an arrangement, encountered bearing problems, it is believed that the difficulties can be resolved, as evidenced by the success in this regard of INTELSATs III and IV.

INTEROPERABILITY

The large investment in UHF and SHF communications satellites and terminals is likely to dictate that future systems in new frequency bands provide some cross-connections to the earlier bands. Differences in the sizes of the user platforms lead to differences in antenna diameters and thus in data rates. Differences in mission may be reflected in substantial differences in the required data rate and the degree of covertness and resistance to interference (friendly or unfriendly). Processing onboard the satellite, i.e., the "switchboard in the sky" concept, is a means of coping with differences in carrier frequency, data rate, type of modulation, error correction coding and encryption, and temporary overloads or outages. If one wishes to avoid isolation between the various classes of users within each Service and between the Services, there is a need for interoperability. Onboard processing is a means of providing for such interoperability.

Accommodation just to the introduction of a new frequency band--isolated from all other changes--would be relatively simple. Even the earliest communications satellites (repeaters which provided a relatively transparent channel to the users) provided a shift between the up and downlink frequencies. Accommodation to large differences in data rate and type of modulation, however, involves much more complex onboard processing than a mere frequency translation. Demodulation

*Private communication with personnel from Varian of Canada.

and remodulation in the satellite was inappropriate in early communications satellites; the general recommendations in 1960 were to avoid it. The LES-8 and -9 satellites, however, have recently demonstrated the feasibility of onboard demodulation and remodulation, and it is likely to become commonplace in the 1980s. The trend in the INTELSAT commercial satellites has been to maximize capacity per satellite and to simplify connectivity by concentrating all users within a single regional satellite beam. Economic factors are likely to continue to force military satellites in the same direction--toward larger, multipurpose, multi-frequency satellites. At some point, the use of a satellite-to-satellite link becomes attractive. Beyond this point, these economic factors no longer apply.

With an onboard information processor, the satellite can dynamically reallocate its resources to maximize overall system efficiency. Uplinks and downlinks can be decoupled so that each can be optimized independently. Dynamic variation in user data rate (separately for each user), with onboard storage when necessary, rapidly changing connectivity, and allocation of power output level on a per link basis as needed, can greatly improve overall system performance. For a description of some types of processing, applications, the current status, and possible future developments, see Ref. 67.

XI. GAPS IN TECHNOLOGY

The trends in subsystem technology were discussed in previous sections of this report. Some important gaps relative to operation in the 20 to 300 GHz region are worth noting:

- Lens antennas of approximately earth coverage are needed for the reception of acquisition signals at the satellite.
- Lightweight antennas which have very low sidelobes and which, together with their drive systems, can be stacked compactly in a launch vehicle are needed. These antennas might be shielded paraboloids, fed by conical horns. A separate receiver and transmitter are assumed to be mounted on the structural support of each antenna.
- Space-qualified packaged amplifiers are needed with output power levels of from 5 to 500 W, efficiencies of 25 to 50 percent, and 20 to 30 dB gain.
- Efficient broadband, solid state drivers for the final amplifiers are needed at about the 0.1 to 1 W level.

No detailed description of these gaps is practical at this time in the absence of a specific system concept, program plan, or selection of a particular frequency band; these are all obviously closely interrelated.

XII. CONCLUSIONS

The feasibility of employing frequencies ranging from 21.2 GHz to 265 GHz for earth-satellite communications has been examined. As a basis for estimating link performance, a model has been evolved which estimates the statistical distribution of signal attenuation, sky noise temperature, and total system performance degradation arising from atmospheric components such as humidity, clouds, and rain, at selected frequencies in each of six atmospheric windows. The six frequencies are: 21.2, 31, 48, 101, 152, and 265 GHz. The following conclusions have been reached:

Communications link performance generally compatible with the needs of small mobile users can be obtained in the windows of the millimeter-wave band with very small (10 cm diameter) terminal antennas. In one case, these were used in conjunction with 4.4-m diameter satellite antennas (the largest size antenna compatible with the space shuttle without folding, unfurling, or extending). Assuming typical values* for the other link parameters, a data rate of 10^6 bps (sufficient to provide a 16 kbps voice channel to each of 60 TDMA users) can be transmitted over a downlink to a receiver in a relatively high rainfall area (Washington, D.C.) with an estimated availability (freedom from weather outages), averaged over a year, which ranges from 98.7 percent at 21.2 GHz to 89 percent at 265 GHz (see Fig. 10). If users are separated by 10 to 30 km or more (so that heavy raincells are uncorrelated), the availability figures can be interpreted as meaning that 89 to 98.7 percent of the users can be communicated with at any time. These small (10 cm diameter) terminal antennas have broad beams, which greatly simplifies the problems of incorporating a directional antenna into a small mobile platform.

Wide-band data relay users can also obtain performance compatible with their needs in this frequency region. As an extreme case for this category of user, we assumed a 10 m terminal antenna diameter. The performance of this terminal was examined in conjunction with 1-m diameter

*Satellite transmitted power = 10 W, E_b/N_0 = 10, margin = 8 dB, satellite altitude = 30,000 n mi, uncooled amplifier, and elevation angle (at the user) $\geq$ 30 deg.

satellite antennas. Thus, assuming the same values as before for the other parameters, a data rate of 10^8 bps can be obtained with availabilities ranging from 99.7 percent at 21.2 GHz to 93 percent at 265 GHz. With a 17°K receiver, in conjunction with a better quality modem (E_b/N_0 of 5 dB), a data rate of 10^9 bps can be obtained with an estimated availability which ranges from 99.5 percent at 21.2 GHz to 94 percent at 265 GHz (see Fig. 15).

Link performance degrades rapidly as the elevation angle is decreased below 30 deg, especially at the higher frequencies. Thus, in a typical case (Fig. 14) it was found that, with an availability of 98 percent, the estimated data rate at 30 deg elevation exceeds that at 10 deg elevation by a factor which ranges from 4 at 21.2 GHz to 3000 at 265 GHz. It is concluded that the higher the frequency, the more important it is to avoid elevation angles below 30 deg.

If the width of the beam footprint on earth is held constant, the associated satellite antenna diameter decreases with increasing frequency; performance in this case degrades more rapidly with frequency than when the satellite antenna diameter is held constant (Fig. 15). This disadvantage is, however, counteracted by the advantage that a larger number of antennas can be mounted in the same total aperture when higher frequencies are employed. This can be effective when coping with a large number of widely dispersed small mobile users.

Table 16 (from Fig. 15) illustrates the situation for the small mobile user. It assumes a user at 30 deg elevation with a constant footprint width of 123 n mi.

Table 16

DOWNLINK PERFORMANCE WITH A CONSTANT FOOTPRINT WIDTH OF 123 N MI

Frequency (GHz)	Antenna Diameter (m)	Number of Antennas for Constant Satellite Aperture[a]	Data Rate per Antenna Beam (bps)	Availability[b] (percent)
21.2	4.4	1	10^6	99
31	3	2	10^6	98
48	1.94	5	10^5	99
101	0.92	23	10^4	97
152	0.61	51	10^4	96
265	0.35	158	10^2	94

[a]Practical considerations, such as mutual coupling and allowable packing fraction (without blockage) are ignored.

[b]Annual average for each satellite antenna beam.

Note, for example, that 158 antennas operating at 265 GHz could be mounted in the aperture completely filled by the single 21.2 GHz antenna. This number is small, however, compared with the total number of beam positions (1900) required to cover all possible user locations with elevation angles above 30 deg from the same satellite altitude.

When subdividing the antenna aperture, the useful limit is reached (with all other parameter values held constant) when the data rate in the beam is just adequate to support one user. Thus, the 158 beams at 265 GHz may be reasonable if only a 75 bps data link is required (one teletype circuit) with 94 percent availability. However, if the requirement is for a 16 kbps digital voice circuit with 95 percent availability, about 50 beams at 152 GHz are preferable.

Atmospheric constituents such as rain degrade link performance in two ways: they attenuate the signal and they increase system noise by adding a sky noise contribution. The additional sky noise effect is most significant at the lower frequencies, where, in the examples treated, it was found to add roughly 4 dB of degradation with uncooled receivers and 8 dB when cooled receivers were employed (see Tables 4 and 8).

With constant antenna diameters, the link performance improves with increasing frequency in relatively good weather because the increased antenna gain more than overcomes the increased atmospheric degradation. During heavy rain, the converse is true. In the example studied, the two effects approximately balance each other when the availability is about 90 percent (Fig. 11).

The estimated annual throughput increases monotonically with frequency up to about 152 GHz for elevation angles of 30 deg and above. Thus, to maximize annual throughput (and hence the transmitted number of bits of information per dollar invested) with fixed antenna diameters at both ends of the link, operation in the 100 to 300 GHz range is indicated (Fig. 12).

Geostationary orbits do not provide elevation angles above 30 deg for users at latitudes above 52.5 deg, regardless of the number of satellites employed; inclined orbits are therefore indicated for use with higher frequency communications systems. A constellation involving nine satellites in circular orbits at 30,000 n mi altitude and 60 deg inclination is attractive in this regard, because, with such a constellation,

the probability of there being one satellite in view above 30 deg elevation is 98.7 percent, averaged over time and over the entire surface of the earth. It is estimated that there will be one satellite in view 100 percent of the time at elevations only slightly below 30 deg. Moreover, the probability that a rainstorm would coincide with the absence of a satellite above 30 deg is quite low. The elevation angle statistics for a number of other constellations are examined in Section V.

The narrow beam footprints obtained at higher frequencies greatly facilitate the rejection of strong interfering sources displaced from the terminal location. Thus, for example, the footprint obtained from a satellite at an altitude of 30,000 n mi with a 4.4-m diameter antenna is only 30 n mi wide at 100 GHz, and still less at higher frequencies (Fig. 23). This permits rejection of strong interfering signals from sources located 300 n mi away. This effect does not vary greatly with look angle because the footprint area increases by only a factor of about two as the elevation angle decreases from 90 deg (overhead) to 30 deg (Fig. 24).

The pointing and tracking problems of the small mobile terminals are greatly simplified by the 10-cm diameter antennas postulated above. This is because the associated beams are relatively broad, ranging from 0.82 deg at 265 GHz to 10.3 deg at 21.2 GHz. The required pointing and tracking accuracies are thus reduced and easy to obtain because the mass of the antenna is small as well.

The pointing and tracking accuracy requirements of the wide-band data relay users will be high at the higher frequencies, but these requirements are well within present technology. Astronomical radio telescopes have already demonstrated pointing accuracies more than ten times better than needed for the largest antennas considered here. Similarly, tracking should be no problem because radars already track to well under one-hundredth of a beamwidth when adequate signal-to-noise ratio is available.

Satellite motion has a negligible effect on the tracking capability required of either a stationary or a mobile user. The roll rate of a ship is 200 to 500 times the maximum angular rate (overhead) of the line of sight for any satellite orbit considered. The angular rates of ground vehicles and aircraft would be even higher than that of ships. Thus,

tracking rates are dominated by the motion of the user platform due to changes in user attitude or earth rotation (for stationary terminals).

Pointing and tracking of the satellite beam should present no problem at higher frequencies, despite the narrow beams involved (0.019 to 0.234 deg for a 4.4-m diameter satellite antenna). While the cost of a relatively coarse (0.1 to 0.3 deg) long-life attitude stabilization system is high (about $800,000), the incremental cost of a sun sensor to improve the performance by an order of magnitude is only about 10 percent. Attitude reference systems whose performance exceeds that required here by an order of magnitude have already been utilized in space, and a system is under development with much higher predicted accuracy at a projected cost no greater than that of present relatively coarse systems.

Use of small terminal antennas (about 10 cm in diameter) and minimum elevation angles exceeding 30 deg permits their use on smaller mobile user platforms than are presently contemplated for SHF terminals. Obstruction of the beam by other components on the platform, whether ship or ground vehicle, can be avoided due to the small antenna size and high elevation angle (and associated flexibility in antenna placement). With aircraft platforms, the radome could be a conformal window. A 40 cm window permits operation down to 30 deg elevation while avoiding projecting radome problems such as drag and rain erosion. The size of the conformal radome is relatively insensitive to frequency (see Fig. 30).

Many tube types may be capable of supplying useful power levels at millimeter wavelengths. Bandwidth, power level, efficiency and gain, as well as lifetime and reliability, are the key parameters affecting the choice. Some of these tube types are: extended interaction klystron amplifiers (EIAs), ubitron (undulating beam interactions) tubes, coupled-cavity TWTs, and gyrotron traveling-wave amplifiers. Power levels as high as 10 kW CW at 300 GHz may prove feasible, although laboratory units have only demonstrated 12 kW at 100 GHz so far.

The weight, size, and power requirements of higher frequency communications systems, and hence their compatibility with the user platforms, depend largely on the efficiency of the power output amplifiers at higher frequencies. A fall-off of efficiency with increasing frequency occurs for each tube type, but the rate of decrease is slow. Measures can be

taken to offset this and a change of tube type can restore high efficiency at the higher frequency (see Fig. 31). Thus, the transmitter weight and prime power requirements need not increase with frequency.

No basic limitation seems to exist that would prevent the fabrication of low-loss radomes for ground vehicle, shipboard, and airborne use up to 300 GHz. Thus, a random triangular-panel radome exhibits a transmission loss of 0.5 dB over any selected pass band out to 325 GHz. Both the location and the width of the pass band are selected by proper choice of radome thickness. The shift in boresight introduced by the radome is less than 0.0006 deg.

Multi-beam antennas such as phased arrays, reflectors, and lenses were examined. Phased arrays are too heavy and too costly in the millimeter-wave band to be considered at all. The other approaches tend to result in high sidelobe levels, which limits the data rate in the presence of interference. The interfering sources can be rejected by adaptive pattern antennas (null-forming) and by signal cancellation. Alternatively, use of a conical horn-fed, shielded parabolic antenna (single beam) can produce far-out sidelobes which are 80 dB below the peak of the main beam (for main beam gains in excess of 40 dB).

Appendix

THE SHAPE AND SIZE OF THE BEAM FOOTPRINT ON THE EARTH

W. Sollfrey

The satellite communications antenna produces a pencil beam which illuminates some region on the ground. The details of the illuminated region depend on the satellite altitude, the antenna beamwidth, and the angle between the beam direction and the subsatellite vertical. We shall calculate the shape and size of the spot under the assumptions that the antenna beamwidth is small and that the beam does not intersect the horizon. The results for the spot diameters and area will be given to the fourth powers of the beamwidth.

The configuration is shown in Fig. A.1. The satellite is at the point S at the altitude H. The center of the beam is directed at the point P, with the beam making an angle β with the vertical. The ground angle from the subsatellite point to P is θ, and the elevation angle of the line of sight P→S is α. The beamwidth to the half-power point is δ (note this is half the more conventional beamwidth between half-power points). The point Q is a representative point on the edge of the intersection between the beam, taken as a cone of semiangle δ, and the surface of the earth.

We use rectangular coordinates, x, y, z, with the z-axis along O→S and the point P in the x-z plane, and also spherical coordinates, ρ, ψ, ϕ, with the pole along the z-axis and the point P as the longitude reference. At the point S, we have $x = y = 0$, $z = R + H$; at P, $x = R \sin\theta$, $y = 0$, $z = R\cos\theta$; and at Q, $x = R\sin\psi\cos\phi$, $y = R\sin\psi\sin\phi$, $z = R\cos\psi$. The range from P or Q to S is:

$$r^2 = R^2 + (R+H)^2 - 2R(R+H)\cos\theta \qquad \text{(A.1a)}$$

$$s^2 = R^2 + (R+H)^2 - 2R(R+H)\cos\psi \ . \qquad \text{(A.1b)}$$

The unit vector from P to S is:

$$\vec{i}_P = \left[-\vec{i}_x R\sin\theta + \vec{i}_z (R + H - R\cos\theta)\right]/r \ , \qquad \text{(A.2)}$$

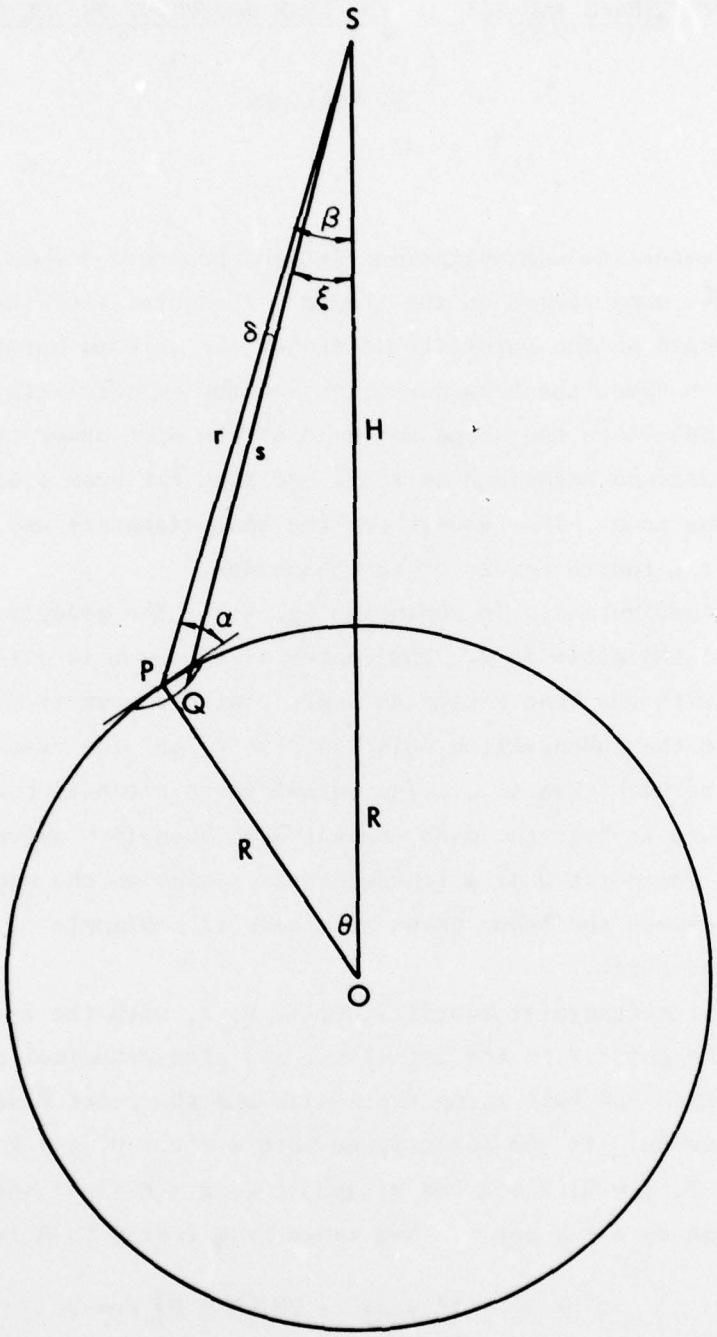

Fig. A-1 — Geometrical configuration

and the unit vector from Q to S is

$$\vec{i}_Q = \Big[- \vec{i}_x R \sin\psi \cos\phi - \vec{i}_y R \sin\psi \sin\phi + \vec{i}_z \left(R + H - R\cos\psi\right)\Big] \Big/ s \quad . \tag{A.3}$$

The condition that Q is on the beam half-power cone is:

$$\vec{i}_P \cdot \vec{i}_Q = \cos\delta \tag{A.4a}$$

$$= \Big[R^2 \sin\theta \sin\psi \cos\phi + \left(R + H - R\cos\theta\right)\left(R + H - R\cos\psi\right)\Big] \Big/ rs \quad . \tag{A.4b}$$

This expression may be simplified by expressing it in terms of the angles β and ξ, respectively the angles from the vertical of the lines P→S and Q→S. The result is:

$$\cos\delta = \cos\beta \cos\xi + \sin\beta \sin\xi \cos\phi \quad . \tag{A.5}$$

The colatitude ψ is related to the angle ξ by:

$$\psi = \sin^{-1}\left(\frac{(R + H)\sin\xi}{R}\right) - \xi \quad . \tag{A.6}$$

We see from Eq. (A.5) that the maximum excursion of ξ from β is $\pm\,\delta$, which occurs at $\phi = 0$. It follows that the length of the illuminated spot along the meridian connecting P and the subsatellite point is:

$$D_{||} = R\left[\sin^{-1}\left(\frac{(R + H)\sin(\beta + \delta)}{R}\right) - \sin^{-1}\left(\frac{(R + H)\sin(\beta - \delta)}{R}\right) - 2\delta\right] . \tag{A.7}$$

The law of sines applied to the triangle O→P→S permits us to express the angle β in terms of the angle α by:

$$\sin\beta = R\cos\alpha \Big/ \left(R + H\right) . \tag{A.8}$$

Equation (A.7) may be expanded in powers of δ. The even powers cancel, and it may be shown after extensive manipulation that:

$$D_{||} \sim \frac{2\,r\,\delta}{\sin\alpha} + \frac{H\,(2\,R + H)(1 + 2\cos^2\alpha)\,\{(R + H)^2 - R^2\cos^2\alpha\}^{\frac{1}{2}}\,\delta^3}{3\,R^2\sin^5\alpha} \quad . \tag{A.9}$$

The derivation of the perpendicular diameter is somewhat more complicated. We introduce an angle σ, which is an azimuthal angle in the tangent plane at the point P, referenced to the meridian line. In terms of σ, Eq. (A.5) is parametrized by:

$$\cos\xi = \cos\beta\cos\delta - \sin\beta\sin\delta\cos\sigma \tag{A.10a}$$

$$\sin\xi\cos\phi = \sin\beta\cos\delta + \cos\beta\sin\delta\cos\sigma \quad . \tag{A.10b}$$

The curve defined by Eq. (A.5) is covered by $0 \leq \sigma \leq 2\pi$. To third order in δ, the variables ξ and ϕ are given by:

$$\xi = \beta + \delta\cos\sigma + \frac{\delta^2\cos\beta\sin^2\sigma}{2\sin\beta} - \frac{\delta^3\,(1 + 2\cos^2\beta)\cos\sigma\sin^2\sigma}{6\sin^2\beta} \tag{A.11a}$$

$$\phi = \frac{\sin\sigma}{\sin\beta}\left[\delta - \frac{\delta^2\cos\beta\cos\sigma}{\sin\beta} + \frac{\delta^3\,(\cos^2\sigma - \cos^2\beta + 3\cos^2\beta\cos^2\sigma)}{3\sin^2\beta}\right] \tag{A.11b}$$

in which it has been assumed that we are not near the subsatellite point, so the longitudinal width is small.

The point Q is at the lateral distance from the meridian along the spherical surface:

$$q = R\,\phi\sin\psi \quad . \tag{A.12}$$

When the expansion of Eq. (A.11a) is substituted into Eq. (A.6) for ψ, the expansion of Eq. (A.11b) is inserted into Eq. (A.12), and the angle β is eliminated using Eq. (A.8), the eventual reduced expression is:

$$q = r\,\delta\sin\sigma\left[1 + \delta\frac{\cos\alpha\cos\sigma}{\sin\alpha} + \delta^2\left\{\frac{\{(R + H)^2 - R^2\cos^2\alpha\}^{\frac{1}{2}}}{2\,R\sin\alpha} + \frac{H\,(2\,R + H)\cos^2\alpha\cos^2\sigma}{2\,r\,R\sin^3\alpha} - \frac{R^2\cos^2\alpha - (R + H)^2\sin^2\sigma}{6\,R^2\cos^2\alpha}\right\}\right] \tag{A.13}$$

This may be differentiated with respect to σ to find the maximum lateral distance the curve extends from the meridian. The value of σ for which the maximum occurs is:

$$\sigma_o = \frac{\pi}{2} + \delta \frac{\cos \alpha}{\sin \alpha} + 3^{rd} \text{ order terms} , \tag{A.14}$$

and the transverse diameter of the spot is:

$$D_{\perp} \sim 2 r \delta \left[1 + \delta^2 \left\{ \frac{r}{2 R \sin \alpha} + \frac{1}{2 \sin^2 \alpha} + \frac{(R + H)^2 - R^2 \cos^2 \alpha}{6 R^2 \cos^2 \alpha} \right\} \right] . \tag{A.15}$$

If only the first order terms had been kept, the surface spot would be an ellipse, with the major axis along the meridian of length $2 r \delta / \sin \alpha$, the minor axis of length $2 r \delta$. This can be seen directly from Fig. A.1. If the beamwidth is small enough that the diameters of the spot are small compared to the radius of the earth, then the spot is the intersection of an inclined plane with the conical beam, yielding an ellipse of appropriate size and shape. The third order corrections to the diameters are usually fairly small.

The illuminated area is given by the formula:

$$A = 2 R^2 \int_{\psi_{min}}^{\psi_{max}} \phi \left(\psi \right) \sin \psi \, d \psi , \tag{A.16}$$

where the limits are the extreme values of the colatitude ψ, and the longitude is to be expressed in terms of the colatitude via Eq. (A.4b). Integrate by parts, use the fact that the longitude vanishes at the extremes, and change to σ as the independent variable. The result is:

$$A = 2 R^2 \int_{o}^{\pi} \cos \psi \frac{d \phi}{d \sigma} d \sigma . \tag{A.17}$$

Express cos ψ in terms of ξ from Eq. (A.6), then use the expansions of Eqs. (A.11a) and (A.11b). Since the mean value of $d \phi / d \sigma$ is zero, the expansions are accurate enough to give the area to fourth order in δ. After very tedious calculations, the result is:

$$A = \frac{\pi r^2 \sin^2 \delta}{\sin \alpha} + \frac{\pi H^2 (2R + H)^2 (3 - \sin^2 \alpha) \delta^4}{8 R^2 \sin^5 \alpha} . \qquad (A.18)$$

The first term is the area of the ellipse, the second term shows the effect of the distortion.

As a typical example, take a satellite at a height of 10,000 n mi, and let the diameter of the nadir spot be 100 n mi. Then $\delta = 0.005$, corresponding to a 4-ft dish at 31 GHz. Consider an elevation angle of 30 deg. Then the two terms in the meridian diameter are 226.89 and 16.12, in the perpendicular diameter 113.44 and 0.02, and in the area 20,219 and 52. Clearly, the correction terms are quite small, and the figure is only slightly distorted from an ellipse. As long as we are not too close to either the horizon or the subsatellite point, the expressions of Eqs. (A.9) and (A.15) for the diameters and Eq. (A.18) for the area will sufficiently characterize the illuminated region.

REFERENCES

1. *Manual of Regulations and Procedures for Radio Frequency Management*, Executive Office of the President, Office of Telecommunications Policy, 1976.

2. See, for example, S. E. Levine, *A Review of the Mission Success of Communications Satellites and Related Spacecraft*, The Aerospace Corporation, SAMSO-TR-180, October 1977.

3. Feldman, N. E., and S. J. Dudzinsky, Jr., *A New Approach to Millimeter-Wave Communications*, The Rand Corporation, R-1936-RC, November 1976.

4. Deirmendjian, D., *Far Infrared and Submillimeter Scattering, II: Attenuation by Clouds and Rain*, The Rand Corporation, R-1718-PR, February 1975; also *J. of Appl. Meteorol.*, Vol. 14, No. 8, December 1975, pp. 1584-1593.

5. Deirmendjian, D., "Scattering and Polarization Properties of Water Clouds and Hazes," *Appl. Optics*, Vol. 3, 1964, p. 187; also *Electromagnetic Scattering on Spherical Polydispersions*, American Elsevier Publishing Co., New York, 1969; and The Rand Corporation, R-456-PR, May 1969.

6. Deirmendjian, D., *Far Infrared and Submillimeter Scattering, I: The Optical Constants of Water — A Summary*, The Rand Corporation, R-1486-PR, February 1974.

7. Meyer, J. W., "Radar Astronomy at Millimeter and Submillimeter Wavelengths," *Proc. IEEE*, Vol. 54, No. 4, April 1966, pp. 484-492.

8. Feldman, N. E., *Estimates of Communication System Degradation Due to Rain*, The Rand Corporation, P-3027, October 1964.

9. Hannaford, D. A., *Meteorological Factors in Space Communications Systems*, International Conference on Satellite Communication, organized by the Electronics Division of the IEEE, November 1962.

10. Hogg, D. C., and T. S. Chu, "The Role of Rain in Satellite Communications," *Proc. IEEE*, Vol. 63, No. 9, September 1975, pp. 413-418.

11. Wilson, R. W., "Sun Tracker Measurements of Attenuation by Rain at 16 and 30 GHz," *B.S.T.J.*, Vol. 48, No. 5, May-June 1969, pp. 1383-1404.

12. Henry, P., "Measurement and Frequency Extrapolation of Microwave Attenuation Statistics on the Earth-Space Path at 13, 19, and 30 GHz," *IEEE Transactions*, March 1975, pp. 271-273.

13. Wulfsberg, Karl N., "Sky Noise Measurements at Millimeter Wavelengths," *Proc. IEEE*, March 1975, pp. 321-322.

14. Ippolito, L. J., "Summary and Evaluation of Results from the ATS Millimeter-Wave Experiment," *Earth-Satellite Propagation Above 10 GHz*, Sec. 8, Goddard Space Flight Center, Greenbelt, Maryland, May 1972.

15. Filipowsky, R. F., and E. I. Muehldorf, *Space Communications Systems*, Prentice-Hall, Inc., New York, 1965, p. 207.

16. Coleman, H. P., R. M. Brown, and B. D. Wright, "Paraboloidal Reflector Offset Fed With a Corrugated Conical Horn," *IEEE Trans. on Antennas and Propagation*, November 1975, pp. 817-819.

17. *A Forecast of Space Technology 1980-2000*, National Aeronautics and Space Administration, Washington, D.C., January 1976.

18. Villeneuve, A. T., *Microwave Atmospheric Sounding Radiometer Antenna System*, Hughes Aircraft Company, NAS 5-24087, July 1977.

19. Vogel, W. J., A. W. Straiton, and B. M. Fannin, "ATS-6 Ascending: Near Horizon Measurements Over Water at 30 GHz," *Radio Service*, Vol. 12, 1977, pp. 757-765.

20. Hitney, H. V., *Propagation Modeling in the Evaporation Duct*, Naval Electronics Laboratory Center, NELC/TR 1947, April 1975.

21. Richter, J. H. et al., *Propagation Measurements of 37 GHz in the Oceanic Surface Evaporation Duct*, Naval Electronics Laboratory Center, NELC/TN 2422, July 1973.

22. Allen. D. R., *Signal Quality of the Thule, Greenland-CONUS Satellite Link*, to be presented at the AIAA 7th Communications Satellite Systems Conference, April 1978 (preprint).

23. Lindsey, W. C., and M. K. Simon, *Telecommunications Systems Engineering*, Prentice-Hall, Inc., New York, 1973, pp. 252-271.

24. See, for example, S. Silver (ed.), *Microwave Antenna Theory and Design*, Boston Technical Lithographers, Inc., Lexington, Massachusetts, 1963, p. 195.

25. See, for example, D. O. Reudink and Y. S. Yeh, "A Scanning Spot-Beam Satellite System," *B.S.T.J.*, Vol. 56, 1977, pp. 1549-1560.

26. Holmes, D., "Navstar Technology," *Countermeasures*, Vol. 2, 1976, p. 27.

27. Skolnik, M. I., *Introduction to Radar Systems*, McGraw-Hill Book Co., Inc., New York, 1962.

28. *System Specification for Satellite Communication Terminal AN/FSC-78(V)*, SC-SS-1001A, June 30, 1976 (available from the Defense Communications Agency, Washington, D.C.).

29. *Satellite Communication Terminal AN/MSC-61*, U.S. Army Satellite Communications Agency, USASATCOMA Technical Requirements, SCA-2180, Fort Monmouth, New Jersey, April 1, 1976.

30. *Prime Item Specification for Communication Terminal Satellite AN/TSC-86( )*, U.S. Army Satellite Communications Agency, USASATCOMA Technical Requirements, SM-A-775168A, Fort Monmouth, New Jersey, March 3, 1976.

31. LaBanca, Dominic L., and Peter T. Maresca, *Ground Mobile Forces Satellite Communications Program (GMFSCP)*, U.S. Army Satellite Communications Agency, Fort Monmouth, New Jersey, September 27, 1976.

32. *Shipboard Satellite Communication Sets AN/WSC-2 (XN-2) (V)*, Naval Electronic Systems Command, Contract Specifications, ELEX-S-138, February 23, 1973, with Addendum 2, September 10, 1973.

33. *SHF Antenna and Computer Augmented Antenna Point Group--Advanced Airborne Command Post (AABNCP) Phase 1B-2*, The Boeing Company, Aerospace Group, Envelope Drawing No. 226-00045, Rev. A, Seattle, Washington, September 1975.

34. *Precision Rate System Final Report*, RCA Defense Electronic Products, Missile & Surface Radar Division, Moorestown, New Jersey, DS 105-679-6785, July 1966.

35. Proposal for *C-Band Mobile Medium Range Tracking Radar System (MMRTRS)*, RCA Missile & Surface Radar Division, Moorestown, New Jersey, DS 105-694-6885, April 1968.

36. Menzel, D. H., "A New Radio Telescope for Sweden," *Sky and Telescope*, Vol. 52, 1976, pp. 240-242.

37. See, for example, R. M. du Plessis, *Poor Man's Explanation of Kalman Filtering, or How I Stopped Worrying and Learned to Love Matrix Inversion*, The Autonetics Division, Rockwell International, June 1967.

38. Gelb, A. (ed.), *Applied Optical Estimation*, The MIT Press, Cambridge, Massachusetts, 1974, Chap. 4.

39. Mikelson, A. D., W. J. Owen, and H. A. Garcia, *Space Sextant Attitude Reference System (SS-ARS) Study*, Martin Marietta Corporation, AFAL-TR-76-15, March 1976.

40. Baird, J. M. et al., *Millimeter Wave Ubitron Development, Phase I*, Hughes Research Laboratories, Contract F-30602-76-C-0215, February 1977.

41. Godlove, T. F., and V. L. Granatsteen, "Gyrotron: Reborn Tube Is a Millimeter Powerhouse," *Microwave System News*, Vol. 7, No. 11, November 1977, pp. 75-82.

42. Jory, H., *Millimeter Wave Gyrotron Development, Phase I: Final Technical Report*, Varian Associates, Contract F30602-76-C-0237, May 1977.

43. Gapanov, A. P. et al., "Experimental Investigation of Centimeter-Band Gyrotrons," *Radiophysics and Quantum Electronics*, Vol. 18, No. 2, 1975, p. 280.

44. *Development Program for a 200 kW, CW, 28 GHz Gyroklystron*, Quarterly Report No. 5, Varian Associates, Palo Alto, California, July 1977.

45. Kisel, D. V. et al., "An Experimental Study of a Gyrotron, Operating at the Second Harmonic of the Cyclotron Frequency, With Optimized Distribution of the High Frequency Field," *Radio Engineering and Electronic Physics*, Vol. 19, 1974, p. 95.

46. Godlove, T. F. et al., *Prospects for High Power Millimeter Radar Sources and Components*, Naval Research Laboratory, Washington, D.C.

47. Manheimer, W. M., and V. L. Granatsteen, *Development of High-Power Millimeter-Wave Cyclotron Masers at NRL and Its Relevance to CTR*, Naval Research Laboratory, Memo Report 3493, April 1977.

48. Zaytsev, N. I. et al., "Millimeter and Submillimeter Wave Gyrotrons," *Radio Engineering and Electronic Physics*, Vol. 19, 1974, p. 103.

49. Luchinin, A. G., M. M. Ofitserov, T. B. Pankratova, V. G. Usov, and V. A. Flyagin, "High-power cyclotron-resonance masers of short millimeter wave range," Reports of all-union meeting on engineer problems of controlled fusion, *Izd. NIIEFA*, Vol. 4, 1975, pp. 308-313.

50. Godlove, T. F., and V. L. Granatsteen, "Relativistic Electron Beam Sources of Electromagnetic Radiation," *Society of Photo-Optical Instrumentation Engineers, Far Infrared/Submillimeter Wave Technology*, Vol. 105, 1977, pp. 17-21.

51. Sprangle, P., and A. T. Drobot, "The Linear and Self-Consistent Nonlinear Theory of the Electron Cyclotron Maser Instability," *IEEE Trans. on Microwave Theory and Techniques*, Vol. MTT-25, No. 6, June 1977, pp. 528-544.

52. Tentative Data Sheet 6949-1-58, Radio Corporation of America, Electron Tube Division, January 1958.

53. Tentative Data Sheet 6806-3-56, Radio Corporation of America, Electron Tube Division, March 1956.

54. Technical Data Sheet, VA-800H, Varian Associates, Palo Alto Tube Division, April 1974.

55. Preliminary Data Sheet VA-8[illegible] Varian Associates, Palo Alto Tube Division, May 1965.

Catalog on Hughes Travelin[illegible] Wave Tubes, Electron Devices, Lasers; Hughes Electron Dynamic[illegible] Division, undated.

57. [illegible] *Proposal for t[illegible] ESSCO Metal Space Frame Radome and Re[illegible]ories, 3rd Edit[illegible]*, Electronic Space Systems Corporation, Con[illegible] Massachuset[illegible] January 1977.

58. Matthews, [illegible]W., W. G[illegible]cott, and C. C. Han, "Advances in Multi-beam Sa[illegible]e Ante[illegible]a Technology," *Proc. EASCON '76*, 1976, pp. 132A-O.

59. Scott, W. G., D[illegible] *Tradeoffs for Multibeam Antennas in Communication Satel[illegible]*, Aeronutronic Ford Corporation, Palo Alto, California.

60. Binz, E. D.[illegible]d D. K. W[illegible], "Satellite Multibeam Antenna Concept," *A[illegible] CASE 6th Com[illegible]ations Satellite Systems Conference*, M[illegible]cal, Canada, Ap[illegible]-8, 1976.

61. Turrin[illegible] H., "A Multibeam Sphe[illegible]l-Reflector Satellite Antenna for [illegible]20 and 30 GHz Bands," [illegible]., Vol. 54, No. 6, July-Aug[illegible]1975, pp. 1011-1026.

62. Sem[illegible], R. A., "100-GHz Measurements [illegible] Multiple-Beam Offset A[illegible]nna," *B.S.T.J.*, Vol. 56, No. 3, M[illegible] 1977, pp. 385-398.

63. Ku[illegible]awa, H., and M. Karikami, "Multiple[illegible] Antenna for Domestic [illegible]mmunication Satellites," *IEEE Trans. [illegible]ennas and Propagation*, November 1973, pp. 876-878.

64. [illegible]er, P. J., R. M. Rudish, and J. J. Taub, *Guid[illegible]ptical Techniques for Simultaneous Reception of Multiple [illegible]meter Signals*, A.I.L., A Division of Cutler-Hammer, AFAL[illegible]-393, November 1972.

Tang, R. et al., *Limited Scan Antenna Technique Study*, [illegible]es Aircraft Company, AFCRL-TR-75-0448, August 1975.

Buehl, F. W., and R. E. Hammerand, *A Review of Communication Satellites and Related Spacecraft for Factors Influencing Mission Success*, The Aerospace Corporation, TOR-0076(6792)-1, November 1975.

67. Van Trees, H. L., E. V. Hoversten, and T. P. McGarty, "Co[illegible] tions Satellites: Looking to the 1980s," *IEEE [illegible]*, ber 1977, pp. 42-51.

55. Preliminary Data Sheet VA-879, Varian Associates, Palo Alto Tube Division, May 1965.

56. Catalog on Hughes Traveling-Wave Tubes, Electron Devices, Lasers; Hughes Electron Dynamics Division, undated.

57. *Technical Proposal for the ESSCO Metal Space Frame Radome and Accessories, 3rd Edition,* Electronic Space Systems Corporation, Concord, Massachusetts, January 1977.

58. Matthews, E. W., W. G. Scott, and C. C. Han, "Advances in Multibeam Satellite Antenna Technology," *Proc. EASCON '76,* 1976, pp. 132A-O.

59. Scott, W. G., *Design Tradeoffs for Multibeam Antennas in Communication Satellites,* Aeronutronic Ford Corporation, Palo Alto, California.

60. Binz, E. D., and D. K. Wainer, "Satellite Multibeam Antenna Concept," *AIAA/CASE 6th Communications Satellite Systems Conference,* Montreal, Canada, April 5-8, 1976.

61. Turrin, R. H., "A Multibeam Spherical-Reflector Satellite Antenna for the 20 and 30 GHz Bands," *B.S.T.J.,* Vol. 54, No. 6, July-August 1975, pp. 1011-1026.

62. Semplak, R. A., "100-GHz Measurements on a Multiple-Beam Offset Antenna," *B.S.T.J.,* Vol. 56, No. 3, March 1977, pp. 385-398.

63. Kumazawa, H., and M. Karikami, "Multiple Beam Antenna for Domestic Communication Satellites," *IEEE Trans. on Antennas and Propagation,* November 1973, pp. 876-878.

64. Meier, P. J., R. M. Rudish, and J. J. Taub, *Quasi-Optical Techniques for Simultaneous Reception of Multiple Millimeter Signals,* A.I.L., A Division of Cutler-Hammer, AFAL-TR-72-393, November 1972.

65. Tang, R. et al., *Limited Scan Antenna Technique Study,* Hughes Aircraft Company, AFCRL-TR-75-0448, August 1975.

66. Buehl, F. W., and R. E. Hammerand, *A Review of Communications Satellites and Related Spacecraft for Factors Influencing Mission Success,* The Aerospace Corporation, TOR-0076(6792)-1, November 1975.

67. Van Trees, H. L., E. V. Hoversten, and T. P. McGarty, "Communications Satellites: Looking to the 1980s," *IEEE Spectrum,* December 1977, pp. 42-51.